New Formula for Clearwater Equilibrium Scour Depth around a Log Vane based on Literatures

A thesis submitted towards partial fulfilment of the requirements for the degree of

Master of Engineering

in

Water Resources and Hydraulic Engineering

Submitted by

Asraf Hossain

Examination Roll No. M6WRP24003

Registration No. 160490 of 2021-2022

Under the guidance of

Dr. Subhasish Das

Associate Professor

School of Water Resources Engineering

Jadavpur University

School of Water Resources Engineering

M.E. (Water Resources & Hydraulic Engineering)

Course affiliated to ***Faculty Council of Engineering & Technology***

Jadavpur University

Kolkata-700032, West Bengal, India

2024

Declaration of Originality and Compliance of Academic Ethics

I hereby declare that this thesis contains a literature survey and original research work by the undersigned candidate, as part of my **Master of Engineering (Six Semester)** in **Water Resources and Hydraulic Engineering** in the Faculty Council of Interdisciplinary Studies, Law & Management, Jadavpur University during the academic session 2023-24.

All information in this document have been obtained and presented in accordance with academic rules and ethical conduct.

I also declare that, as required by these rules and conduct, I have fully cited and referenced all material and results that are not original to this work.

Name	**:**	**Asraf Hossain**
Exam. Roll Number	**:**	**M6WRP24003**
Thesis Title	**:**	New Formula for Clearwater Equilibrium Scour Depth around a Log Vane based on Literatures
Signature with Date	**:**	

M.E. (Water Resources & Hydraulic Engg.) course affiliated to
Faculty Council of Engineering & Technology
Jadavpur University
Kolkata, India

Certificate of Recommendation

This is to certify that the thesis entitled "***New Formula for Clearwater Equilibrium Scour Depth around a Log Vane based on Literatures"*** is a Bonafide work carried out by **Mr. Asraf Hossain** under my supervision and guidance for partial fulfilment of the requirement for the Post Graduate Degree of Master of Engineering in Water Resources and Hydraulic Engineering (Six Semester) during the academic session 2023-24.

THESIS ADVISOR
Dr. Subhasish Das
Associate Professor
School of Water Resources Engineering
Jadavpur University

DIRECTOR
Prof. (Dr.) Asis Mazumdar
School of Water Resources Engineering
Jadavpur University

DEAN
Prof. (Dr.) Ratan Mondal
Faculty Council of Interdisciplinary Studies, Law & Management
Jadavpur University

M.E. (Water Resources & Hydraulic Engg.) course affiliated to
Faculty Council of Engineering & Technology
Jadavpur University
Kolkata, India

CERTIFICATE OF APPROVAL **

This foregoing thesis is hereby approved as a credible study of an engineering subject carried out and presented in a manner satisfactorily to warranty its acceptance as a prerequisite to the degree for which it has been submitted. It is understood that by this approval the undersigned do not endorse or approve any statement made or opinion expressed or conclusion drawn therein but approve the thesis only for the purpose for which it has been submitted.

Committee of

Final Examination

for the evaluation

of the thesis

** Only in case the thesis is approved.

ACKNOWLEDGEMENTS

I express my sincere gratitude to my supervisor, ***Dr. Subhasish Das,*** *Associate Professor, School of Water Resources Engineering, Jadavpur University, under his supervision and guidance this work has been carried out. It would have been impossible to carry out this thesis work with confidence without his wholehearted involvement, advice, support and constant encouragement throughout. He has not only helped me in carrying out my thesis but also has given me valuable advice to proceed further in my life.*

I also express my sincere gratitude to, ***Prof. (Dr.) Asis Mazumdar****, Director,* ***Prof. (Dr.) Arunabha Majumder****, Emeritus Professor;* ***Prof. (Dr.) Pankaj Kr. Roy, Dr. Rajib Das, Dr. Gourab Banerjee,*** *Faculty members of School of Water Resources Engineering, Jadavpur University for their valuable suggestions.*

I would also express my sincere thanks to ***Mr., Buddhadev Nandi,*** *Research Scholar of School of Water Resources Engineering, Jadavpur University for his unconditional support and affection during my work. Also, thanks to my classmate* ***Mr. Sudarshan Mondal****, my MAA* ***Mrs. Fatema Bibi*** *and my soulmate* ***Mrs. Manuyara Khatun*** *for their unconditional love in encouraging me to prepare this thesis.*

Thanks, are also due to all staff of the School of Water Resources Engineering and the Regional -cum-Facilitation Centre (RCFC), NMPB, Jadavpur University for their help and support.

Date : 31.05.2024

Place : Jadavpur University

Mr. Asraf Hossain
(Exam. Roll No: M6WRP24003)

ABSTRACT

River restoration aims to enhance the natural form and processes of a river, often involving techniques to manage the riverbed, stabilize channel alignment, protect stream banks, and rebuild natural habitat methods such as rebuilding meanders, establishing pool-riffle sequences, and managing large wood contribute to stabilizing rivers and restoring habitat. Common measures include the installation of single-wing, double-wing, and triangular deflectors, as well as log vanes constructed along the riverbank to prevent erosion. Despite several studies on the topic, no literature comprehensively covers all the necessary data and equations for thorough comparative analysis. Studying equilibrium scour around log vanes can help fill gaps in understanding the unique mechanisms and characteristics of sediment erosion and deposition, contributing to improved design and management strategies for riverine structures. This study aims to analyze influential parameters affecting the equilibrium scour depth of a log vane through dimensional analysis to develop a new formula for predicting equilibrium scour near the downstream of a log vane. The experimental data utilized in this study were sourced from various literatures where the authors conducted experiments under clear water scour conditions. Upon analyzing these available data, it becomes evident that parameters such as tail water depth, orientation angle of log vanes, aspect ratio of the vane, and downstream water fall significantly influence scour depth. There are two formulas in literatures based on some literature data. However, these two formulas were tested on only a limited number of data. Therefore, a new formula is developed based on all accessible literature data to describe the scour process using nonlinear regression and its dependency on these factors. The statistical performance indicators including coefficient of determination, root mean squared error, sum of squared error, and mean squared error are used for the evaluation of this newly developed formula as well as the two formulas collected from the literatures. Two new formulas have been established which are non-dimensionalized by the length of the vane and height of the vane. These two new formulas outperform the other two literature formulas in terms of all statistical indicators. Furthermore, the scour in the river is influenced by a non-dimensional parameter, ψ, which is a function of the particle Froude number, height of the log vane and water fall depth. Plotting the data with the new formulas shows a 30% deviation from the perfect agreement line, with no data below -30%, indicating overestimated non-dimensional scour depths and reduced likelihood of structural failure due to scouring.

CONTENT

Serial Number	Chapter No	Topic	Page No
1	**Chapter 1**	**INTRODUCTION**	
		1.1. Scour processes around log vane	1
		1.2. Definition of scour	2
		1.3. Factors affecting scour	3
		1.3.1. Types of scour	3
		1.3.2. Local Scour	4
		1.3.3. Clearwater and live bed scour	5
2	**Chapter 2**	**REVIEW OF LITERATURES**	
		2.1. Literature review	6
		2.2. Research gap	14
		2.3. Need of the work	14
3	**Chapter 3**	**LOCAL SCOUR CHARACTERISTICS AROUND LOG VANE**	
		3.1. Local scour mechanism	15
		3.1.1. Wake vortex	15
		3.1.2. Horseshoe vortex and downflow	16
		3.2. Classification of scour parameters	17
		3.2.1. Flow intensity	17
		3.2.2. Floe depth	17
		3.2.3. Effective width of vane	17
		3.2.4. Sediment size	18
		3.2.5. Flow Froude number	18
		3.2.6. Densimetric Froude number	19
4	**Chapter 4**	**SYNTHESIS OF EXISTING RESEARCH: DATA, METHODS, AND EQUATIONS**	
		4.1. Review of experimental procedure	20
		4.2. Ranges of different author data	22
		4.3. Functional relationship used in literature to find scour	23
5	**Chapter 5**	**OBJECTIVES AND METHODOLOGY**	
		5.1. Objectives	26
		5.2. Methodology	26
		5.3. Statistical influence indicator	27
6	**Chapter 6**	**DIMENSIONAL ANALYSIS**	

		6.1. Analyses of scouring parameters	30
		6.2. Dimensionless analysis	30
		6.3 Classification of non-dimensional Parameters	33
		6.4 Ranges of non-dimensional parameters used in literatures	34
7	**Chapter 7**	**ANALYSIS OF PARAMETERS USING CORRELATION AND REGRESSION METHOD**	
		7.1. Introduction to reduction method	35
		7.1.1. Correlation	35
		7.1.1.1. Scatter diagram	35
		7.1.1.2 Pearson correlation	36
		7.1.1.3 Spearman's rho Correlation	36
		7.1.1.4 Kendall's Tau B Correlation	36
		7.2. Regression	37
		7.2.1. Forward regression	37
		7.2.2. Backward regression analysis	37
		7.2.3. Stepwise regression analysis	37
		7.2.4. Subset regression analysis	38
8	**Chapter 8**	**RESULTS AND DISCUSSION**	
		8.1. Results	39
		8.1.1. Behavior of scour with Froude number and role of vane angle on it	39
		8.1.2. Behavior of scour with tailwater depth and role of vane angle on it	41
		8.1.3. Behavior of scour with aspect ratio and role of vane angle on it.	43
		8.1.4. Behavior of scour with densimetric Froude number and role of vane angle on it	45
		8.1.5. Behavior of scour with waterfall and role of vane angle on it	47
		8.1.6. Behavior of scour with Froude number and role of vane angle on it	49
		8.1.7. Behavior of scour with tailwater depth (h_{tw}/H) and role of vane angle on it	51
		8.1.8. Behavior of scour with non-dimensional parameter(η) and role of vane angle on it	53
		8.1.9. Behavior of densimetric Froude number F_d with dimensionless waterfall ($\Delta y/H$) and role of different parameters on it	56

		8.2(a). Formula derivation by using different statistical techniques	59
		8.2(b). Formula derivation by using different statistical techniques	71
		8.3. General discussion on newly developed formulas	84
		8.4. Comparison between shortlisted formulas	86
		8.5. Validation of formula	87
9	**Chapter 9**	**CONCLUSIVE REMARKS**	
		9.1. Conclusions	92
		9.2. limitations of the study	93
		9.3 Future Scopes	94
		9.4 Notations	95
		References	96

Chapter – 01

Introduction

1.1. Scour processes around log vane

A submerged log vane is a vortex-generating device that can control riverbed evolution in natural stream channels. The log vane is a low-height baffle that is positioned on the river bottom at a particular angle of attack which diverts the flow of a river and thereby generates secondary currents in the mainstream. Therefore, the intensity and direction of the bottom shear stresses are modified, and sediments are redistributed within the channel cross-section. For this reason, these devices have found many applications in river hydraulics, such as bank protection for curved channels, protection of bridge abutments and piers, and prevention of sediment drift in hydropower or irrigation channel junctions. Moreover, they are used to produce the optimal depth of the riverbed, reduce unwanted scour or the deposition of sediments and improve overall river navigability, settle braided and wandering rivers with the consequent removal of bars and shoals, and create a suitable habitat for aquatic fauna. Control of sediment in alluvial channels is one of the most difficult problems encountered by hydraulic engineers. Control may be required for the provision of greater channel capacity, maintenance of a certain optimum flow depth, improvement of non-regime channels, prevention of bed and bank erosion, or diversion of flow from one channel to another or a water intake. A log vane is an effective measure for sediment management in alluvial rivers. By installing several log vanes on the streambed at an angle to the flow, the flow pattern downstream of the log vane is changed and the shear stress on the channel bed is redistributed. As a result, the bed material is transported transversely in a channel cross-section. With proper configuration of the log vanes, a certain portion of the streambed affected by the vanes can practically be modified into any designated profile that is favored for the management of the river. The effectiveness (in terms of sediment control) of a log vane is related to its dimensions and shape. Most vanes in field applications are rectangular plates, mainly due to their simplicity to manufacture and construct, but here log vanes are made of wood. Some sophisticated designs tested in laboratory studies have airfoil-like cross-sectional profiles. Vanes are structures to divert the flow of a river, however, as it is a structure placed on the riverbed, local scour around it is also a common phenomenon. Local scour around structures is the main cause of the destruction of many manmade structures inside rivers. An estimate of the maximum possible scour around any manmade structure is necessary for its safe design. For example, it has been observed that in the free surface flow around a bridge pier, horseshoe vortices formed, and the turbulence is intensified in front of, around and behind the piers. In

addition, a uniquely shaped scour hole on the loose bed around a pier is observed. Experimental studies have found that both the flow and the sediment transport processes during the scour hole development are highly complex. Another aspect of this scour around structures is that the sediments are transported downstream to the river. In many small channels, it is observed that due to deposition the depth of the channel reduces significantly. This in turn makes it non-navigable. Hence if the sediments could be shifted to one side of the bank of the small channel, it may help in navigation. Also, stream bank erosion and deposition in small channels is a major resource management problem. Bank erosion generally occurs in curves of river channels, where the interaction between the vertical gradient of the velocity and the curvature of the flow generates a so-called secondary or spiraling flow. Our present study has attempted to establish a new equation for more accurately predicting the equilibrium scour depth, which in turn may give us a clear idea of the scour phenomena around a log vane. From this study, we may be able to understand the scour pattern around a log vane which is dependent on several hydraulic parameters.

1.2. Definition of scour

Scouring is a natural phenomenon caused by the flow of water in the river and stream. It is the process by which flowing water exerts force (on the bed and banks), dislodging and carrying away sediment particles(see **Fig. 1.1**) from the bed and banks of streams and the vicinity of bridge piers and abutments (Breusers et al., 1977). Scouring occurs naturally as part of the morphological changes of rivers and can also be influenced by human-made structures such as bridges. Scour can either be caused by the normal flow or flood flow. Normal flow cannot make a big scour, but during a peak flow make a big scour hole in which the flow velocity is higher than normal flow.

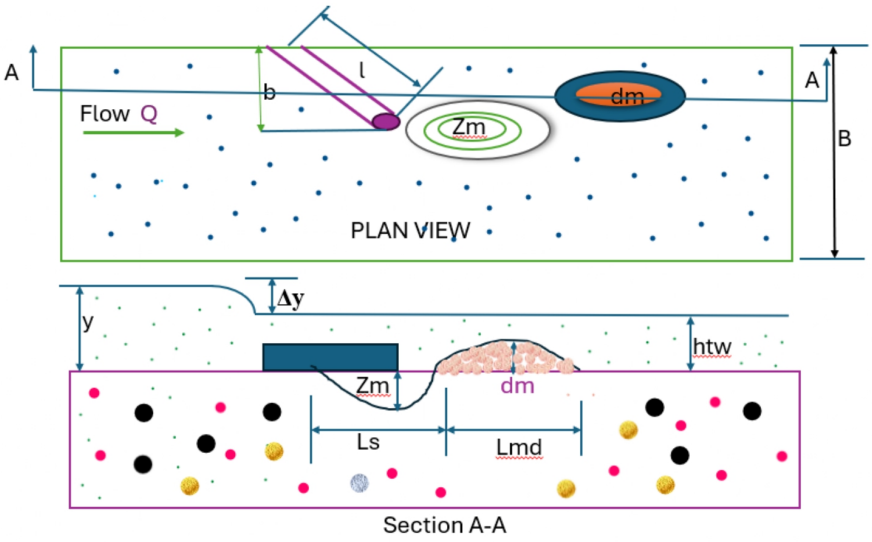


Fig. 1.1. Process of scouring near the log vane

1.3. Factors affecting scour

Scour depends upon various factors such as flow velocity, depth of flow, Vane width, Froude number, bed materials, presence of obstructions/man-made structures, and channel morphology.

- Flow velocity (V): Higher water velocities in the river exerted higher force on the bed and banks which increased the scouring.
- Depth of flow (y): The Froude number is inversely related to flow depth. Lower flow depth increases the velocity which generates more force on the bed and banks as a consequence of higher scouring.
- Vane width: The width of a vane, which is a structural element used in river engineering to manage flow patterns and reduce erosion, can affect scour in several ways.
- Froude number (Fr): While the Froude number itself may not directly influence the scouring process; it is indicative of the flow conditions within a river. Understanding the flow regime, as characterized by the Froude number, is crucial for assessing the potential for scouring.
- Bed materials: The type, size, and amount of sediment present in the riverbed influence scouring rates.
- Presence of obstructions/Man-made structures: Presence of obstacles such as rocks, vane dikes, cross vane, Bridge piers and abutments can alter the scour process.
- Channel morphology: The shape, size and roughness of the channel also change the scour distribution on the beds.

1.3.1 Types of scour

Scouring occurs naturally as a part of the morphologic changes of rivers and as the result of manmade structures. Generally, any hazard may cause a scour in the river bed. Scour can be classified into two major types, namely general scour, and localized scour. Some other subdivisions of scour are shown (**Fig. 1.2.**) below:

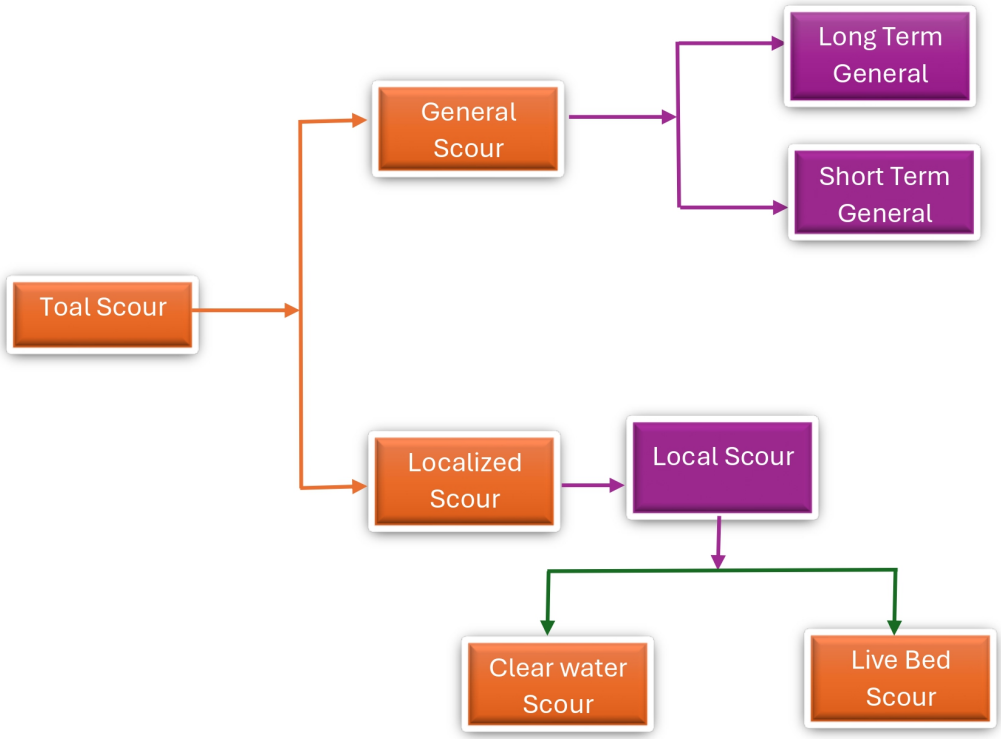


Fig. 1.2. Different types of local scour

1.3.2. Local scour

The scour that occurs near a vane dyke, log vane, pier, abutment, erosion control device, or other structure obstructing the flow is called local scour. These obstructions cause flow acceleration and create vortices that remove the surrounding sediments. Generally, depths of local scour are much larger than general or contraction scour depths, often by a factor of ten. Local scour can affect the stability of structures such as riprap revetments and lead to failures. Factors that influence local scour include:

a) Width of the obstruction.
b) Projection length of the obstruction into the flow.
c) Length of the obstruction.
d) Angle of incidence of the structure to the approaching flow.
e) The velocity of the approach flow.
f) Size of the bed material.
g) Depth of flow.
h) Shape of the obstruction.
i) Bed configuration.

The depth of the scour is directly dependent on the width of the obstruction. Thus, the wider the obstruction, the deeper the scour. Though not addressed by most of the empirical relations, the ratio of obstruction width to channel width is probably a better measure of scour potential than the obstruction width alone. The projected length of an obstruction into the

stream influences the depth of the scour. With an increase in the projected length of a vane dyke into the flow, there is an increase in scour. This happened because the velocity distribution across the river is parabolic. Johnsen et al. (2001) also showed that the scour towards the bank is less as compared to the center of the channel.

1.3.3. Clearwater and live bed scour

Clear water scour refers to the erosion of sediment around a structure in a river or coastal area under conditions where the water is clear and free from sediment transport. This type of scour typically occurs when the flow velocity exceeds a critical threshold, causing sediment particles to be entrained and eroded from the bed.

On the other hand, live bed scour occurs when sediment transport is actively happening in the water column, leading to the erosion and deposition of sediment around a structure. This type of scour is common in rivers and coastal areas where sediment is continuously transported by the flow.

Both clear water scour and live bed scour are important considerations in hydraulic engineering and geomorphology, particularly in the design and maintenance of structures such as bridges, culverts, and coastal defences. Understanding the mechanisms and characteristics of these scour processes is essential for ensuring the stability and safety of such Structures. **Fig. 1.2.** shows how scour changes with time for both cases. From **Fig. 1.2**. it is also clear that scour is a continuous process for clear water conditions whereas in live bed conditions scour and sediment particles are deposited simultaneously on the riverbed.

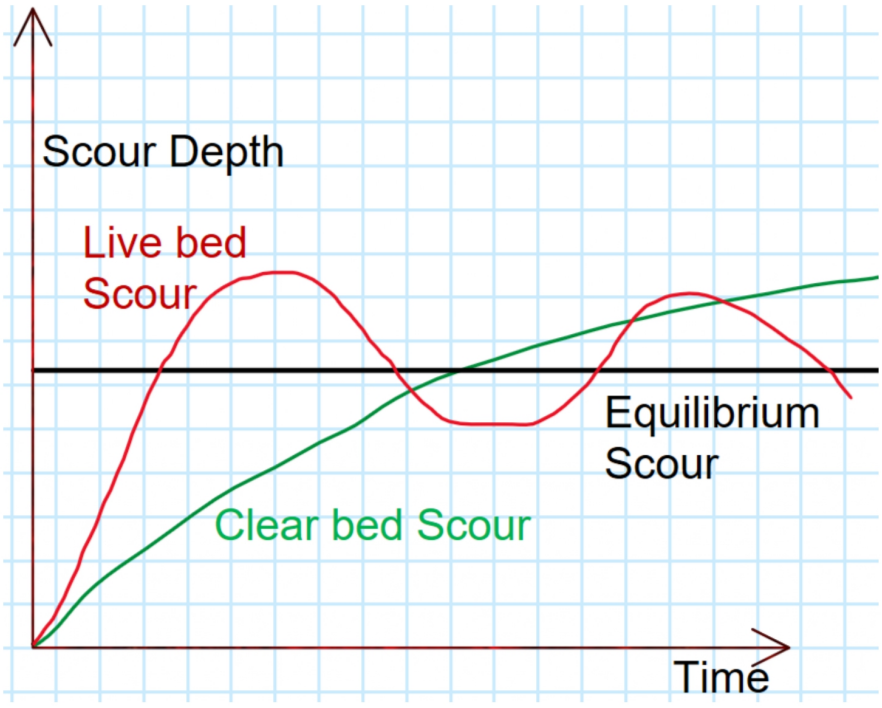


Fig. 1.2. Correlation between scour and time

Chapter 02

Review of literatures

2.1. Literature Review

It is crucial to accurately predict the scour depth around the hydraulic structures such as bridge piers, abutments, log vane, and spur dikes experimentally, numerically as well as using machine learning techniques. There are numerous studies available for isolated bridge piers and a combination of bridge piers. The study on isolated pier scour depth computation formula conducted by Melville and Chiew (1999), Oliveto and Hager (2002), Azamathulla et al. (2010), Nandi and Das (2023*a*), Nandi et al. (2024*a*) and Nandi et al. (2024*b*). The study of eccentric multiple piers conducted by several researchers (Das et al., 2014*a*; Das et al., 2014*b*; Das et al., 2016; Das and Mazumdar, 2018; Das et al., 2019; Nandi and Das, 2023*b*). The flow characteristic near the pier was studied by Das et al. (2013), Das et al. (2014*c*), Das et al. (2017), Jaman et al. (2017), and Das et al. (2019).

Reviews on some important experimental works were carried out by Odgaard and Spoljaric (1986), Breusers et al. (1977), Melville (1992), Dey et al. (1995), Ahmed and Rajaratnam (1998); Dey (1999), Muzzammil and Gangadhariah (2003), Barbhuiya and Dey (2004), Dey and Raikar (2007), Khwairakpam et al. (2014) and Das et al. (2013). The selection of an appropriate design method to estimate equilibrium depths of local scour at bridge piers has perplexed designers for many years. There was a wide variety of formulas available and no obvious similarity in either their appearance or their predictions. The apparent conflicts arose from earlier studies, some of which showed live-bed scour exceeding clear-water scour and others which showed the reverse (Breusers et al. 1977).

Some of the significant works on Bridge and pier scours are reported below:

Melville and Raudkivi (1977) (also see Melville 1975) were the pioneers in measuring the turbulent flow field within a scour hole at a circular pier with the aid of the DISA Hot-Film Anemometer. The experiments aim to obtain information for such a case on flow patterns, turbulence intensity distributions, boundary shear stress distribution in the scour zone, and interaction of the vortices shed by the cylinder with the horseshoe vortex. The flow patterns were traced using the hydrogen-bubble method. They measured the flow field in the upstream axis of symmetry and the near-bed turbulence intensity for the case of a flatbed, intermediate (scour hole after 30 minutes from the commencement of erosion), and equilibrium scour hole. He also estimated the bed-shear stresses from the measured near-bed velocities. The experiments were confined to the clear water scour condition and the development of one scour hole from the initial flatbed through to the equilibrium scour hole condition.

Raudkivi and Ettema (1983) calculated the equilibrium depth of local scour in this study. Based on the data of laboratory experiments on the clear-water local scour of

cohesionless bed sediment at cylindrical piers, it was suggested that the equilibrium depth of local scour is related to the particle size distribution of the bed sediment, the mean particle size of the bed sediment, relative to the pier diameter, flow depth relative to both the pier diameter and the mean particle size of the bed sediment. A formula for estimating the maximum depth of local scour for non-uniform alluvial sediments can be estimated in terms of the geometric standard deviation of the sediment.

Darghi (1990) found that clear water scouring around a circular cylinder is driven by the three-dimensional separation of the upstream boundary layer and periodic vortex shedding in the cylinder's wake. Horseshoe vortices in the upstream region and primary wake vortices behind the cylinder cause periodic sediment transport and scouring patterns, with the periodicity governed by the shedding frequency of the wake vortices. Adding collars to the cylinder can influence the scouring dynamics.

Melville (1992) presented a series of laboratory data to demonstrate the effects on scour depth of abutment length, flow depth, and abutment shape and alignment. In addition to this, some data also presented for the effects of sediment characteristics, flow intensity, and approach channel geometry are given. The data are rationalized in terms of the ratio of abutment length to flow depth, L/y. For large and small values of L/y, the abutments are termed long and short, respectively, and it is shown that the maximum scour depths measured in the laboratory for these cases are $2L$ and $10y$. Most actual cases of abutment scour lie between the limiting cases, and it is demonstrated that, in such situations, scour depth is proportional to the square root of the product Ly. These relationships are formulated in a simple design method in this study. These equations do not include the effects of sediment characteristics, lateral distribution of flow, or river geometric features including overbank flow and may lead to excessively conservative estimates of scour depth in some instances.

Dey et al. (1995) studied the quasi-steady vortex flow around circular piers in a clear water scour(quasi-equilibrium) hole. They used a five-hole pitot sphere to measure velocity vectors at different angles: 0°, 15°, 30°, 45°, 60°, and 75°. They analyzed how circulation changed with the pier Reynolds number (it is defined as the ratio of inertia force and viscous force of fluid) for eighteen different tests. The results matched well with Melville's observations from 1975.

Ahmed and Rajaratnam (1998) conducted a laboratory study on how water flows past cylindrical piers on smooth, rough, and mobile beds. They measured flow in the plane of symmetry, focusing on frontal downflow and the impact of bed roughness and scour holes. The roughness induced a steeper pressure gradient and thus stronger downflow in front of the cylinder. The scour hole allowed fluid to pass through it, which was reflected in stronger downflow. The Clauser-type defect scheme better described the velocity profiles as compared to the log-law and defect law. They observed frontal downflows reaching up to 95% of the approach flow. Bed roughness increased bed shear stress. Ahmed and Rajaratnam (2000) extended this work to rectangular bridge abutments, a topic not considered herein.

Barbhuiya and Dey (2004) obtained similar results from a semi-circular pier arrangement placed at the channel sidewall. The vortex size, vortex velocity and vortex strength were determined in terms of the relevant hydraulic and geometric parameters and the temporal scour hole evolution.

Dey and Raikar (2007) presented the outcome of an experimental study on the turbulent horseshoe vortex flow within the developing intermediate stages and equilibrium scour holes at cylindrical and square piers measured by an Acoustic Doppler Velocimeter. The contours of the time-averaged velocities, turbulence intensities, and Reynolds stresses at different azimuthal planes 0°, 45°, and 90° were presented.

Jueyi et al. (2010) identified clear water scours around semi-elliptical abutments with armored beds. An experimental study has been carried out under a clear-water scour condition to explore the local scour around semi-elliptical model bridge abutments with armor-layer bed, compared with the local scour process around semi-circular abutment. The researcher concluded that for both semi-elliptical and semi-circular abutments, with the increase in flow velocity in all the runs the equilibrium scour depth of the scour hole will be increased. The equilibrium scour depth of the scour hole is not dependent either on the condition of the bed material or armor-layer. For any armor-layer having the same grain size, with the increase in the particle size of bed material and the velocity, the equilibrium scour depth of the scour hole will be increased. However, for any bed material having the same grain size, with the increase in the particle size of armor-layer and the velocity, scour depth will be decreased. Therefore, an increase in the particle size of armor-layer will result in a reduction in scour depth of the equilibrium scour hole. However, with an increase in the particle size of the bed material, the equilibrium scour depth of the scour hole will be increased. For all of the runs, the equilibrium scour depth of the scour hole around the semicircular abutment is more than that around the semi-elliptical one. The equilibrium scour depth of the scour hole can be described as an empirical equation as a function of excess approaching flow Froude number (it is the ratio of inertia force and gravitational force), the grain size of bed material, grain size of armor-layer and water depth of approaching flow.

Khwairakpam et al. (2012) conducted clear water scour experiments with a circular pier in a tilting flume, varying the densimetric Froude number and inflow depths. Das et al. (2013a, b, 2014a) studied the geometry and circulation of scour holes at a circular pier, measuring data with an ADV. They presented velocity vector plots and vorticity contours for the flow field upstream and downstream of the pier. Das et al. (2013c) compared horseshoe vortex characteristics at circular and square piers. Das et al. (2014b) investigated how clear water scour geometry varies with piers of different widths.

Al-Shukur and Obeid (2016) focused on the impact of pier shape on local scours around bridge piers, important for safe design. Experiments were conducted in a laboratory flume with sand beds, keeping flow depth and bed material constant, and varying velocities at 0.18, 0.25, and 0.3 m/sec. Ten pier shapes were tested: Circular, Rectangular, Octagonal, Chamfered, Hexagonal, Elliptical, Sharp, Joukowsky, Oblong, and Streamline. The results showed that scour depth is proportional to the exposed area of the upstream nose of the pier. The rectangular pier had the largest scour depth (0.076 m), while the streamline shape had the smallest (0.003 m). There are several studies around multiple piers focusing on the prediction of scour depth. For a pier in a group, combined effects are significant besides those parameters that affect scouring around a single pier.

Michael et al. (1991) explained how inline eccentric piers can enhance the sediment transport rate towards the riverbank flowing downstream. Stream bank erosion and deposition in small channels is a major resource management problem. Bank erosion generally occurs in

curves of river channels, where the interaction between the vertical gradient of the velocity and the curvature of the flow generates a so called secondary or spiraling flow. The secondary flow moves the high velocity, near surface current outward (and low velocity, near bed current inward) and thereby produces larger depths and velocities near the outer banks. The deepening of the channel diminishes the toe support of the bank, and the larger velocities attack it, setting the stage for bank erosion. A technique developed at the Iowa Institute of Hydraulic Research (IIHR) may alleviate the problem. The technique consists of installing small, submerged vanes on the streambed to counter the flow spiral. The vanes are small-aspect ratio foils placed along the outer bank, at angles of 10-15° with the mean flow, to direct the near bed current outward toward the bank. The height of the vanes is 20-30% of the high flow water depth. The analytical basis for the functioning of the vanes was described earlier by Odgaard and Kennedy (1982, 1983).

Some of the very important and significant works on scours due to vane are reported below:

Odgaard and Kennedy (1983) studied river-bend bank protection using submerged vanes. They demonstrated, both theoretically and with a physical model, that short, vertical vanes placed in the outer half of a river-bend can significantly reduce secondary currents and protect the outer bank from erosion. The effect of the vanes on secondary flow was estimated using a simple torque calculation based on the Kutta-Joukowski theorem. They derived a design formula for vane spacing by balancing the torque from flow curvature with the lateral force on the vanes. This formula was verified using a model of a bend in the Sacramento River, California.

Odgaard and Spoiljaric (1986) described here a procedure developed for a rational design of a system of submerged vanes for depth control in alluvial-river channels. The vanes were vertical, small-aspect ratio foils installed on the channel bed at an angle of attack of 10° -15° with the flow. Their height was 0.2-0.5 times the water depth at design flow (stage). The design procedure was based on a calculation of the transverse bed slope generated by the vane induced transverse component of the near bed velocity vector. The streamwise extent of the vanes impact was governed by the momentum equation. The effectiveness of the technique was tested in a series of laboratory experiments, showing that the bank protection technique was a feasible and realistic alternative to the traditional techniques, e.g., rock, riprap, and spur dikes. Although the design could be improved, the vanes of this design were seen to effectively stabilize the bed topography by preventing near bank scour and, instead, cutting in on the point bar. The design produced a reduction of the high flow transverse bed slope of at least 50% and a reduction of the near bank velocity of, generally, 10%-20%, moving the velocity maximum toward the Centre of the channel. This study also showed that a system of submerged vanes for sediment control could be designed on a rational basis using hydro-dynamical principles. The change in flow depth induced by a vane was proportional to the vane-induced transverse velocity component near the bed, which was a function of the vane's angle of incidence with the flow. The optimum angle was about 15°; a vane at a 15° angle can produce a change in depth of the order of 10%. At angles greater than 15°, flow separation became significant and caused excessive scouring around the vane. A change in flow depth

beyond that which a single 15° vane could accomplish could be generated by a lateral array of two or more vanes spaced one to two water depths apart.

Odgaard and Wang (1991) carried out an experiment to show sediment management with submerged vanes. It was suggested that small, submerged vanes can produce significant changes in the distributions of velocity and depth in river channels. By introducing relatively small changes in the bed shear stresses, arrays of vanes can generate local changes in the bed elevation of the order of the vane height. The major controlling parameters were vane height, vane aspect ratio and angle, vane density (spacing), channel resistance, and sediment Froude number. An increase of any of these parameters causes the induced changes in bed elevation to increase. The major uncertainties in the calculations were associated with the transverse bed-slope factor and the velocity-profile factor. The transverse bed-slope factor represented the bed sediment's motion-resistance properties. Its value was reported to range from three to six, possibly depending on sediment gradation. The velocity-profile factor was the ratio of the depth-averaged velocity to its velocity in the near-bed layer affected by the vanes. The calculations were performed with the transverse bed-slope factor of 4 and velocity-profile factor of 1.

Marelius and S.K Sinha (1998) described the physics of the flow past a submerged vane at high angles of attack in this paper. The data presented were collected during an experimental study of flow past vanes at various angles of attacks in a deformable-bed straight rectangular channel. The first few experimental runs were undertaken to establish the optimal angle of attack required to generate the strongest secondary circulation in the flow. At this optimal angle of attack, the flow features responsible for the transverse movement of bed sediment are clearly identified. The differences between the flow features observed near the vanes at both low and high angles of attack are also outlined. These include, among others, two counter rotating vortices for vanes at high angles of attack as opposed to the widely acclaimed hypothesis of a single vortex for low angles of attack. This paper presents a detailed analysis of the flow field past submerged vanes at a high angle of attack. It is shown that the vane produced the strongest circulation for an angle of attack of about 40°. The flow features responsible for the transverse movement of sediment transport are clearly identified. The differences between the flow features observed for vanes with low and high angles of attack are outlined.

Johnson et al. (2001) attempted a project work where rock vanes were single-arm structures angled to the flow with a pitch into the streambed such that the tip of the vane is submerged even during low flow. Vanes have primarily been used in recent years for the treatment of bank erosion in stream stability projects. These structures roll the water away from the eroding banks, thus limiting erosion of the channel banks. They have proven to be very effective treatments over a range of flow conditions. In this project, the effectiveness of vanes for preventing scour at single-span bridges with vertical wall abutments was evaluated based on laboratory experiments. The vanes were tested in small-scale experiments in a re-circulating flume and subjected to a range of flow conditions, including bank full and several overbank flows, which were forced to return to the channel at the abutment. The results showed that the vanes were highly effective in moving the scour away from the abutment into the Centre of the channel under all flow conditions tested. Based on the experimental results,

optimum design settings for the vane angle and height, the most effective number of vanes, and the distance upstream for placement of the first vane were determined.

Flokstra (2006) developed a morphological simulation system to study the effects of submerged vanes on an alluvial bed. The simulation results matched well with the experimental data. Physical model tests, mainly in a flume with a fixed bed and one or more submerged vanes, were also conducted and discussed. Measurements focused on flow velocity downstream of the vanes and the lift and drag forces on the vanes. The morphological model, based on wing theory by Odgaard, accurately simulated bed level changes for the test cases, with tuning parameters within the expected range.

Gupta et al. (2007) attempted to use tapered submerged vanes in the Wapsipinicon River bend in the USA and outside a new water intake in Nepal. The taper angle is the angle made by the leading edge of the vane with horizontal in a vertical plane. A tapered vane also induces something called the vortex lift (at high angles of attack) which is a secondary lift caused by a reattachment of the flow due to a spanwise leading edge vortex. The aptitude of the vane or foil to form this leading-edge vortex is highly dependent on the shape of the leading edge, generally a sharp leading edge will form a strong vortex whilst a rounded leading edge will form a weaker vortex (with the vortex Centre further downstream). In this paper, the effect of taper angle variation within a range of 33.7° to 45°on moment of momentum (MOM) has been investigated and it is observed that for a given optimal angle of attack as 40°, MOM can be further increased by keeping the taper angle as 33.7°.

Ghorbani and Kells (2008) studied the effect of a submerged vane as a countermeasure technique on local scour at a cylindrical pier. For this purpose, several heights of the vane, angles of orientation, and flow depths were evaluated, all for a constant Froude number. It was found that for an isolated vane, a greater depth of scour was experienced at higher flow rates and/or at greater flow depths with all vane combinations and orientations. It was also found that not all types of single isolated submerged vanes can be used as a scour countermeasure at cylindrical piers. The highest reduction in scour was achieved for an angle of 8.5° and a flow depth of 20 cm for a vane height equal to 0 cm while the most exacerbated case occurred with a vane angle of 18.5° and a flow depth of 10 cm for a vane height equal to 5.7 cm. So, it was concluded that for vane heights other than the 0 cm investigated in this study, an increasing scour depth is experienced at cylindrical piers compared to the control. For two vanes attached to the pier, a reduction of 87.7% in scour depth next to the pier was achieved for a constant flow depth (i.e., 15 cm), a constant vane angle (i.e., 18.5), and at 0 distance upstream from the pier for a vane height of 0 cm.

Behbahan (2011) investigated the effect of vane shapes on riverbank protection, a series of experiments on a straight canal with 20 m length; 0.7 m width, and 0.6 m depth were carried out using galvanized vanes in different shapes. These vanes with 1 mm thickness, 15 cm width and 13 cm height were installed on the canal bed such that the height of the vanes above the river bed was 7 cm. Three types of same-size vanes were used in these experiments. The first type was flat, which was installed at an angle of attack of 20° to the flow direction. The second type was angled vanes with an angle of 20° in the middle of the vanes, which were installed such that the first- half of these vanes were in an angle of attack of 10° and the second half in 30° of flow direction. The third type includes two parts flat and cured, these vanes were installed such that the flat part was at an angle of 20° with flow direction. Using measured

data, the canal and related vanes were modeled by ANSYS and SURFER software. Results show that the curved and angled vanes compared to flat vanes are more effective in river-bank protection by 35% and 20% respectively.

Bejestan and Azizi (2012) performed physical hydraulic model testing to investigate four shapes of vanes: a simple rectangular vane, and three vanes that are beveled at the leading edge in 30°, 45°, and 60° to the base, respectively. The experiments showed that cutting the leading edge of the vanes reduces the local scour around the vanes. Maximum scour depth reduction occurred due to the maximum chamfer at the leading edge of the vanes. Based on the results, cutting the leading edge of the vanes was a performance-improving and cost-saving modification, too.

Bejestan et al. (2015) studied submerged vanes as a countermeasure for bridge safety and riverbank erosion. The study aimed to evaluate the performance of submerged vanes near abutments. Tests were conducted with and without vanes, examining different positions and angles. A single vane at the upstream nose of an abutment was most effective in reducing and shifting scour holes. The optimal vane angle was found to be 40°, with the technique achieving up to 95% efficiency under certain flow conditions.

Few contributions are focused on scouring downstream of instream structures like Pagliara and Palermo (2008), Pagliara et al. (2009, 2011, 2012), Bhuiyan et al. (2007), Scurlock et al. (2011, 2012a, b), Pagliara and Kurdistani (2013), Pagliara et al. (2013, 2014a, b), Pagliara and Kurdistani (2014) compared scour hole characteristics downstream of the cross vane and W-weirs, highlighting similitudes and differences in the respective ranges of application. The main purpose of this paper is to experimentally analyze the scour morphology and characteristics downstream of log deflectors in horizontal straight channels.

Some of the very important and significant works on scours due to different vanes (i.e. log vane, cross vane, deflector, W-weir vane etc.) are reported below:

Pagliara et al. (2014) used Log-Vane as a grade-control structure to stabilize riverbed and river banks. The purpose of this paper is to study the scour phenomena downstream of Log-Vanes in straight rivers. The main goal is to obtain design equations to determine the main scour parameters and the scour morphology along with types of scour formation. All the experiments have been carried out in a horizontal channel and in clear water conditions. Log-Vanes made of wood, with different heights and vane angles, were tested. Different hydraulic conditions including densimetric Froude numbers, water drops, and tail water values were tested. Results show that the tail water depth is an important variable in determining the maximum scour depth. The vane angle results are an important parameter to predict the scour parameters. Dimensional analysis allows us to derive design equations useful to estimate the maximum scour depth, maximum length of the scour and maximum height and length of the dune. The results show that by increasing η, all the scour geometry parameters increase. Pagliara et al. (2014) compared scour downstream of two different low-head control structures i.e. Log-Vane and J Hook vane. The analysis contains the results of laboratory experiments conducted at the PITLAB hydraulic laboratory of the University of Pisa and a detailed comparison of scour hole characteristics, highlighting similitudes and differences in

the respective ranges of application. All tests have been done in clear water conditions using uniform sand as channel bed material.

The main scour parameters for different combinations of hydraulic conditions downstream of Log-Vanes and J-Hook Vanes have been studied. Results showed that tailwater is an important variable in predicting the maximum scour depth. The effect of the vane installation angle θ on the maximum scour depth is negligible. The results show that by increasing η, the maximum scour depth increases while increasing tailwater depth decreases the maximum scour depth. Results showed that the vane installation angle θ also is not an effective parameter on scour formation. Scour typology included two major types of scours. Type A where "the dune is developed beside the scour hole close to the channel bank" and Type B where "the dune is developed along the scour hole towards the center of the channel". The combination of the results of Pagliara et al. (2013) with Log-Vane observed data indicates that there are three zones for each morphology type. Zone 1: long scour-long ridge; Zone 2: short scour-short ridge and Zone 3: short scour-short ridge.

Pagliara et al. (2015) investigated the scour phenomena downstream of log deflectors in straight horizontal channels. The main goal was to obtain design equations to predict the main scour parameters and describe the scour morphology. All the experiments have been carried out in a horizontal channel and in clear water conditions. Log deflectors with different heights and angles were tested. Different hydraulic conditions including densimetric Froude numbers, water head drops, and tailwater values were studied. Results show that the tailwater depth and deflector angle are important variables in determining the scour parameters. Dimensional analysis leads to design equations to estimate the maximum scour depth, maximum length of the scour, and maximum height and length of the dune. Two types of scour morphology downstream of log deflectors have been defined.

Ferro et al. (2019) introduced a new river restoration technique for bank protection and restoration of meander bends by combining a permeable groin with a triangular vane. Nine different combinations of permeable groins with triangular vane including three different effective lengths and three angles of vane were investigated in a 180° mild laboratory flume bend in clear water conditions. Based on experimental tests, scour geometrical patterns were analyzed, classified, and compared with each other. This analysis showed that a triangular vane dramatically enhances the performance of the permeable groin to protect the outer bank from erosion. Then, using Buckingham's theorem of the dimensional analysis and the incomplete self-similarity (ISS) condition, generalized functional relationships for estimating scour main characteristics around an enhanced permeable groin (EPG) were deduced. This analysis showed that scour patterns depend on the upstream densimetric particle Froude number and the ratio between the effective lengths of the triangular vane and the permeable groin. The results showed that scour geometric characteristics estimated by the proposed equations agree reasonably well with the experimental values.

Several experimental studies focusing on the scour downstream of grade-control structures can be found in the literature. Przedwojski (1995) investigated the effect of groins on river scour processes. He showed that the maximum scour depth occurs when the groin is located downstream of the bend apex. Pagliara et al. (2015a, b, c) and Pagliara and Kurdistani (2017) studied the scour morphology in straight rivers downstream of different types of wood-made structures such as log-vane, log-deflector, and log-frame deflector structures. Kurdistani

and Pagliara (2015) conducted a series of experiments focusing on the installation angle of woody structures and analyzed the scour occurrence close to the channel bank. Pagliara and Kurdistani (2015) studied the main scour characteristics and morphology downstream of J-hook vanes in a curved channel, showing that the values of all scour parameters decrease with the tailwater depth and the bend radius. Pagliara et al. (2016) studied scour morphology downstream of rock-made sills in curved and straight horizontal channels. Pagliara and Kurdistani found that using log-frame deflectors instead of log deflectors results in more efficient riverbank protection. Kurdistani and Pagliara (2017) experimentally studied the effect of channel curvature and the structure orientation on scour morphology downstream of cross-vanes. Kurdistani et al. (2018) showed that the meandering process in rivers is deeply influenced by the distance between log-frame deflectors when located at both left and right riverbanks.

2.2. Research gap

Several laboratory researches have been done on log vane, however, no literature has comprehensively covered all the literature data and formulas developed in literatures for a comparative and robust analysis. Pagliara et al. (2014) compared their formula with the J-hook data of Pagliara et al. (2013). In the very next year, Pagliara et al. (2015) compared their formula with the cross-vane data suggested by Pagliara et al. (2013). Additionally, Pagliara and Kurdistani (2016) used the spur dike data provided by Khunle et al. (1999, 2002) to compare their formula. In this field, a greater amount of field data is required so that anyone can easily validate their work.

2.3 Need of the work

- Studying equilibrium scour around log vanes can help fill gaps in understanding the unique mechanisms and characteristics of sediment erosion and deposition, contributing to improved design and management strategies for riverine structures.
- Understanding equilibrium scour around log vanes is crucial for optimizing their design and effectiveness in river engineering and restoration projects.
- Researching equilibrium scour around log vanes can aid in devising strategies to mitigate the risk of scour-related failures, enhancing infrastructure safety.
- Developing reliable and accurate methods for predicting equilibrium scour around log vanes is essential for effective design and management. A thesis can focus on refining existing prediction models or developing new methodologies tailored specifically to log vane structures.
- In summary, conducting a thesis on equilibrium scour around log vanes can address important research gaps, contribute to engineering practice and environmental management, and provide valuable insights into the behavior of river systems.

Chapter 03

Local scour characteristics around log vane

3.1. Local scour mechanism

The boundary layer flow passed a submerged vane undergoes a three-dimensional separation. This separated shear layer rolls up along the obstruction to form a vortex system in front of the element which is swept downstream by the open channel flow. Viewed from the top, this vortex system has the characteristic shape of a horseshoe and thus is called a horseshoe vortex (**Fig. 3.1.**). The formation of the horseshoe vortex and the associated downflow at the upstream part of the submerged vane dyke results in increased shear stress and hence a local increase in sediment transport capacity of the flow. This leads to the development of a deep scour hole at the upstream part of the vane, which in turn, changes the flow pattern causing a reduction in shear stress by the flow thus reducing its sediment transport capacity. The temporal variation of scour and the maximum depth of scour at vane dykes therefore mainly depend on the characteristics of flow, vane orientation, and river/channel bed material. The formation of the horseshoe vortex and the associated downflow cause scour at the vane dike, bridge pier, abutment, and spur dike.

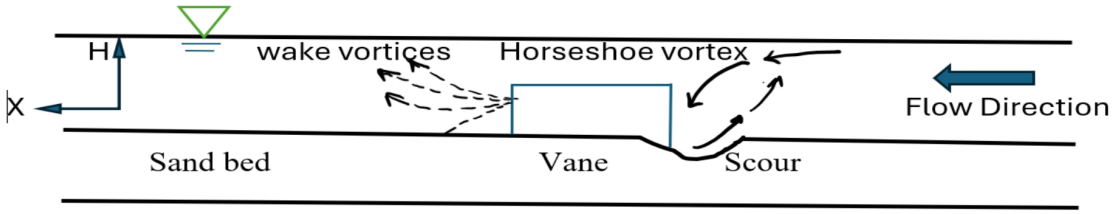


Fig. 3.1. Flow structure around submerged vane (side view)

3.1.1. Wake vortex

Wake vortices form at the downstream side of the vane and are the result of flow separation at the sides of the vane (**Fig. 3.1.**). These are called cast-off vortices and have vertical axes. One vortex develops on one side, sheds away, and is moved downstream. Immediately, other forms on the other side, finally shedding also. The wake vortices dissipate as they move down the stream. The frequency of the vortex shedding is directly proportional to the approach flow velocity and inversely proportional to the effective width of the vane. Information on the wake vortex scour is particularly scanty. As a wake vortex scour occurs downstream of the pier, it has little or no destructive potential. Because the horseshoe vortex scour occurs at the downstream face of the vane and thus can threaten the underwater constructions, this type of

scour has been given considerable theoretical thought by Bruesers et al. (1977) and is well documented in the model studies given by Raudkivi (1986). Knowledge about wake vortex scour due to bridge piers has come mainly from a few laboratory tests Melville (1975). To describe the scouring action, Melville wrote “Each of the concentrated vortices acts with its low-pressure center as a vacuum cleaner, picking up material from the bed, which is then transported downstream”. There is concern that the holes may enlarge or move upstream endangering the vane dykes and the bridges. We have made observations in the vicinity of the scour holes and have concluded that, in each case, the scour is caused by two streams of wake vortices from adjacent vanes intersecting downstream. The vortices that result from the two conflicting velocity fields create local scour. At one bridge, the scour is enhanced by the vortices that occur at the confluence of the main channel and its side channel. This is known as confluence scour.

3.1.2. Horseshoe vortex and downflow

The flow deflected by sediment-embedded vane dike causes scour at its foundations. Scour may endanger the stability of the complete vane dyke system. In riverbank protection, rectangular-shaped vane dikes are commonly used. Due to the similar flow structures of airflow around circular bodies in wind tunnels, the basic research concerns flow visualization in aerodynamics. The main flow features involve a vertically deflected flow along the upstream edge of the vane, a horseshoe vortex system upstream of the vane, a flow separation beside the vane and a wake zone downstream of it shown in **Fig. 3.2**. In general, the pressure distribution beneath the horseshoe vortex system is measured and the horseshoe vortex position is determined experimentally. For all the flow conditions, a horseshoe vortex system consists of at least two vortices.

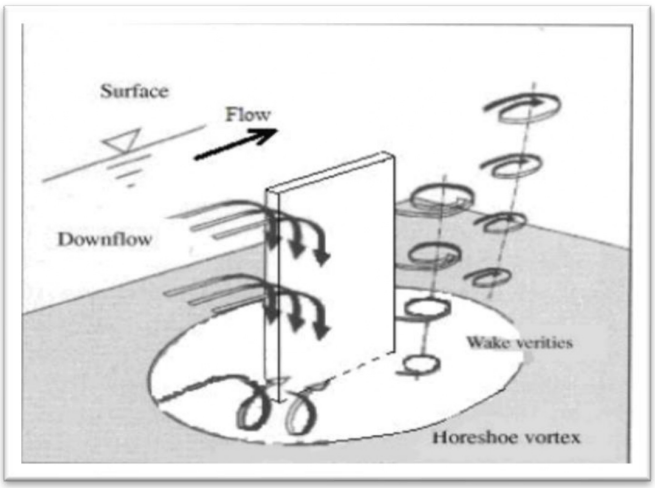


Fig. 3.2. Vortex formation around Vane.

3.2. Classification of scour parameters

3.2.1 Flow Intensity

Flow intensity is defined as the ratio of the shear velocity (u^*) to the critical shear velocity (u^*_c) or the ratio of the mean approach velocity to the critical mean velocity (Melville and Chiew, 1999). Under clear water conditions, the local scour depth in uniformly graded sediment increases almost linearly with the velocity and reaches a maximum at the threshold velocity (Melville and Coleman, 2000). The maximum scour depth is reached when the ratio u^*/u^*_c is equal to one and the corresponding maximum scour depth is called the threshold peak. As the velocity exceeds the threshold velocity, the local scour depth in uniform sediment first decreases and then increases again to a second peak, but the threshold peak is not exceeded provided the sediment is uniform.

3.2.2. Flow Depth

In the past, the influence of flow depth on the scour depth has been discussed by many authors like Breusers and Raudkivi (1991), Melville and Coleman (2000) etc. The presence of the vane dike in a channel causes a surface roller around the vane and a horseshoe vortex at the downstream base of the vane. Flow depth affects local scour depth when the horseshoe vortex is affected by the formation of the surface roller (or bow wave) that forms at the leading edge of the vane. The two rollers that are the bow wave and the horseshoe vortex rotate in opposite directions. In principle, if there is no interference between the two rollers, the local scour depth does not depend on the flow depth but depends only on the vane shape and size. In such an instance, often called deep flow, the local scour is said to occur at narrow vanes. As the flow depth decreases, the surface roller becomes relatively more dominant and causes the horseshoe vortex to be less capable of entraining sediment. Therefore, for shallower flows, the local scour depth is reduced. Subsequently, in a very shallow flow, the local scour is dependent on the flow depth and the local scour is said to occur at a wide pier.

3.2.3 Effective Width of Vane

Previous experiments have clearly shown that it is possible to relate the scour depth to the size of the vane. This observation can be explained physically by the fact that scouring is due to the horseshoe vortex system whose dimension is a function of the diameter of the pier. It has also been observed that the horseshoe vortex, being one of the main scouring agents, is proportional to the vane Reynolds number (Re), which in turn is a function of the vane effective width. For the same value of mean approach flow velocity, therefore, the scour depth is proportional to the vane effective width. The influence of vane size and angle of incidence on the local scour depth is of interest when data from the laboratory are interpreted for field use. Under clear water conditions, vane size influences the time taken to reach the

ultimate scour depth but not its relative magnitude (ratio of scour depth to effective vane width), if the influence of relative depth, and relative grain size (ratio of effective vane width to median grain diameter) D/d_{50} on the local scour depth are excluded. They also believed that the volume of the local scour hole formed around the downstream half of the perimeter of the vane may be proportional to the power of the effective vane width. The larger the effective vane width the larger the scour hole volume and the longer the time taken for the development of the scour hole for a given shear stress ratio. Hardly any study states that the effect of scour due to vane is almost like the effect of the pier. So, we can consider that the effective width of the vane may also have the same impact as that of the pier width.

3.2.4 Sediment Size

The effects of the grain size and the density of the sediment material are often expressed as a function of the critical flow velocity for the initiation of sediment motion. From the pier scour study, it is observed that a sediment size of $d_{50} \leq 0.7$ mm leads to a formation of ripples, whereas the sediment size of $d_{50} \geq 0.7$ mm does not cause ripples. The results for grain sizes which lead to the formation of ripples ($d_{50} \leq 0.7$ mm) are different from those for larger grain sizes for which ripples do not form ($d_{50} \geq 0.7$ mm). For non-ripple forming sediments ($d_{50} \geq 0.7$ mm), experiments can be run successfully with a flow condition, $u^* \sim 0.95u^*_c$, without the upstream bed being disturbed by the approach flow, whereas with finer sands ($d_{50} < 0.7$ mm) a flatbed cannot be maintained for the same flow condition. Therefore, if the sediment is uniform sand with grain size $d_{50} < 0.7$ mm, a flatbed cannot be maintained near the threshold shear stress condition because ripples will develop, with a small amount of general sediment transport taking place to replenish some of the sand getting scoured at the vane. Thus, true clear water scour conditions cannot be maintained in this case.

3.2.5 Flow Froude Number

The flow Froude number is a dimensionless number comparing inertia and gravitational forces (**Eq. 3.1.**). It may be used to quantify the resistance of an object moving through water and compare objects of different sizes. Named after William Froude, the Froude number is based on the speed/length ratio as defined by him.

$$\mathrm{Fr} = \left(\frac{V}{\sqrt{\mathrm{g}\, y}} \right) \tag{3.1}$$

where, V is a characteristic velocity and y is the approach depth for rectangular cross-sections, For Fr< 1, the flow is called a subcritical flow, further for Fr > 1 the flow is characterized as supercritical flow. When Fr ≈ 1 the flow is denoted as critical flow.

3.2.6 Densimetric Froude Number

The Deinsimetrric Froude number or particle Froude number is defined as $\mathrm{F_d} = \left(\frac{Q'}{lH\sqrt{\mathrm{g}' d_{50}}} \right)$

where g' is the reduced gravity $g' = \left(\frac{\rho_s - \rho_w}{\rho_w} \right) = g\left(\frac{\rho_s}{\rho_w} - 1 \right)$, g is the acceleration due to gravity, ρ_s is the density of sediment particles and ρ_w is the density of water, Q is the discharge of the river and $Q' = Q\left(\frac{b}{B} \right)$.

It is clearly seen that if we neglect the effect of the *b/B* ratio, then the remaining term is also referred to as the Deinsimetric Froude number. Pagliara et al. (2015) considered this effect in some cases or sometimes neglect it. So, in my present study, considered both cases. when the effect of *b/B* is not considered, then it is represented by $\mathrm{F'_d}$.

Chapter 04

Synthesis of existing research: data, methods and equations

4.1. Review of experimental procedure

Pagliara and Kurdistani (2016) conducted 17 experiments in a straight horizontal channel (0.5 m wide, 15 m long, and 0.5 m high) at the Hydraulic Laboratory of the University of Pisa. Stable inflow was provided by an overhead tank, and discharge was measured with ±0.0001 m^3/s precision using a magnetic current meter. Water surface profiles were monitored at the start and hourly during each test using a point gauge with ±0.0001 m accuracy. Bed morphology was surveyed at the end of each test using a laser scanner (HDS-4500) with ±0.001 m precision, including key hydraulic and geometric parameters. Uniform sand (G_s = 2.60, d_{50} = 1.77 mm, σ = 1.26) was used as bed material. Channel bed leveling was performed before each experiment, and bed material mixing was done post-test to maintain gradation consistency. The study utilized an inception Froude number, derived from Shields' criterion, to regulate clear water conditions. The inception Froude number accounts for the relationship between fluid dynamics, sedimentology, and relative flow depth, increasing with relative flow depth. Tests ran until equilibrium bed conditions were reached (1-3 hours), with approaching Re varying between 82000 to 198000 indicating turbulent flow conditions. All experiments were conducted under subcritical flow and clear water conditions.

Pagliara et al. (2015) conducted experiments in a horizontal channel at the hydraulic laboratory of the University of Pisa, measuring 0.8 m wide, 20 m long, and 0.75 m deep. Stable flow was supplied by an overhead tank, and discharge was measured with a calibrated tank with a precision of ±0.0001 m^3/s. An ultrasonic distance meter with a precision of 0.001 m was used to record water surface profiles. Single-wing deflectors with *b/B* ratios ranging from 0.33 to 0.25 were used, made of tree branches and stabilized with two attached stones. The channel bed was carefully levelled before each experiment. The sand particles used had a uniform size of d_{50} = 1.7 mm, with G_s = 2.60 and σ = 1.26. Two series of experiments were conducted: one with single-wing deflectors at deflector angles (θ) of 30° and 60°, and another with double-wing deflectors. Tests were conducted until an equilibrium bed condition was reached, typically within 1 to 3 hours, ensuring no bed material movement. All experiments were conducted under clear water conditions.

Pagliara et al. (2014) conducted experiments that were carried out in a horizontal channel 0.8 m wide, 20 m long and 0.75 m deep located in the PITLAB hydraulic laboratory of the University of Pisa. Stable inflow was supplied by an overhead tank. The flow discharge was measured using a calibrated tank with a precision of ±0.0001 m^3/s. An ultrasonic distance

meter Baumer sensor with a precision of 0.001m has been used to read the water surface profile and the bathymetry of the mobile bed. Uniform non-cohesive sand with a σ = 1.16, G_s = 2.60 and d_{50} = 1.70mm was used. At the beginning of each experiment, the channel bed was carefully levelled. All the tests have been conducted in clear water conditions. Three series of experiments were carried out. The first series included tests on Log-Vane in a horizontal channel with θ=30° for different values of the height of the structure, discharge and Δy. The second and third series of experiments were done for Log-Vanes with vane angles of 60° and 90° respectively. The duration of tests was long enough to reach an equilibrium bed condition depending on the single test (between 1 and 3 h).

4.2. Ranges of different Author data

In this analysis, a total of 88 numbers of data was used in different experiments which are present in **Table 4.1.** along with their ranges.

Table 4.1. Ranges of experimental data

Literature	Range	Q	V	y	h_{tw}	Δy	B	H	l	b	θ	F_d	d_{50}	σ	G_s	Z_m
		m^3/s	m/s	m	m	m	m	m	m	m	-	-	m	-	-	m
Pagilara and Kurdistani (2016)	min	0.02	0.54	0.07	0.06	0.00	0.50	0.06	0.33	0.17	30.00	0.94	0.00	1.26	2.60	0.05
	max	0.06	0.72	0.16	0.16	0.01	0.50	0.09	0.33	0.17	30.00	3.98	0.00	1.26	2.60	0.07
Pagilara et al. (2014)	min	0.00	0.15	0.02	0.02	0.00	0.80	0.04	0.27	0.27	90.00	0.25	0.00	1.16	2.60	0.03
	max	0.06	0.43	0.16	0.16	0.01	0.80	0.09	0.53	0.27	150.00	3.43	0.00	1.16	2.60	0.11
Pagilara et al. (2015)	min	0.01	0.25	0.03	0.02	0.00	0.80	0.04	0.23	0.20	30.00	0.21	0.00	1.16	2.60	0.01
	max	0.06	0.43	0.16	0.16	0.01	0.80	0.09	0.53	0.26	60.00	3.46	0.00	1.16	2.60	0.08
Present study	min	0.00	0.15	0.02	0.02	0.00	0.50	0.04	0.23	0.17	30.00	0.21	0.00	1.16	2.60	0.01
	max	0.06	0.72	0.16	0.16	0.01	0.80	0.09	0.53	0.27	150.00	3.98	0.00	1.16	2.60	0.11

4.3. Functional relationship used in literature to find scour

Pagliara et al. (2014)

Dimensional analysis has been applied to obtain analytical functions in order to predict the main scour parameters downstream of Log vanes such as maximum scour depth, maximum scour length, etc. For the maximum scour depth, the main variables are as follows:

$$\phi\left(Z_m, l, H, h_{tw}, B, \Delta y, Q, \rho_s, \rho, g, d_{50}, \theta\right) = 0 \tag{4.1}$$

The final formula suggested for the log vane is given below

$$\frac{Z_m}{H} = 1.6\left(\frac{h_{tw}}{H}\right)^{-0.5}(\eta)^{0.3} \tag{4.2}$$

where, η is the non-dimensional parameter.

Pagliara and Kurdistani (2013) and Pagliara et al. (2013) defined the non-dimensional scour parameter.

$$\eta = \left(\frac{\Delta y}{H}\right)\left(F_d{}^2\right) \tag{4.3}$$

From the equation, the non-dimensional scour parameter is the function of η and h_{tw}/H. Therefore, it can be represented as follows

$$\frac{Z_m}{H} = \phi_1\left(\frac{h_{tw}}{H}\right) \text{ and } \frac{Z_m}{H} = \phi_2(\eta)$$

Pagliara and Kurdistani (2016)

One of the most important scour morphological features downstream of grade-control structures is the value of the maximum scour depth. Maximum scour depth downstream of woody stream restoration structures is governed by the following functional relationship:

$$\phi_3\left(Z_m, l, H, h_{tw}, B, \Delta y, Q', \rho_s, \rho, g, d_{50}\right) = 0 \tag{4.4}$$

in which f is a functional symbol. Pagliara and Kurdistani (2013), based on dimensional analysis and incomplete self-similarity (Barenblatt, 1987) as it has also been used by D'Agostino and Ferro (2004) and Scurlock et al. (2012 *a*, *b*), presented the following nondimensional functional expression derived from above equation as follows

$$\frac{Z_m}{H} = \phi_4\left(\frac{h_{tw}}{H}, F_d, \frac{l}{B}, \frac{\Delta y}{H}\right) \tag{4.5}$$

Based on dimensional analysis and experimental data, the general **Eq**. **4.6.** has been derived to predict the maximum scour depth downstream of log-deflectors in straight channels that is valid for different values of tailwater depths as follows.

$$\frac{Z_m}{H} = 6.6\left(\frac{h_{tw}}{H}\right)^{-1}\left(\frac{l}{B}\right)(\eta)^{0.7} \tag{4.6}$$

From the equation, the non-dimensional scour parameter is the function of η, *l/B,* and h_{tw}/H. So, it can be represented as follows

$$\frac{Z_m}{H}=\phi_1\left(\frac{h_{tw}}{H}\right),\ \frac{Z_m}{H}=\phi_5\left(\frac{l}{B}\right)\text{ and }\frac{Z_m}{H}=\phi_2(\eta)$$

Pagliara et al. (2015)

Dimensional analysis has been applied to obtain analytical functions fin order to predict the main scour parameters downstream of Log vanes such as maximum scour depth, maximum scour length, etc. For the maximum scour depth, the main variables are as follows:

$$\phi\left(Z_m,l,H,h_{tw},B,\Delta y,Q,\rho_s,\rho,g,d_{50},\theta\right)=0 \tag{4.1}$$

in which ϕ is a functional symbol. Pagliara and Kurdistani (2013), based on dimensional analysis and incomplete self-similarity (Barenblatt, 1987) as it has also been used by D'Agostino and Ferro (2004) and Scurlock et al. (2012a,b), presented the following nondimensional functional expression derived from above equation as follows

$$\frac{Z_m}{H}=\phi_4\left(\frac{h_{tw}}{H},F_d,\frac{l}{B},\frac{\Delta y}{H}\right) \tag{4.5}$$

Based on dimensional analysis and experimental data, the general Eq. (4.6) has been derived to predict the maximum scour depth downstream of log-deflectors in straight channels that are valid for different values of tailwater depths as follows.

$$\frac{Z_m}{H}=6.6\left(\frac{h_{tw}}{H}\right)^{-1}\left(\frac{l}{B}\right)(\eta)^{0.7} \tag{4.6}$$

From the equation, the non-dimensional scour parameter is the function of η, l/B and h_{tw}/H. So, it can be represented as follows

$$\frac{Z_m}{H}=\phi_1\left(\frac{h_{tw}}{H}\right),\ \frac{Z_m}{H}=\phi_5\left(\frac{l}{B}\right)\text{ and }\frac{Z_m}{H}=\phi_2(\eta)$$

In all the cases mainly two formulas are suggested in which three functional groups is used which are shown just above the paragraph.

Table 4.5. The functional relationship along with the formula.

Sl. No.	Research groups	Formula	Functional groups
1	Pagliara et al. (2014)	$\frac{Z_m}{H}=1.6\left(\frac{h_{tw}}{H}\right)^{-0.5}(\eta)^{0.3}$	$\frac{Z_m}{H}=\phi_1\left(\frac{h_{tw}}{H}\right)$ $\frac{Z_m}{H}=\phi_2(\eta)$
2	Pagliara and kurdistani (2016)	$\frac{Z_m}{H}=6.6\left(\frac{h_{tw}}{H}\right)^{-1}\left(\frac{l}{B}\right)(\eta)^{0.7}$	$\frac{Z_m}{H}=\phi_1\left(\frac{h_{tw}}{H}\right)$ $\frac{Z_m}{H}=\phi_2(\eta)$, $\frac{Z_m}{H}=\phi_5\left(\frac{l}{B}\right)$

3	Pagliara et al. (2015)	$\frac{Z_m}{H}=6.6\left(\frac{h_{tw}}{H}\right)^{-1}\left(\frac{l}{B}\right)(\eta)^{0.7}$	$\frac{Z_m}{H}=\phi_1\left(\frac{h_{tw}}{H}\right)$ $\frac{Z_m}{H}=\phi_2(\eta)$, $\frac{Z_m}{H}=\phi_5\left(\frac{l}{B}\right)$
4	Present Study	$\frac{Z_m}{l}=f_9\left(\frac{V^2}{l\,\mathrm{g}},\frac{h_{tw}}{l},\frac{B}{l},\frac{b}{l},\frac{H}{l},F_d,\frac{\Delta y}{l}\right)$ $\frac{Z_m}{H}=f_{10}\left(\frac{V^2}{H\,\mathrm{g}},\frac{h_{tw}}{H},\frac{b}{l},\frac{l}{H},\frac{B}{H},\frac{b}{H},F_d,\frac{\Delta y}{H}\right)$	Totaal 13 numbers non-dimensional parameter is used.

Chapter 05

Objectives and methodology

5.1. Objectives

The main purpose of this study is to develop a new formula for equilibrium scour around a log vane under clear water conditions by analyzing the different non-dimensional parameters, which may be used to compare the other literature formulas suggested by different researchers.

- To analyze the influential parameters influencing the equilibrium scour depth of a log vane through dimensional analysis.
- The main objective of my present study was to develop a new formula for finding equilibrium scour near the downstream of the log vane on the river bed.
- To assess the findings derived from the formulated equation in this current study against existing formulas found in literatures.
- To evaluate the formula from the present study as well as from the literature study.

5.2. Methodology

- **Research paper Collection**: The initial step involved a thorough search across reputable databases such as Research gate, Scopus, Google, and Google Scholar to compile a diverse range of papers relevant to vane dykes and log vanes.
- **Data and formula collection:** From the different research papers raw data and formulas are extracted for future analysis.
- **Preliminary Screening**: Raw data goes through several screening procedures on the basics of types of scours (i.e. clear water or live bed scour) or type of vane used for the study. In my present study data was collected for single arm log vane structure for findings of formula using.
- **Parameter Identification**: Key parameters such as vane (log) dike dimensions (length, height, vertical projection from river bed), Maximum scour depth, fluid properties (density, kinematic viscosity), hydraulic factors (acceleration due to gravity, depth of flow, flow velocity, critical flow velocity), geometric factors (Vane dike orientation angle, median diameter of sediment, sediment density), and flow characteristics (Froude number, Geometric Standard Deviation) were identified. This step ensured a comprehensive understanding of the variables affecting scour depth.
- **Dimensionless Framework**: Dimensionless analysis was conducted to reduce the number of parameters involved in the study of log-vane scour depth. This process involved

transforming the dimensional parameters into dimensionless forms using relevant scaling parameters. By doing so, the analysis aimed to simplify the model and improve its generalizability across different conditions. This technique allowed researchers to focus on the essential characteristics influencing scour depth while minimizing the complexity of the model. In this study, we try to increase the dependency of different parameters with scour depth. For this dimension analysis was done firstly by taking the length of vane(l) as a repeating variable and secondly same analysis was done using the height of vane(H) as a repeating variable. Above both cases number of non-dimensional parameters remains 12 (including the non-dimensional scour parameter).

- **Parameters reduction through physical understanding**: By going through the datasheet, a few parameters can easily be neglected by observing their range. In this method, 4 parameters were reduced in case-1 and 3 in case-2. Thus, the number of parameters remaining is 8 and 9, respectively.
- **Dimensionality Reduction**: Six dimensionality reduction methods (Pearson Correlation coefficient, Spearman's rho correlation coefficient, Kendall's tau b correlation coefficient, Forward, Backward, Removed and Stepwise regression) were applied to reduce the non-dimensional parameters for future use. Further, a few non-dimensional parameters were reduced by using the Subset regression method. This step aimed to refine the model and improve its efficiency.
- **Data Visualization**: Graphical representations were utilized to validate the collected data against empirical formulas, ensuring the correctness and consistency of the dataset and providing visual insights into the relationship between variables.
- **Formula Development**: A new formula was predicted using the non-linear regression method. Dozens of formulas were predicted, of which one was suggested for further use. The developed formula was then validated using different formulas suggested in the paper. This process aimed to predict the formula with high accuracy and reliability.

- **Comparison and Evaluation**: The predicted formula was compared with two empirical formulas from the literature using data from the preliminary screening and statistical metrics like R^2, SSE, RMSE, %In etc.

5.3 Statistical Influence Indicator

Statistical analysis is used to evaluate the provided accuracy of the literature formulas and newly predicted formulas. Various cost and beneficial criteria are used to assess how well the estimated and observed Z_m values agree. Now, the following formulas have been used to define the various performance indices such as R, R^2, RMSE and SSE. Here, (Z_m/l) o is the observed values and (Z_m/l) c is the computed and, n represents the total number of input samples.

Coefficient of Correlation (R)

R is a statistical measure of how well the regression line approximates the real data points. It ranges from 0 to 1, where 0 indicates the model fails to explain any of the variability of the response data around its mean, 1 indicates the model perfectly explains all the variability of the response data around its mean and 0<R<1 indicates the model explains some proportion of the variability in the response data around its mean. The closer R is to 1, the better the model fits the data. The formula is:

$$R = \left\{ \frac{\sum_{i=1}^{n} \left\{ \left(\frac{Z_m}{l} \right)_{oi} - \overline{\left(\frac{Z_m}{l} \right)_{o}} \right\} \left\{ \left(\frac{Z_m}{l} \right)_{ci} - \overline{\left(\frac{Z_m}{l} \right)_{c}} \right\}}{\left[\sum_{i=1}^{n} \left(\left(\frac{Z_m}{l} \right)_{oi} - \overline{\left(\frac{Z_m}{l} \right)_{o}} \right)^2 \right]^{0.5} \sum_{i=1}^{n} \left\{ \left(\frac{Z_m}{l} \right)_{ci} - \overline{\left(\frac{Z_m}{l} \right)_{c}} \right\}^2} \right\} \tag{5.1}$$

Coefficient of Determination (R^2)

R-squared is a statistical measure of how well the regression line approximates the real data points. It ranges from 0 to 1(Legates et al.1999), where 0 indicates the model fails to explain any of the variability of the response data around its mean, 1 indicates the model perfectly explains all the variability of the response data around its mean and $0<R^2<1$ indicates the model explains some proportion of the variability in the response data around its mean. The closer R^2 is to 1, the better the model fits the data. The formula is:

$$R^2 = \left\{ \frac{\sum_{i=1}^{n} \left\{ \left(\frac{Z_m}{l} \right)_{oi} - \overline{\left(\frac{Z_m}{l} \right)_{o}} \right\} \left\{ \left(\frac{Z_m}{l} \right)_{ci} - \overline{\left(\frac{Z_m}{l} \right)_{c}} \right\}}{\left[\sum_{i=1}^{n} \left(\left(\frac{Z_m}{l} \right)_{oi} - \overline{\left(\frac{Z_m}{l} \right)_{o}} \right)^2 \right]^{0.5} \sum_{i=1}^{n} \left\{ \left(\frac{Z_m}{l} \right)_{ci} - \overline{\left(\frac{Z_m}{l} \right)_{c}} \right\}^2} \right\}^2 \tag{5.2}$$

Root Mean Square Error (RMSE)

RMSE is a measure of the differences between values predicted by a model or an estimator and the observed values. It is calculated by taking the square root of the average of the squared differences between the predicted and observed values. RMSE values typically range from 0 to infinity (Willmott, 1981), with lower values indicating better model performance. The formula is

$$\text{RMSE} = \sqrt{\sum_{i=1}^{n} \frac{\left\{\left(\frac{Z_m}{l}\right)_{ci} - \left(\frac{Z_m}{l}\right)_{oi}\right\}^2}{n}} = \sqrt{\sum_{i=1}^{n} \frac{SSE}{n}} = \sqrt{\sum_{i=1}^{n} MSE} \qquad (5.3)$$

where, SSE= Sum of squares error
MSE=Mean squared error

Chapter 06

Dimensional analysis

6.1. Analysis of scouring parameters

The designer focuses on the equilibrium depth, Z_m for vane dike scouring. This depth is reached after enough time has passed (say 2 to 5 hours). Z_m is measured below the bed level. The study is limited to Log-vane structures in steady, uniform river flows. Many factors can affect scouring.

Variables characterizing the fluid:

- g acceleration due to gravity,
- ρ density of the water, and

Variables characterizing the bed material:

- ρ_s density of the sediment.
- σ Geometric Standard Deviation/Sediment Gradation,
- d_{50} Median Grain Size, and

Variables characterizing the flow:

- h_{tw} depth of water at d/s,
- Δy Difference between u/s and d/s water level
- V mean velocity of flow, and
- F_d Densimetric Froude Number.

*V*ariable characterizing the Flume property:

- B Width of the flume.

Variables characterizing the Vane dike:

- l its length,
- b Projection of vane from the river bank.
- H Height of the vane

and

- θ its orientation angle

6.2 Dimensionless Analysis

Equilibrium scour depth Z_m can be a function of

$$f(Z_m, \rho, g, h_{tw}, V, d_{50}, \rho_s, l, b, H, \theta, F_d, \sigma, B, \Delta y) = 0 \qquad (6.1)$$

where, $Z_m$is scour depth at sufficient elapsed time and the dimension of Z_m is $[L]$or $\left[M^0 L^1 T^0\right]$

ρ is fluid density for flow which has a dimension of $\left[M^1L^{-3}\right]$ or $\left[M^1L^{-3}T^0\right]$

$[L]$

g is the gravitational acceleration which has a dimension of $\left[LT^{-2}\right]$ or $\left[M^0LT^{-2}\right]$

h_{tw} is depth of water at d/s; the dimension of h_{tw} is $[L]$ or $\left[M^0L^1T^0\right]$

V is approach flow velocity and the dimension is $\left[LT^{-1}\right]$ or $\left[M^0L^1T^{-1}\right]$

d_{50} is the median diameter of sediment which also has an also dimension of length $[L]$ or $\left[M^0L^1T^0\right]$

ρ_s is sediment density having a dimension like the dimension of $\rho$is $\left[ML^{-3}\right]$ or $\left[M^1L^{-3}T^0\right]$ or $[M^1L^{-3}T^0]$

l is the Vane dike length which has a dimension of $[L]$ or $\left[M^0L^1T^0\right]$

b is the Projection of vane from river bank which has a dimension of $[L]$ or $\left[M^0L^1T^0\right]$

H is the height of the dike which has a dimension of $[L]$ or $\left[M^0L^1T^0\right]$

θ is the Vane dike orientation angle which has a dimensionless of $\left[M^0L^0T^0\right]$

F_d is the Densimetric Froude Number which has a dimensionless of $\left[M^0L^0T^0\right]$

σ is Sediment gradation or Geometric Standard Deviation which has a dimensionless of $\left[M^0L^0T^0\right]$

B is the width of the channel which has a dimension of $[L]$ or $\left[M^0L^1T^0\right]$

For non-dimensional analysis, here we have considered the Buckinhhum π theorem method, but not considered the Rayleigh method as the number of variables is more than three (3) or four (4). Here θ, F_d, σ already non-dimensional. Here we have also considered the repeating variable as l, $V$and ρ, where l is the geometric property, V is the flow property and ρ is the fluid property. Here total number of parameters, n = 14 and the number of independent parameters, m = 3. Therefore, we obtain a total $(n-m=12-3=9)$ i.e. 9 numbers of π terms as follows

$$f_1(\pi_1,\pi_2,\pi_3.....,\pi_{n-m})=0$$

$$\text{So, } f_1(\pi_1,\pi_2,\pi_3.....,\pi_9)=0$$

After considering the repeating variable in the above-stated way the Pi $(\pi)the$ term looks like below-

$$\pi_1 = l^{a1}V^{b1}\rho^{c1}Z_m$$

$$\pi 2 = l2V^{b2}\rho^{c2}\Delta y$$

$$\pi 3 = l^{a3}V^{b3}\rho^{c3}g$$

$$\pi 4 = l^{a4}V^{b4}\rho^{c4}h_{tw}$$

$$\pi 5 = l^{a5} V^{b5} \rho^{c5} d_{50}$$
$$\pi_6 = l^{a6} V^{b6} \rho^{c6} \rho_s$$
$$\pi_7 = l^{a7} V^{b7} \rho^{c7} B$$
$$\pi_8 = l^{a8} V^{b8} \rho^{c8} b$$
$$\pi 9 = l^{a9} V^{b9} \rho^{c9} H$$

Now for the first π term, we can write-

$$\pi_1 = l^{a1} V^{b1} \rho^{c1} Z_m$$

Now equating the dimensions left side to the right side, then we get

$$M^0 L^0 T^0 = \left(M^0 L^1 T^0\right)^{a1} \left(M^0 L^1 T^{-1}\right)^{b1} \left(M^1 L^{-3} T^0\right)^{c1} \left(M^0 L^1 T^0\right)$$

Equating the power of *M*, *L* and *T* on either side we get the value of a_1, b_1 and c_1 and by putting this value in the above π term we get the first non-dimensional term a $\pi_1 = l^{-1} V^0 \rho^0 Z_m$

,

so $\pi_1 = \frac{Z_m}{l}$

In a similar manner, we can find all the π term

$$\pi_2 = \frac{\Delta y}{l} \qquad \pi_3 = \frac{\lg}{V^2}$$
$$\pi_4 = \frac{h^{tw}}{l} \qquad \pi_5 = \frac{d_{50}}{l}$$
$$\pi_6 = \frac{\rho_s}{\rho} \qquad \pi_7 = \frac{B}{l}$$
$$\pi_8 = \frac{b}{l} \qquad \pi_8 = \frac{H}{l}$$

Now the non-dimensional group will be in the following form-

$$f_1(\pi_1, \pi_2, \pi_3, \cdots\cdots\cdots, \pi_9) = 0$$

$$f_1\left(\frac{Z_m}{l}, \frac{\Delta y}{l}, \frac{l\,\mathrm{g}}{V^2}, \frac{h_{tw}}{l}, \frac{d_{50}}{l}, \frac{\rho_s}{\rho}, \frac{B}{l}, \frac{b}{l}, \frac{H}{l}, \theta, F_d, \sigma\right) = 0 \tag{6.2}$$

By re-arranging the above dimensionless group, we can write the above equation as follows

$$\frac{Z_m}{l} = f_2\left(\frac{V^2}{l\,\mathrm{g}}, \frac{h_{tw}}{l}, \frac{d_{50}}{l}, \frac{\rho_s}{\rho}, \frac{B}{l}, \frac{b}{l}, \frac{H}{l}, \theta, F_d, \sigma, \frac{\Delta y}{l}\right) \tag{6.3}$$

Hence, the non-dimensional group was reduced to the following form-

$$\frac{Z_m}{l} = f_2\left(\frac{V^2}{l\,\mathrm{g}}, \frac{h_{tw}}{l}, \frac{d_{50}}{l}, \frac{\rho_s}{\rho}, \frac{B}{l}, \frac{b}{l}, \frac{H}{l}, \theta, F_d, \sigma, \frac{\Delta y}{l}\right) \tag{6.4}$$

θ is the function of *l* and b so it may be neglected. From the table of data sheet, the value of specific gravity (*G*) of the sediment is constant i.e. 2.6. So $G = \frac{\rho_s}{\rho}$ may be neglected from

this analysis. Ranges of d_{50} vary from 1.7 mm to 1.77 mm. So, this is the narrow range used in different experiments by the authors. So, we may neglect this term from the analysis. And σ is also used between 1.16 to 1.26. So, we may neglect this term.
Now finally the dimensionless group reduced to

$$\frac{Z_m}{l} = f_3\left(\frac{V^2}{l\,\mathrm{g}}, \frac{h_{tw}}{l}, \frac{B}{l}, \frac{b}{l}, \frac{H}{l}, F_d, \frac{\Delta y}{l}\right) \tag{6.5}$$

where $\frac{b}{l} = \sin\theta$

In this analysis, if l is considered as the repeating variable H in replace of l then the non-dimensional parameter will be:-

$$\frac{Z_m}{H} = f_4\left(\frac{V^2}{H\,\mathrm{g}}, \frac{h_{tw}}{H}, \frac{b}{l}, \frac{l}{H}, \frac{B}{H}, \frac{b}{H}, F_d, \frac{\Delta y}{H}\right) \tag{6.6}$$

6.3 Classification of non-dimensional parameter

b/l ratio:l is the length of the log vane and b is the vertical projection from the river bank. It is the function of θ. It may be represented by:

$$\frac{b}{l} = \sin\theta$$

***H/l*:** This is the important non-dimensional parameter of a complex nature which influences the scouring process. It may be known as the aspect ratio **(Gupta et al. 2007).** The range of the aspect ratio for submerged vane may be varied from 0.25 to 0.50.

The densimetric Froude number (F_d): particle Froude number is defined as $\mathrm{F_d} = \left(\frac{Q'}{lH\sqrt{\mathrm{g}'d_{50}}}\right)$ where g' is the reduced gravity $g' = \left(\frac{\rho_s - \rho_w}{\rho_w}\right) = g\left(\frac{\rho_s}{\rho_w} - 1\right)$, g is the acceleration due to gravity, ρ_s is the density of sediment particles and ρ_w is the density of water, Q is the discharge of the river and $Q' = Q\left(\frac{b}{B}\right)$.

h_{tw}/l* or *h_{tw}/H: This is the non-dimensional tailwater depth at the downstream of the channel. It is an important parameter that controls the scour depth and its morphology. This parameter was also used by Pagliara et al. (2014, 2015) and Pagliara and Kurdistani (2016) for the derivation of their formulas.

V^2/lg* or *V^2/Hg: It is the square of the Froude number. The flow Froude number is a non-dimensional number comparing inertia and gravitational forces. It may be used to quantify the resistance of an object moving through water and compare objects of different sizes.

Named after William Froude, the Froude number is based on the speed/length ratio as defined by him.

$\Delta y/l$ or $\Delta y/H$: It is the non-dimensional water fall at the location of d/s of the log vane. This is the one important parameter which mainly controls the formation of scour.
B/H : It is the ratio width of the channel to the Height of the structure
B/l: It is the ratio of the width of the channel to the length of the log vane.

6.4 Ranges of non-dimensional parameters used in literatures

Table 6.1. Ranges of non-dimensional parameters with respect to the length of the vane (*l*).

References	Range	Z_m/l	V^2/lg	h_{tw}/l	B/l	b/l	H/l	$\Delta y/l$	F_d	F'_d
Pagilara and Kurdistani (2016)	min	0.14	0.09	0.18	1.51	0.50	0.17	0.00	0.94	2.82
	max	0.20	0.16	0.48	1.51	0.50	0.26	0.02	3.98	12.00
Pagilara et al. (2014)	min	0.08	0.01	0.06	1.50	0.50	0.10	0.00	0.25	0.75
	max	0.42	0.07	0.60	3.00	1.00	0.30	0.04	3.43	10.27
Pagilara et al. (2015)	min	0.03	0.02	0.05	1.52	0.50	0.10	0.00	0.21	0.84
	max	0.35	0.06	0.69	3.45	0.87	0.37	0.03	3.46	10.52
Present study	min	0.03	0.01	0.05	1.50	0.50	0.10	0.00	0.21	0.75
	max	0.42	0.16	0.69	3.45	1.00	0.37	0.04	3.98	12.00

Table 6.2. Ranges of non-dimensional parameters with respect to the height of the vane (*H*).

References	Range	Z_m/H	V^2/Hg	h_{tw}/H	B/H	b/H	b/l	l/H	$\Delta y/H$	F_d	F'_d
Pagilara and Kurdistani (2016)	min	0.55	0.34	0.81	5.88	1.95	0.50	3.90	0.02	0.94	2.82
	max	1.18	0.96	2.82	9.09	3.01	0.50	6.03	0.13	3.98	12.00
Pagilara et al. (2014)	min	0.49	0.05	0.35	9.41	3.14	0.50	3.30	0.01	0.25	0.75
	max	1.83	0.45	4.00	20.00	6.67	1.00	9.69	0.19	3.43	10.27
Pagilara et al. (2015)	min	0.12	0.08	0.32	9.41	2.35	0.50	2.73	0.01	0.21	0.84
	max	1.55	0.46	4.00	20.00	6.58	0.87	10.00	0.16	3.46	10.52
Present study	min	0.12	0.05	0.32	5.88	1.95	0.50	2.73	0.01	0.21	0.75
	max	1.83	0.96	4.00	20.00	6.67	1.00	10.00	0.19	3.98	12.00

Chapter 07
Analysis of parameters using correlation and regression method

7.1. Introduction to reduction method

In my present study try to develop the best equation for log vane by using different techniques. For this, we must reduce the number of parameters that are used in the analysis. After the using least number of variables, we can develop equations by non-linear regression method. Thus, we required details knowledge about the process of regression and correlation method which are described below.

7.1.1. Correlation: - It is a statistical technique to ascertain the association or relationship between two or more variables. Correlation analysis is a statistical technique to study the degree and direction of the relationship between two or more variables. A correlation coefficient is a statistical measure of the degree to which changes to the value of one variable predict changes to the value of another. When the fluctuation of one variable reliably predicts a similar fluctuation in another variable, there's often a tendency to think that means that the change in one causes the change in the other. There are mainly four types of correlation methods which are described below.

1. Scatter Diagram
2. Karl Pearson's Coefficient of Correlation
3. Spearman's Rank Coefficient of Correlation
4. Kendall's tau-b Correlation Coefficient

7.1.1.1. Scatter diagram

This is a graphic method of measurement of correlation. It is a diagrammatic representation of bivariate data to ascertain the relationship between two variables. Under this method the given data are plotted on a graph paper in the form of dots i.e. for each pair of X and Y values we put dots and thus obtain as many points as the number of observations. Usually, an independent variable is shown on the X-axis whereas the dependent variable is shown on the Y-axis. Once the values are plotted on the graph it reveals the type of correlation between variable X and Y. A scatter diagram reveals whether the movements in one series are associated with those in the other series.

7.1.1.2 Pearson correlation

A correlation coefficient used in statistics to assess the linear correlation between two sets of data is the **Pearson correlation coefficient** (**PCC**). It is essentially a normalized measurement of covariance, with a value that is always between −1 and 1. It is defined as the ratio between the covariance of two variables and the product of their standard deviations. Like covariance, this measure only captures a linear correlation between variables; it leaves out a wide range of other correlations and relationship patterns. Karl Pearson created it based on a similar concept that Francis Galton had presented in the 1880s; Auguste Bravais derived and published the mathematical formula for it in 1844.

The covariance of the two variables divided by the product of their standard deviations yields Pearson's correlation coefficient. The modifier "product-moment" in the name comes from the definition's form, which involves a "product moment," which is the mean (the first moment about the origin) of the product of the mean-adjusted random variables.
Pearson correlation coefficient, given a pair of random variables (X, Y), the formula for ρ is.

$$\rho_{X,Y} = \frac{\operatorname{cov}(X,Y)}{\sigma_X \sigma_Y}$$

where
cov is the covariance
σ_X is the standard deviation of X
σ_Y is the standard deviation of Y

7.1.1.3. Spearman's rho correlation

When quantification of variables becomes difficult then this method of rank correlation is useful which was developed by British psychologist Charles Edward Spearman in 1904. In this method ranks are allotted to each element either in ascending or descending order. The correlation coefficient between these allotted two series of ranks is popularly called as "Spearman's Rank Correlation" and is denoted by "R".

$$R = 1 - \frac{6\sum D^2}{N(N^2-1)}$$

where, D =Difference of the ranks between paired items in two series.
N = Number of pairs of ranks

7.1.1.4. Kendall's tau-b correlation

In statistics, the Kendall rank correlation coefficient, commonly referred to as Kendall's τ coefficient is a statistic used to measure the ordinal association between two measured quantities. A τ test is a non-parametric hypothesis test for statistical dependence based on the τ coefficient. It is a measure of rank correlation: the similarity of the orderings of the data when ranked by each of the quantities. It is named after Maurice Kendall, who developed it

in 1938, though Gustav Fechner had proposed a similar measure in the context of time series in 1897.

Intuitively, the Kendall correlation between two variables will be high when observations have a similar (or identical for a correlation of 1) rank (i.e. relative position label of the observations within the variable: 1st, 2nd, 3rd, etc.) between the two variables, and low when observations have a dissimilar (or fully different for a correlation of −1) rank between the two variables.

7.2. Regression

A study of measuring the relationship between associated variables, wherein one variable is dependent on another independent variable, called as Regression. It was developed by Sir Francis Galton in 1877 to measure the relationship of height between parents and their children. Regression analysis is a statistical tool to study the nature and extent of the functional relationship between two or more variables and to estimate (or predict) the unknown values of the dependent variable from the known values of the independent variable.

7.2.1 Forward regression analysis

Forward regression is a linear regression method where variables are added to the model one by one based on how much they improve the model. It starts with no variables and adds the most helpful ones step by step. This continues until no further improvement is seen or a stopping (Efroymson, 1960) point is reached. It's useful for identifying key predictors from many possibilities. Variables with a P value less than 0.05 and a larger R^2 are considered significant and are included in the model.

7.2.2. Backward regression analysis

Backward regression is a variable selection method where all variables are initially included in the model, then sequentially eliminated based on their partial correlation with the dependent variable. The variable with the smallest partial correlation is removed first, and this process continues until no variables meet the removal criteria (Efroymson, 1960). Variables with the highest R^2 and low p-values (<0.05) are considered significant and retained in the model.

7.2.3. Stepwise regression analysis

At each step, if the probability of F is small enough, enter the independent variable that is not included in the equation and has the smallest value of F. The F variable that is already in the equal regression will be removed if its probabilities are large enough. This method ends when there are no more variables available to include or exclude. This method combines forward and backward regression to add and remove predictors based on their contribution to the

model to avoid incomplete models (Efroymson, 1960). The model included variables with the largest R^2 and low P values (less than 0.05) that were considered statistically significant.

7.2.4. Subset regression analysis

The best subsets regression command involves examining all the models for all possible combinations of predictor variables and determining the best set of predictors for each subset size based on predefined criteria such as the Akaike Information Criterion (AIC) or Bayesian Information Criterion (BIC) (Doe and Smith, 2020). It can be used alternatively in place of the stepwise regression techniques. The best subsets regression is also known as all possible subsets' regression. This method command selects the subset of predictors at each step that fits best, based on the criterion of having the largest R^2.

Chapter 08

Results and discussion

8.1. Results

After the reduction method, our next task is to find the different results and their interpretation. For this, we require an idea about the non-dimensional parameters, and how they behave with different conditions. For this, we draw different graphs between the non-dimensional parameters and try to find out the relationship between them. Based on the graphs between two non-dimensional parameters we get a better visualization about their behavior. Using this idea, we can easily discuss the various results and outcomes of the analysis. After the completion of the graph, we go for different regression methods and finally find out the different equations in which we get different outcomes that are our main findings.

8.1.1 Behavior of scour with Froude number and role of vane angle on it

We know that riverbed scours increase with a higher Froude number (Fr). However, **Fig. 8.1.** shows that non-dimensional scour depth (Z_m/H) remains nearly constant with Fr^2, which contradicts the expected behavior of the parameter. When graphing the effect of Froude number on Z_m/H with different vane orientation angles (θ), the results align with the physical meaning of the parameters, except for $\theta = 150°$, as shown in **Fig. 8.2.** This indicates that the effect of Froude number on scour depth is more accurately depicted when considering the vane orientation angle.

Fig. 8.2. indicates that the non-dimensional scour depth (Z_m/H) increases with the vane angle (θ) for a given Froude number (Fr). Additionally, **Fig. 8.3.** shows that the comparative study of scour due to the Froude number aligns with the expected physical behavior of the parameters. This demonstrates that the vane angle significantly influences scour depth and provides a more accurate representation of the effect of the Froude number on scour depth.

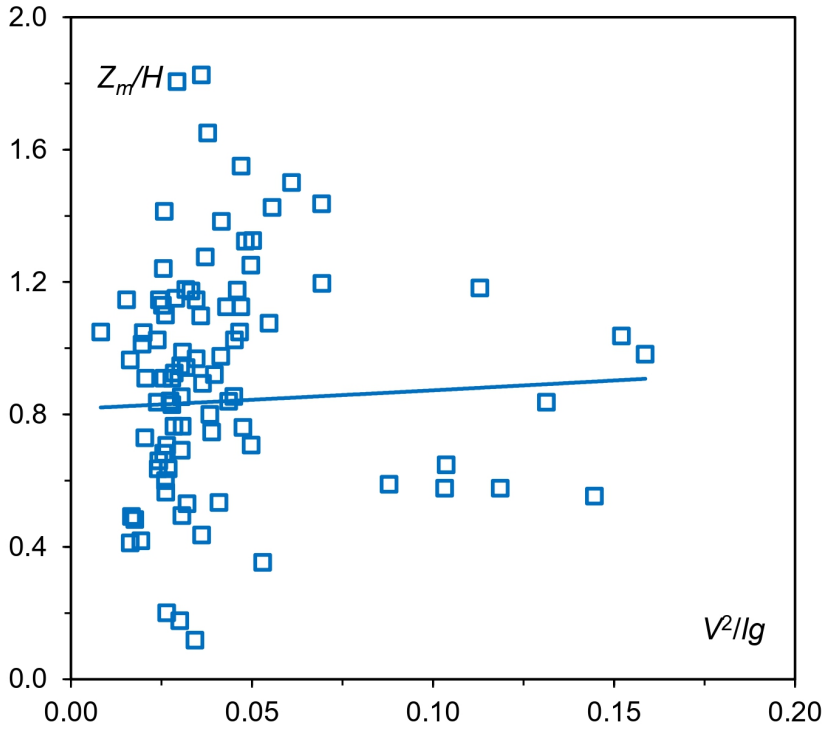


Fig. 8.1. The effect of Froude number (Fr) on non-dimensional scour depth (Z_m/H)

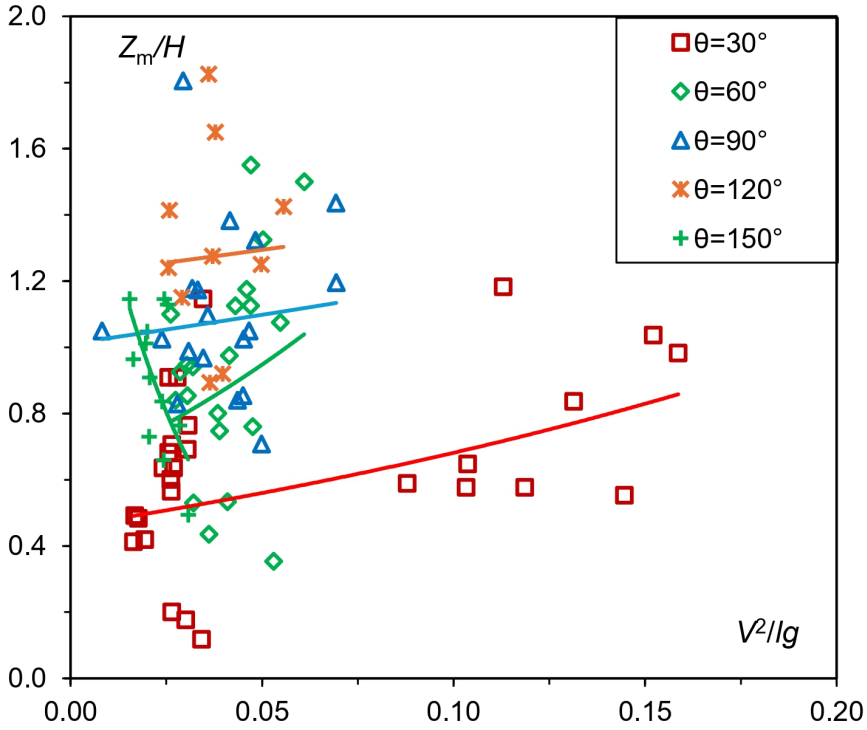


Fig 8.2. The role of vane angle on dimensionless scour depth (Z_m/H) under different Froude numbers.

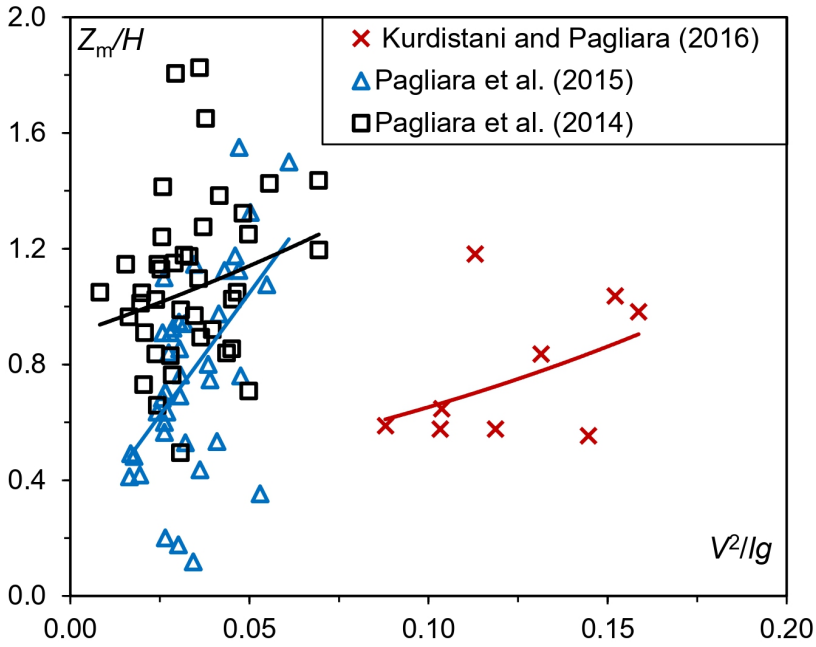


Fig 8.3. Comparative review of Froude number influence on non-dimensional scour depth (Z_m/H)

8.1.2. Behavior of Scour with tailwater depth and role of vane angle on it

It is understood that riverbed scours decrease with increasing tailwater depth. However, in **Fig. 8.4**, Z_m/H is shown to vary proportionally with h_{tw}/l, contradicting typical flow behavior. When the effect of h_{tw}/l on Z_m/H is graphed for different vane angles (θ), a clear inverse trend is observed i.e. consistent with physical expectations, except for θ=30° and θ =90°, as depicted in **Fig. 8.5.** This indicates that the effect of h_{tw}/l on scour depth is more accurately depicted when considering the vane orientation angle. Additionally, **Fig. 8.6** shows that the comparative study of scour due to h_{tw}/l does not obey the expected physical behavior of the parameters except the data of Pagliara and Kurdistani (2016).

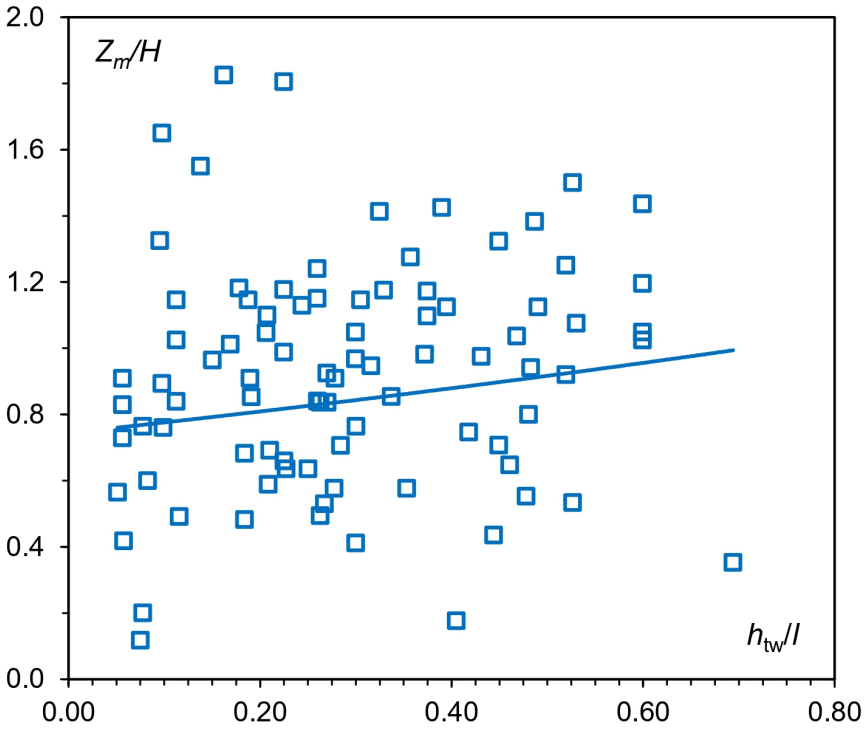


Fig 8.4. The effect of dimensionless tail water depth (h_{tw}/l) on non-dimensional scour depth (Z_m/H).

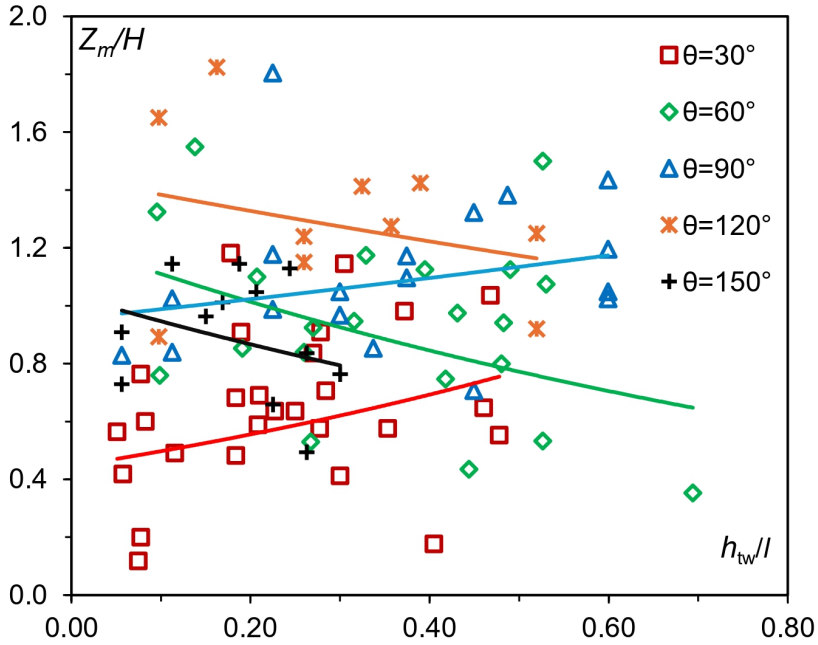


Fig 8.5. The role of vane angle on non-dimensional scour depth (Z_m/H) under different non - dimensional tail water depths (h_{tw}/l).

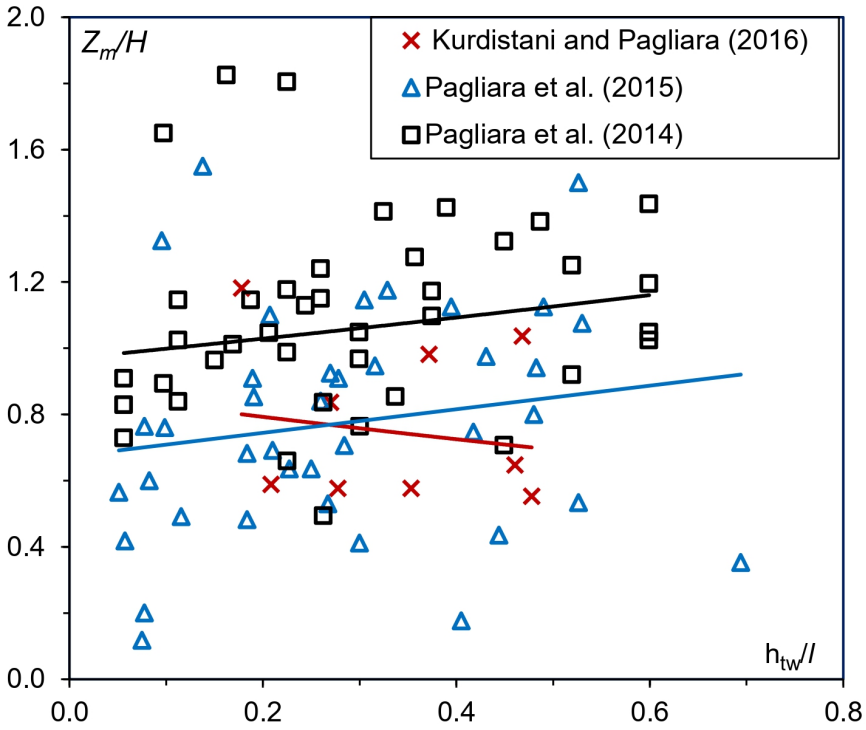


Fig. 8.6. Comparative plots of non-dimensional tail water depth ((h_{tw}/l)) influence on dimensionless scour depth (Z_m/H).

8.1.3. Behavior of Scour with aspect ratio and role of vane angle on it.

The aspect ratio, defined as the ratio of the height of the vane to its length (Odgard and Spoiljaric, 1986), can be increased either by decreasing the vane length (l) while keeping the height (H) constant or by increasing H while keeping l constant. In the first case, the scour is reduced and second case scour depth increases. As shown in **Fig. 4.7**, the scour depth is inversely related to the aspect ratio of the log vane. **Fig. 4.8** also demonstrates this inverse relationship, consistent with physical flow phenomena, except at θ =90°.

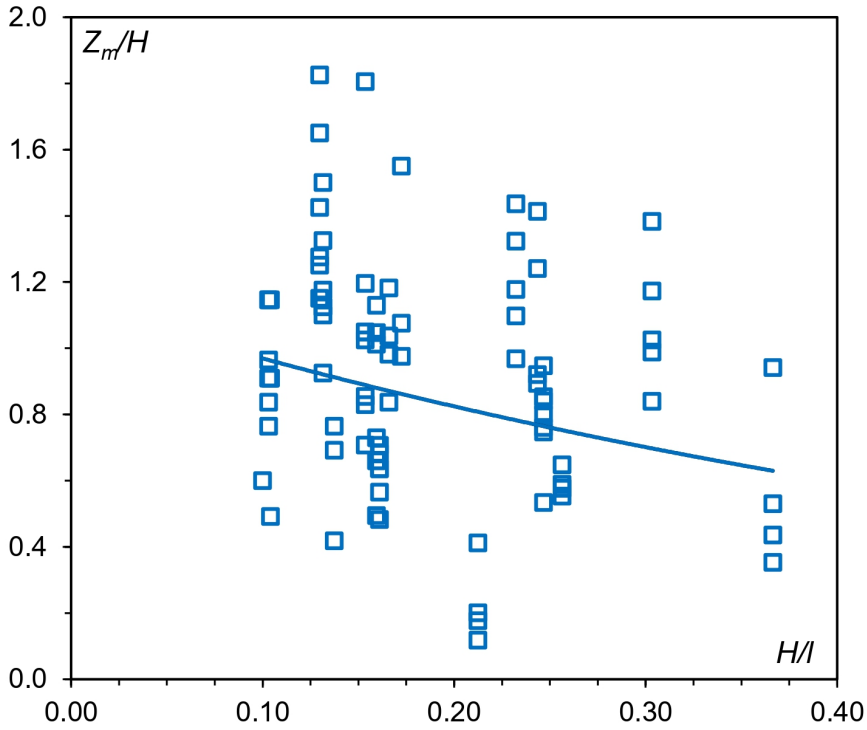


Fig. 8.7. The effect of aspect ratio (H/l) on non-dimensional scour depth (Z_m/H).

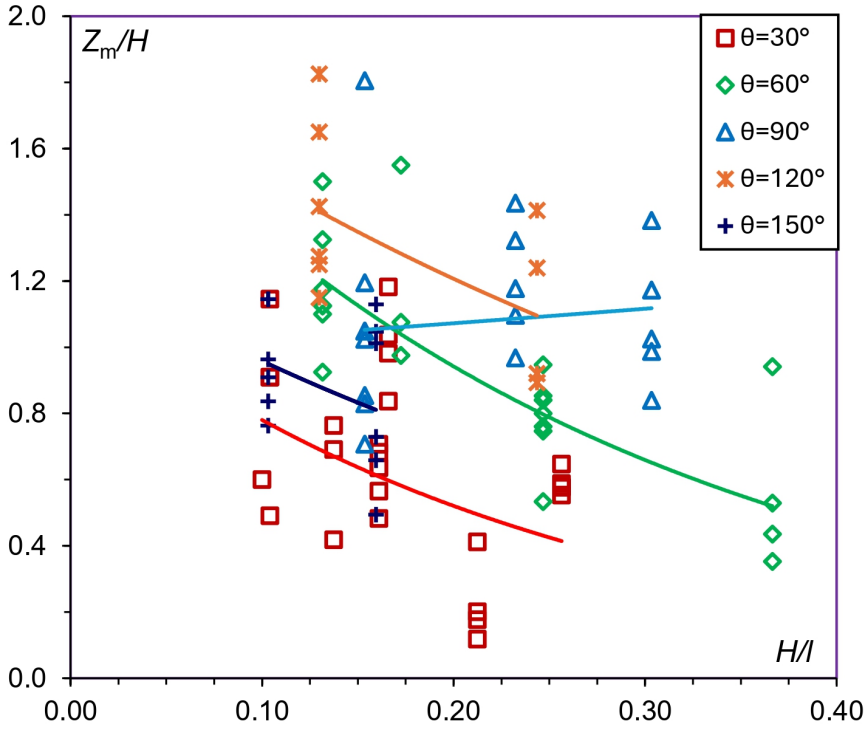


Fig. 8.8. The role of vane angle on dimensionless scour depth (Z_m/H) under different aspect ratios (H/l)

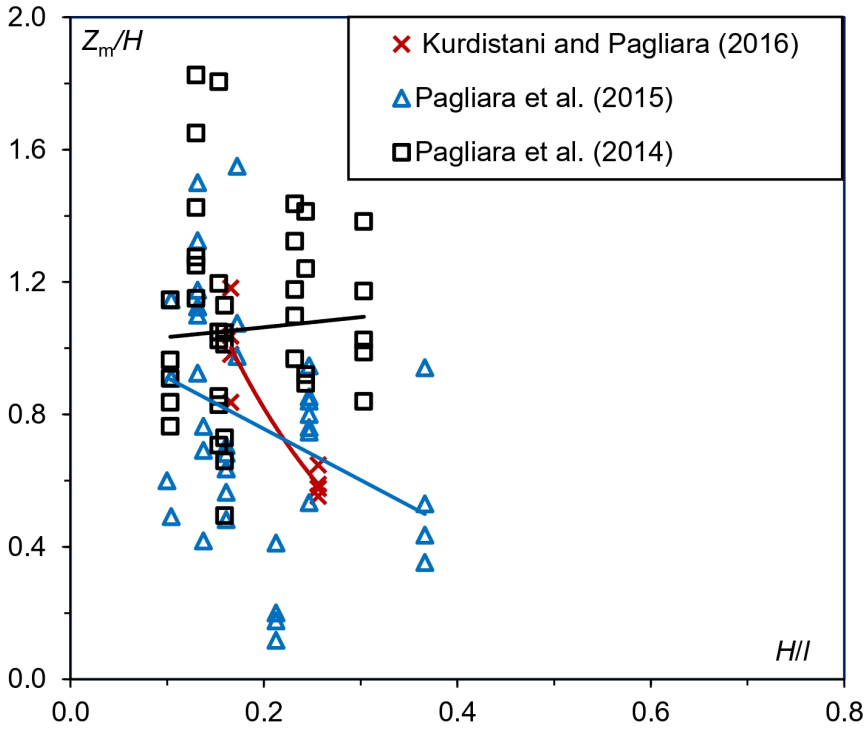


Fig 8.9. Comparative review of aspect ratio(H/l) influence on dimensionless scour depth (Z_m/H)

8.1.4. Behavior of scour with densimetric Froude number and role of vane angle on it

We know that riverbed scours increase with higher densimetric Froude numbers (F_d). However, **Fig. 8.10** shows that non-dimensional scour depth (Z_m/H) increases with the F_d which follows the flow physics.

When graphing the effect of F_d on Z_m/H with different vane orientation angles (θ), the results align with the physical meaning of the parameters, except for $\theta = 150°$, as shown in **Fig. 8.11** This indicates that the effect of the Froude number on scour depth is more accurately depicted when considering the vane orientation angle.

Fig. 8.11 indicates that the non-dimensional scour depth (Z_m/H) increases with the vane angle (θ) for the given Froude number F_d. Additionally, **Fig. 8.12** shows that the comparative study of scour due to F_d aligns with the expected physical behavior of the parameters. This demonstrates that the vane angle significantly influences scour depth and provides a more accurate representation of the effect of the Froude number on scour depth.

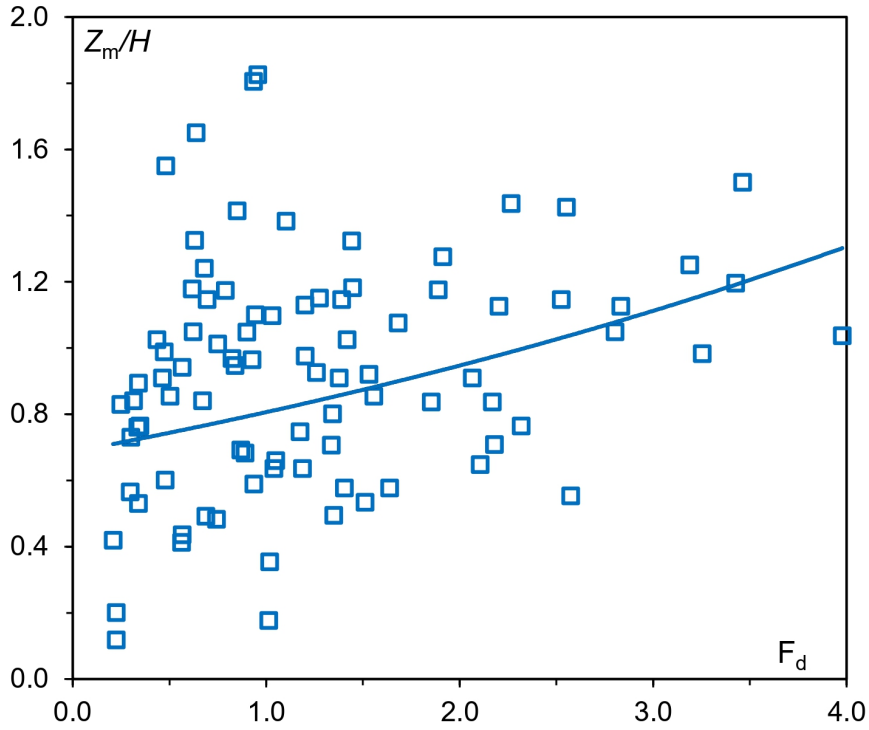


Fig. 8.10. The effect of densimetric Froude number (F_d) on non-dimensional scour depth (Z_m/H).

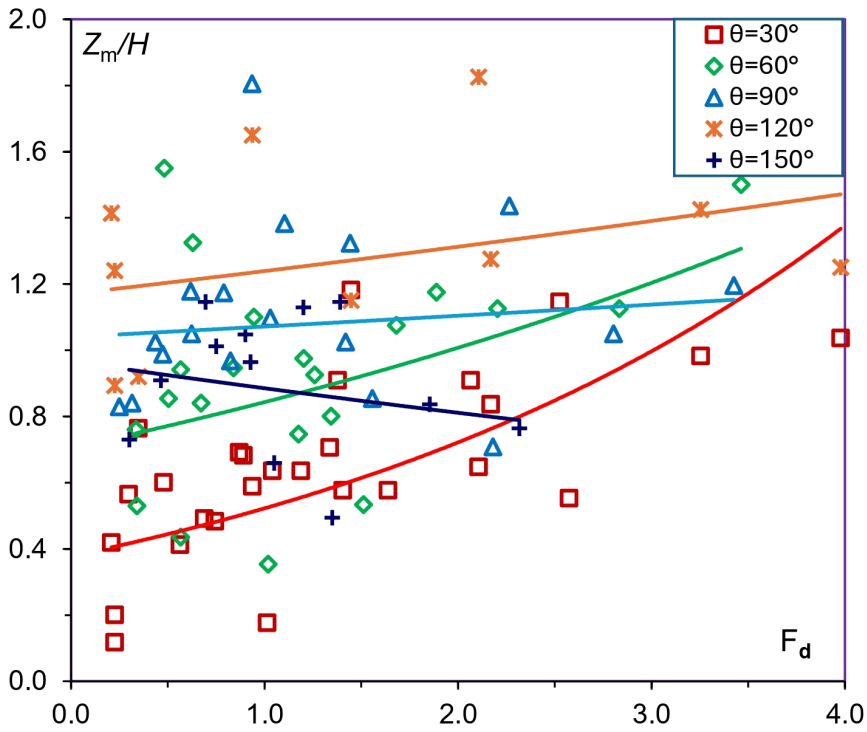


Fig. 8.11. The role of vane angle on non-dimensional scour depth (Z_m/H) under different densimetric Froude numbers (F_d)

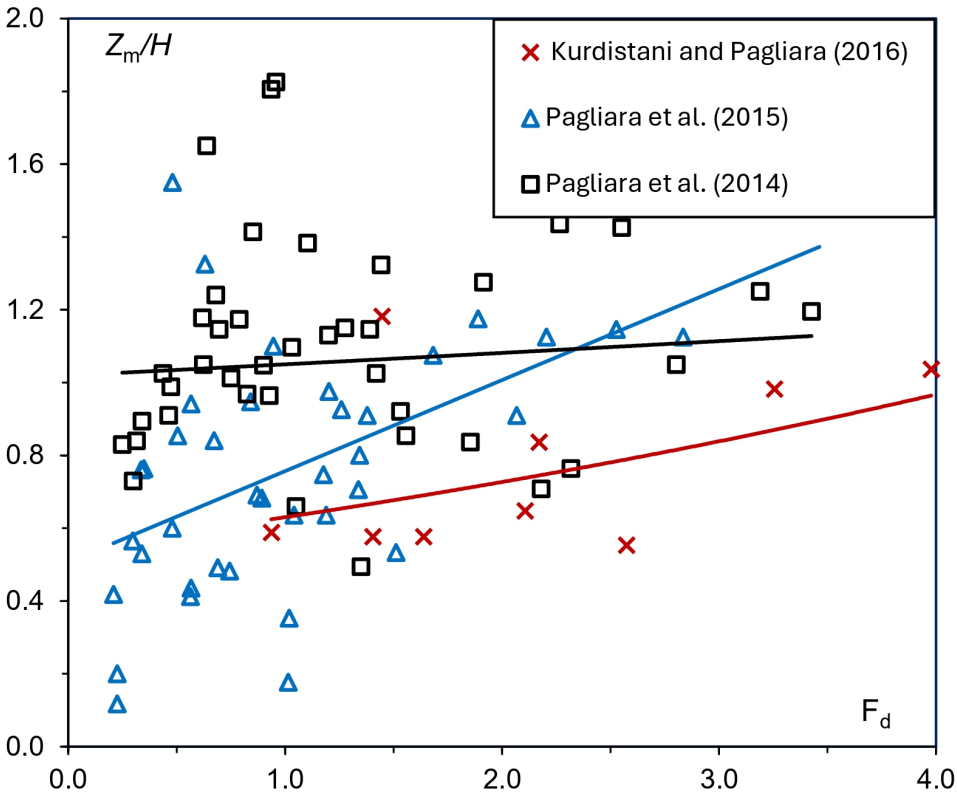


Fig. 8.12. Comparative review of densimetric Froude number (F_d) influence on non-dimensional scour depth (Z_m/H)

8.1.5. Behavior of Scour with waterfall and role of Vane Angle on it

A waterfall is defined as the difference in u/s and d/s water level. This is an important parameter which influences the scour of the channel. **Fig. 8.13** shows the variation of scour with water fall and it indicates that scour directly varies with water fall. When graphing the effect of $\Delta y/l$ on Z_m/H with different vane orientation angles (θ), the results align with the physical meaning of the parameters, only for $\theta = 90°$and $\theta = 150°$, as shown in **Fig. 8.14**.

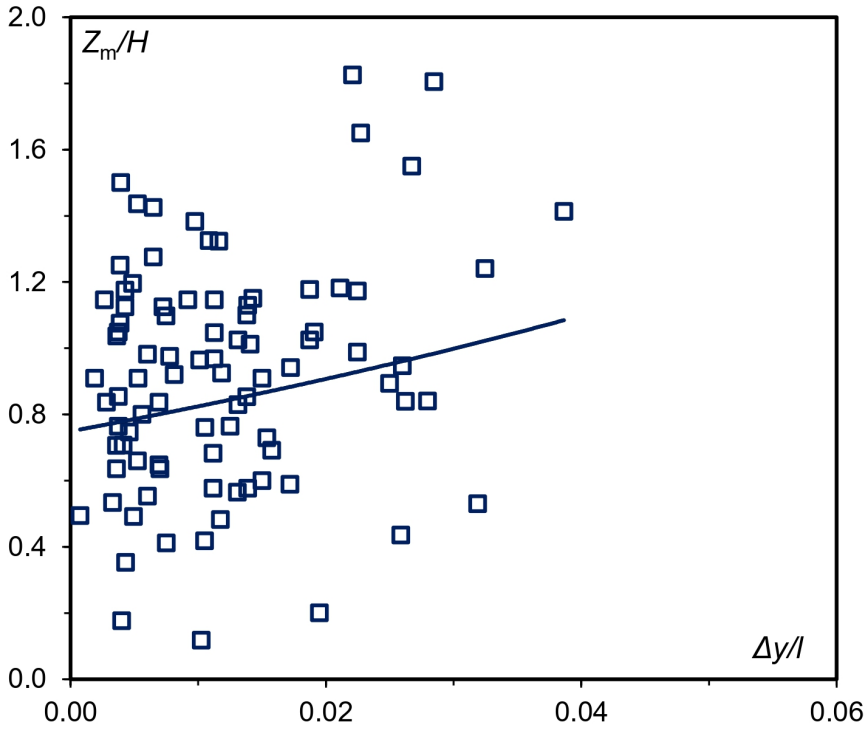


Fig 8.13. The effect of the non-dimensional waterfall ($\Delta y/l$) on non-dimensional scour depth (Z_m/H).

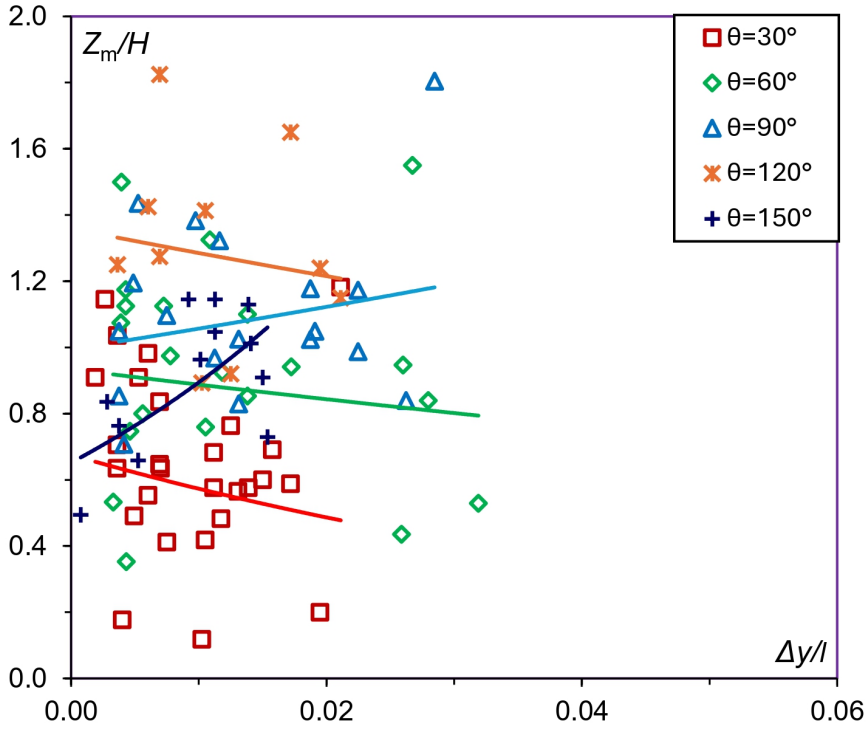


Fig 8.14. The role of vane angle on non-dimensional scour depth (Z_m/H) under different non-dimensional water falls ($\Delta y/l$)

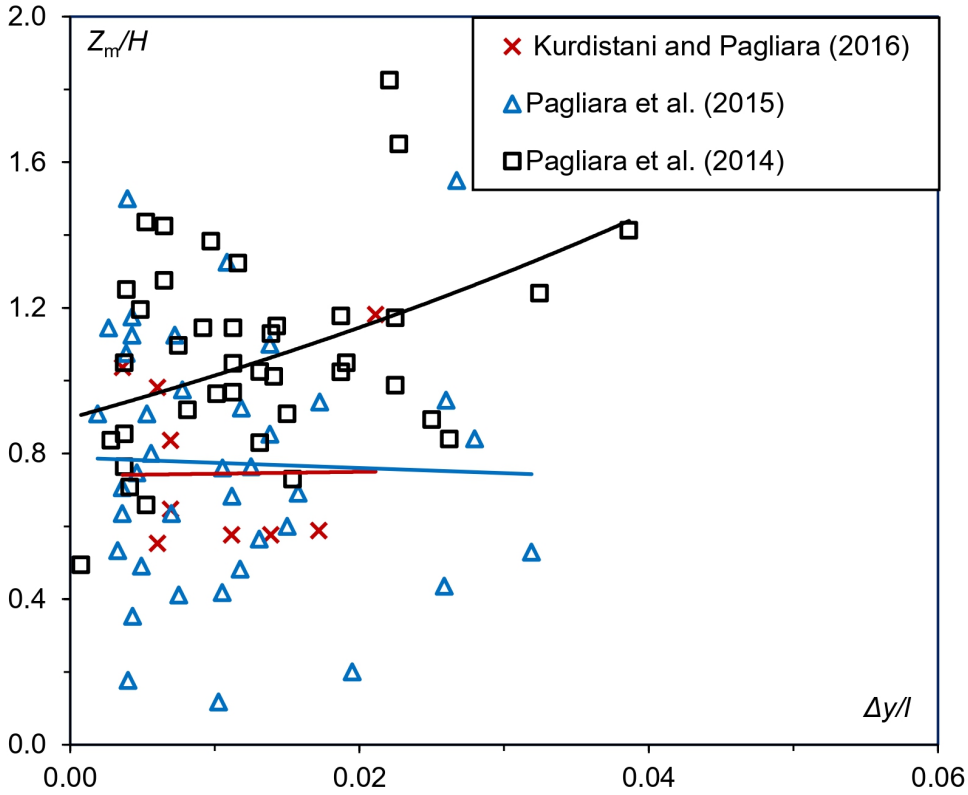


Fig 8.15. Comparative review of non-dimensional waterfall ($\Delta y/l$) influence on non-dimensional scour depth (Z_m/H)

8.1.6. Behavior of Scour with non-dimensional waterfall and role of vane angle on it

Figure 8.16 shows the variation of scour with water fall and it indicates that scour directly varies with waterfall. When graphing the effect of $\Delta y/H$ on Z_m/H with different vane orientation angles (θ), the results align with nearly constant values. But in actuality, this pattern does not represent the true picture of the figure.

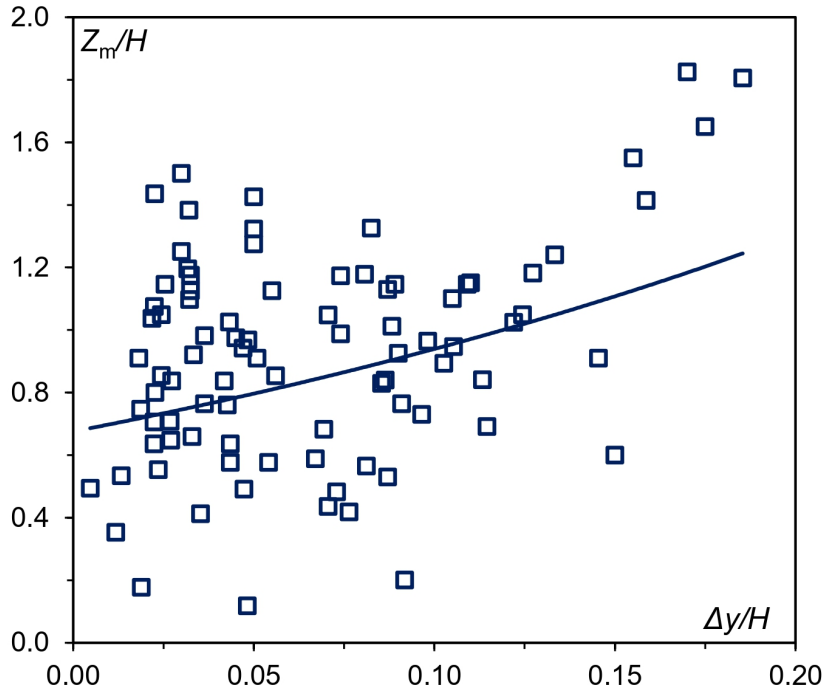


Fig 8.16. The effect of non-dimensional waterfall ($\Delta y/H$) on non-dimensional scour depth (Z_m/H).

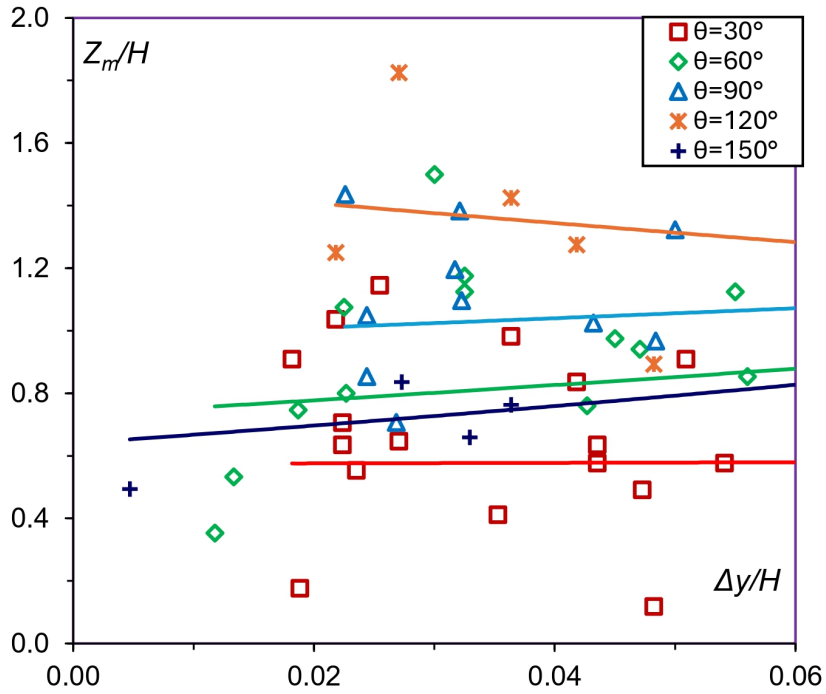


Fig 8.17. The role of vane angle on non-dimensional scour depth (Z_m/H) under different non-dimensional water falls ($\Delta y/H$)

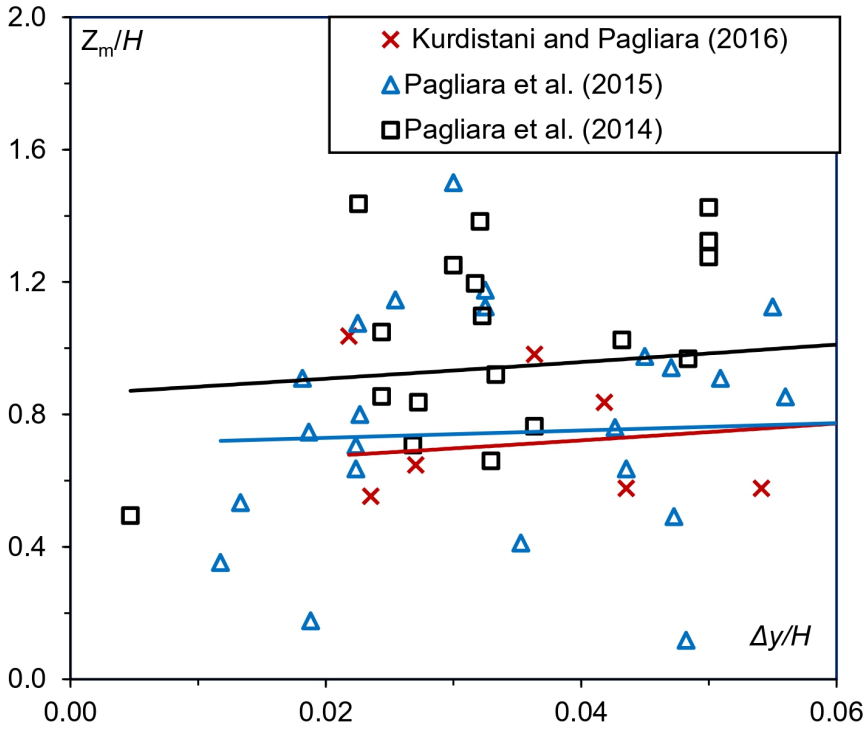


Fig. 8.18. Comparative review of non-dimensional waterfall ($\Delta y/H$) influence on dimensionless scour depth (Z_m/H)

8.1.7. Behavior of Scour with tailwater depth (h_{tw}/H) and role of vane angle on it

It is understood that riverbed scours decrease with increasing tailwater depth. However, in **Fig. 8.19**, Z_m/H is shown to vary proportionally with h_{tw}/H, contradicting typical flow behavior. When the effect of h_{tw}/H on Z_m/H is graphed for different vane angles (θ), a clear inverse trend is observed only for θ=150°, as depicted in **Fig. 8.20.** This indicates that the effect of h_{tw}/H on scour depth is more accurately depicted when considering the vane orientation angle. Additionally, **Fig. 8.21** shows that the comparative study of scour due to h_{tw}/H does not obey the expected physical behavior of the parameters.

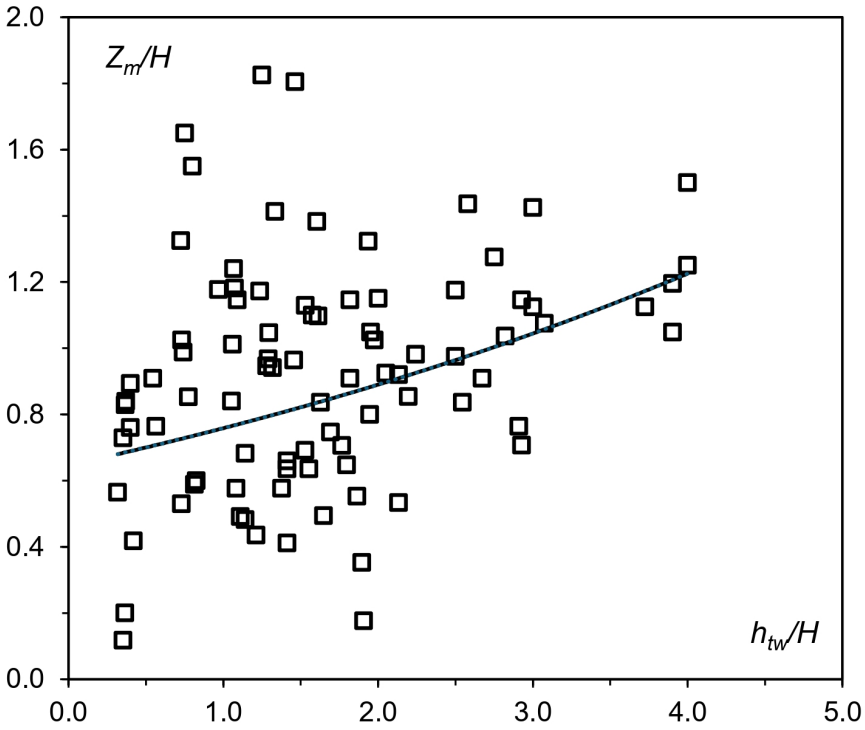


Fig 8.19. The effect of non-dimensional tail water depth (h_{tw}/H) on non-dimensional scour depth (Z_m/H).

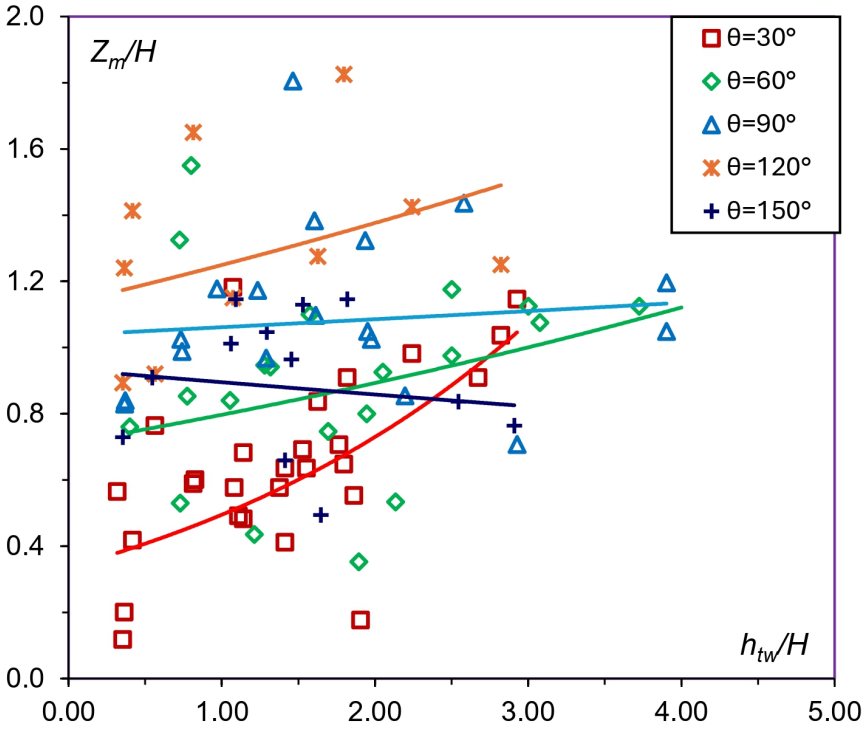


Fig. 8.20. The role of vane angle on non-dimensional scour depth (Z_m/H) under different non-dimensional tail water depths (h_{tw}/H).

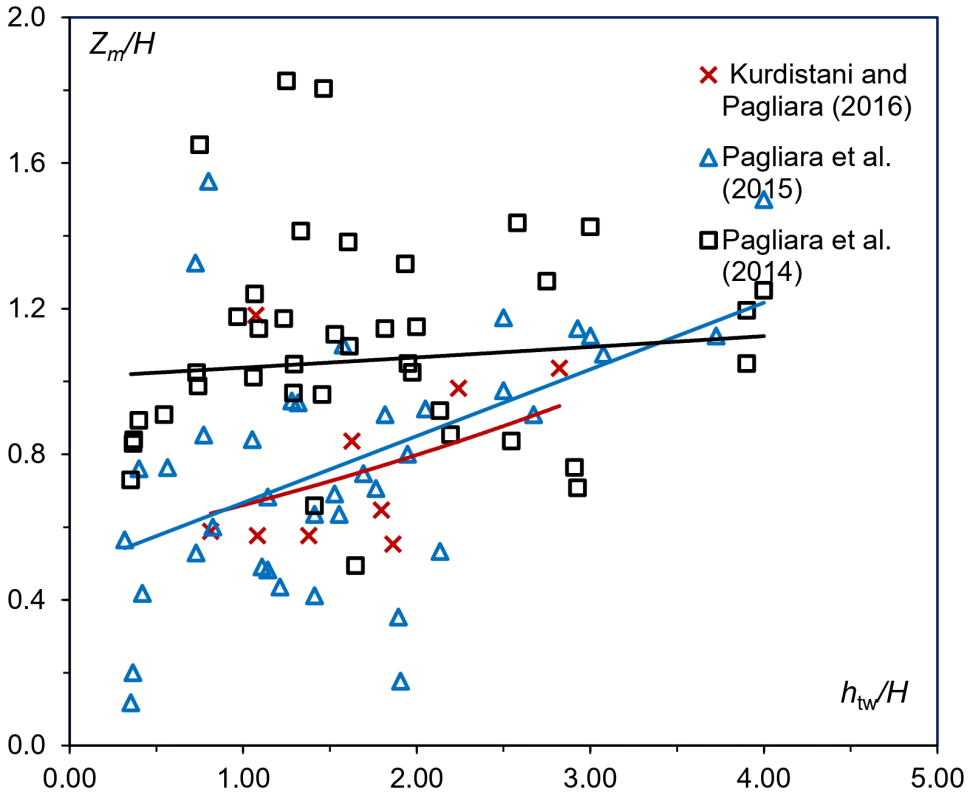


Fig. 8.21. Comparative review of non-dimensional tail water depth ((h_{tw}/H) influence on non-dimensional scour depth (Z_m/H)

8.1.8. Behavior of Scour with non-dimensional parameter (η) and role of vane angle on it

Pagliara and Kurdistani (2013) introduced a non-dimensional scour parameter $\eta = \mathrm{F_d}^2\left(\frac{\Delta y}{H}\right)$, which is the function of $\mathrm{F_d}, \Delta y$ and H respectively. We already know that scour is directly proportional to the $\mathrm{F_d}$ and Δy. So, η will be power relations with scour depth. However, in **Fig. 8.22**, Z_m/H is varying with η by following the power law. When the effect of η on Z_m/H is graphed for different vane angles (θ) and B/l ratio, a clear trend is observed for all the cases of θ and B/l ratio as depicted in **Fig. 8.23** and **Fig. 8.24** respectively. In **Fig. 8.25**, the variation of scour depth with η is shown by changing the h_{tw}/H ratio while keeping the B/l ratio and θ are constant and it is observed that it also followed the power law in this case.

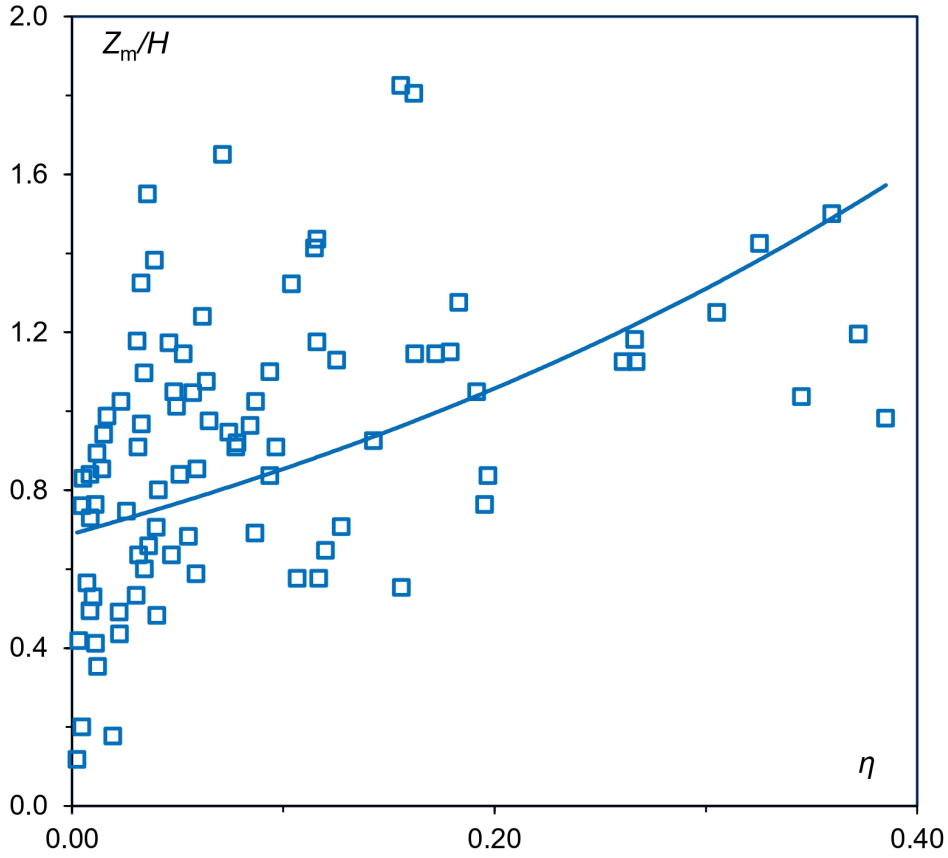


Fig. 8.22. The effect of non-dimensional parameter (η) on non-dimensional scour depth (Z_m/H).

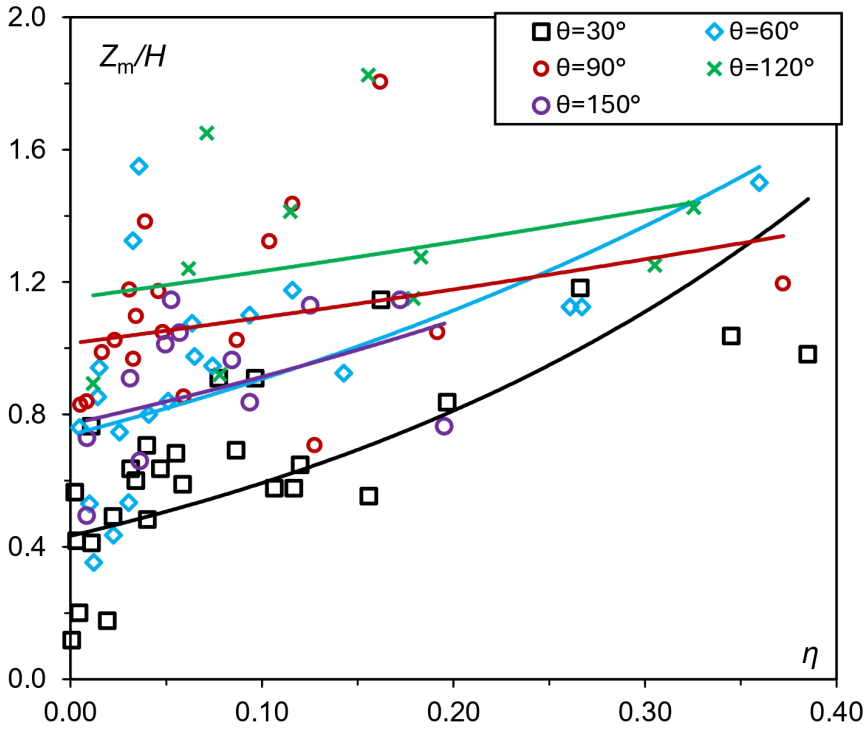


Fig. 8.23. The role of vane angle on non-dimensional scour depth (Z_m/H) under different non-dimensional parameters (η).

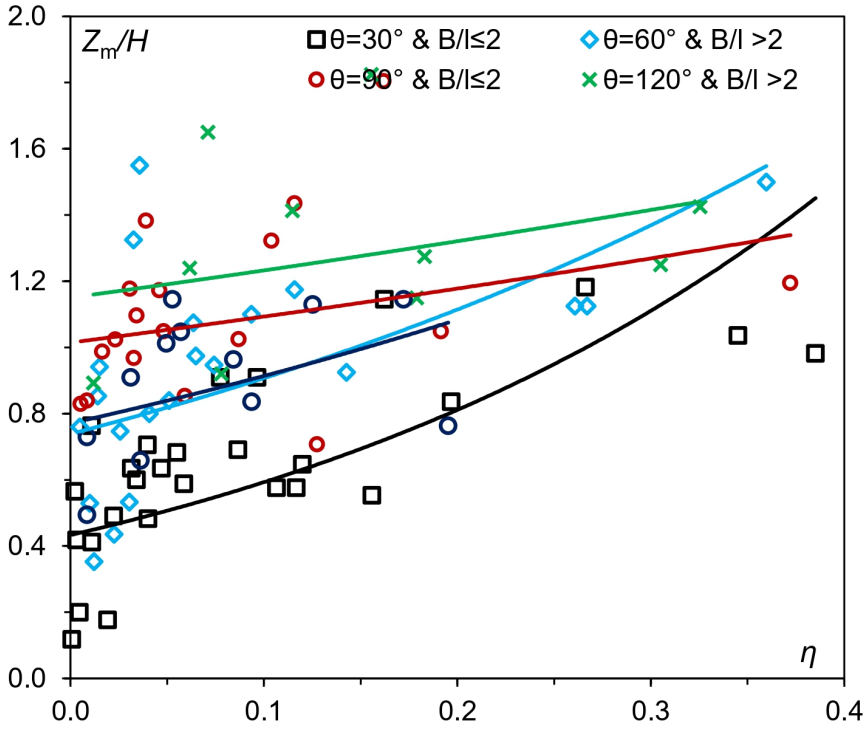


Fig. 8.24. The role of vane angle and B/l ratio on non-dimensional scour depth (Z_m/H) under different non-dimensional parameters (η).

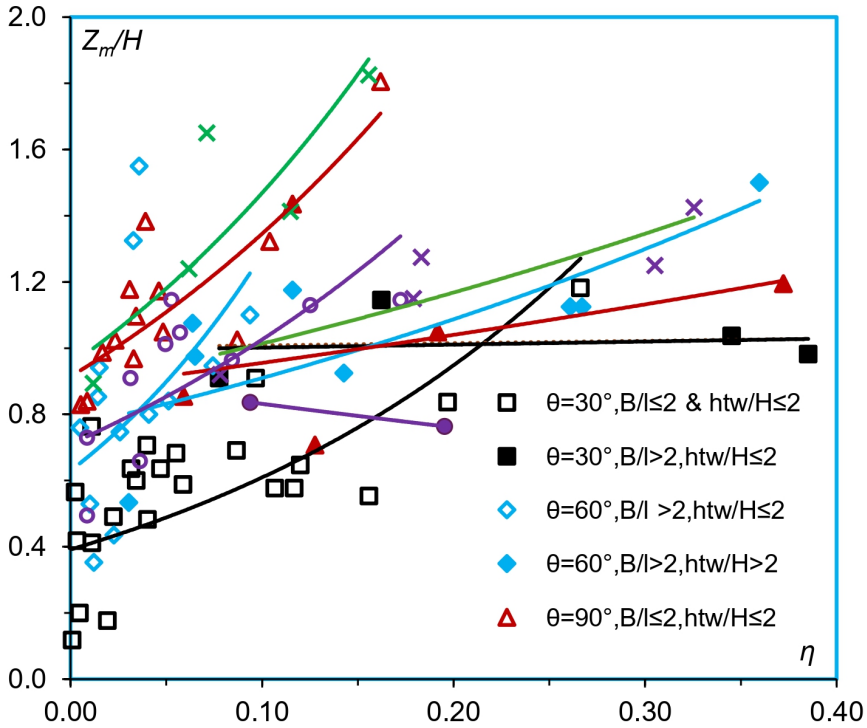


Fig. 8.25. The role of vane angle, *B/l* ratio and h_{tw}/H on non-dimensional scour depth (Z_m/H) under different non-dimensional parameters (η).

8.1.9. Behavior of densimetric Froude number F_d with dimensionless waterfall (Δy/H) and role of different parameters on it

Figure 8.26 shows the variation of F_d with water fall and it indicates that F_d inversely varies with water fall. When graphing the effect of $\Delta y/H$ on F_d with different vane orientation angles (θ), the results show a clear exponential trend line. If F_d increases, then water depth at the downstream will decrease. **Figure 8.27** and **Fig. 8.28** also follow the same trend line.

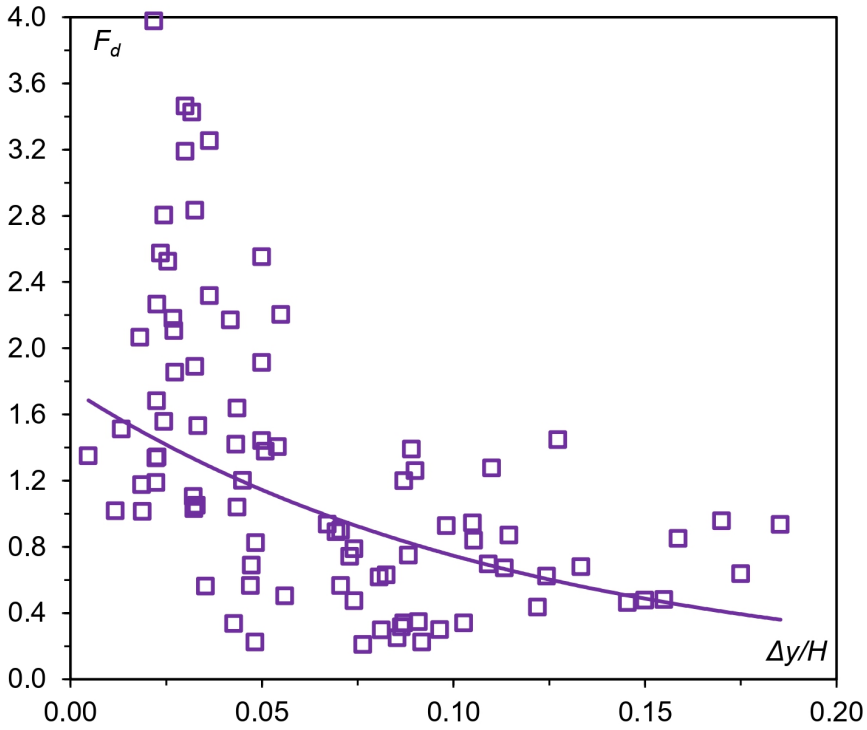


Fig. 8.26. The effect of deinsimetric Froude number F_d on non-dimensional scour depth (Z_m/H).

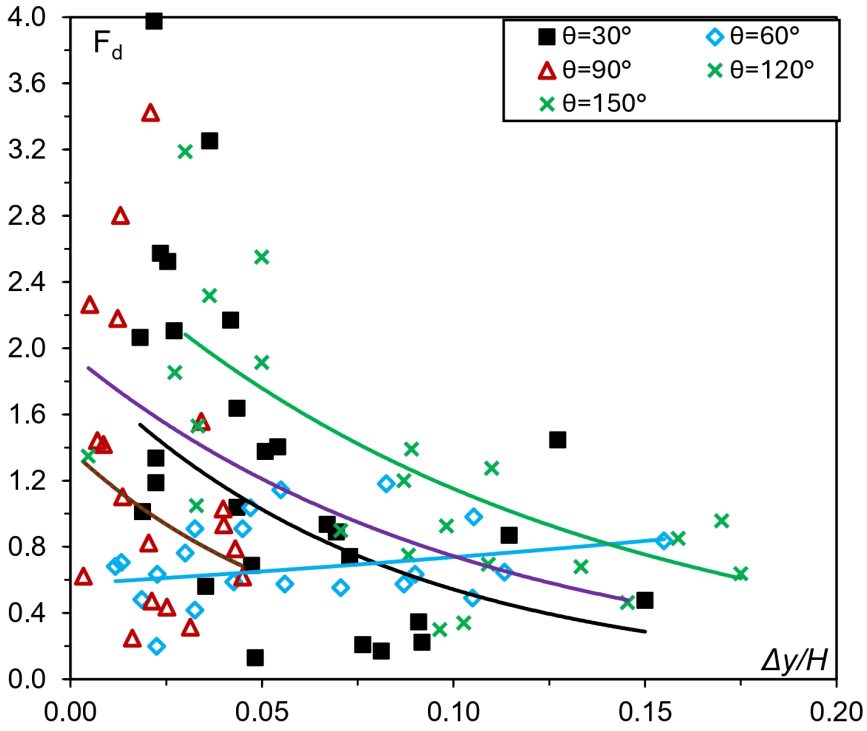


Fig. 8.27. The role of vane angle on non-dimensional scour depth (Z_m/H) under different deinsimetric Froude numbers (F_d).

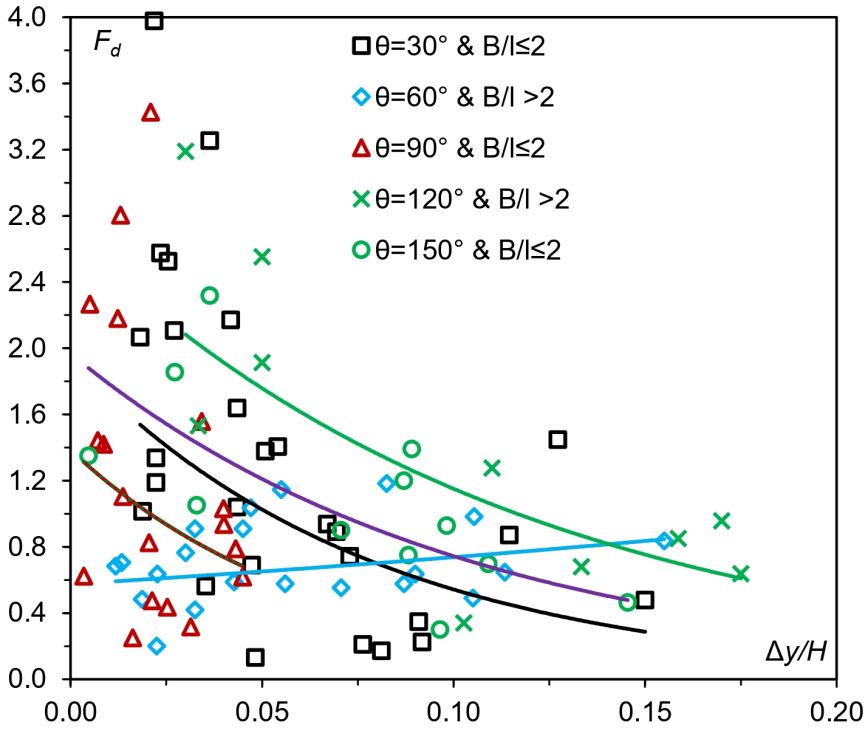


Fig. 8.28. The role of vane angle and *B/l* ratio on non-dimensional scour depth (Z_m/H) under different deinsimetric Froude number F_d.

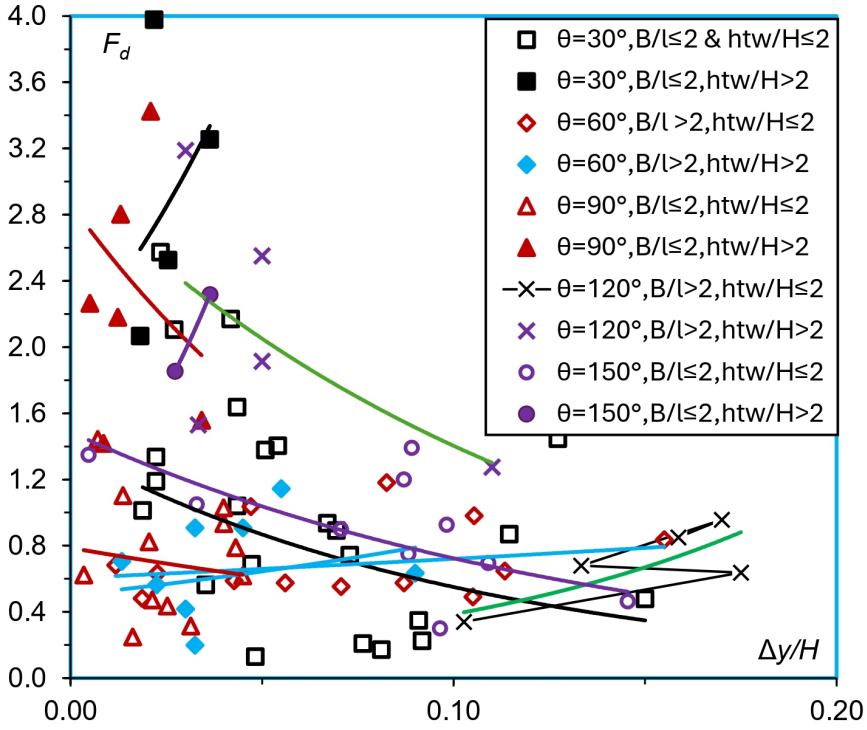


Fig. 8.29. The role of vane angle, *B/l* ratio and h_{tw}/H on dimensionless scour depth (Z_m/H) under different densimetric Froude number F_d

8.2(a). Formula derivation by using different statistical techniques.

In this method, at first, the equations are developed by taking the non-dimensional parameter with respect to *l*, i.e. the parameter obtained from dimensionless analysis (Eq. 6.5.)

Formula derivation by using Pearson correlation and subset regression method.

Table 8.1. Pearson correlation coefficient

Variables	Z_m/l	V^2/lg	h_{tw}/l	B/l	b/l	H/l	$\Delta y/l$	F_d	F'_d
Z_m/l	1								
V^2/lg	0.106	1							
h_{tw}/l	0.340	0.356	1						
B/l	0.592	-0.153	0.397	1					
b/l	0.676	-0.123	0.392	0.927	1				
H/l	0.532	0.188	0.357	0.443	0.345	1			
$\Delta y/l$	0.461	-0.189	-0.387	0.304	0.265	0.374	1		
F_d	-0.009	0.589	0.663	-0.103	0.005	-0.251	-0.579	1	
F'_d	-0.025	0.589	0.692	-0.071	0.000	-0.234	-0.589	0.994	1

Note:- * Correlation is significant at the 0.05 level (2-tailed); ** correlation is significant at the 0.01 level (2-tailed). The correlation values between *B/l* and *b/l*, F_d, and F'_d are 0.927, and 0.994 respectively, indicating strong correlations. So, in both cases significance number <0.001 with ** Consequently, we may neglect one of the terms from *B/l* and *b/l* or F_d and F'_d. However, to create more options for analysis, we will consider one term from each group**. Hence, the non-dimensional group was reduced to the following form-**

Case-1 $$\frac{Z_m}{l} = f_3\left(\frac{V^2}{lg}, \frac{h_{tw}}{l}, \frac{B}{l}, \frac{H}{l}, F_d, \frac{\Delta y}{l}\right)$$

Case-2 $$\frac{Z_m}{l} = f_3\left(\frac{V^2}{lg}, \frac{h_{tw}}{l}, \frac{b}{l}, \frac{H}{l}, F_d, \frac{\Delta y}{l}\right)$$

Case-3 $$\frac{Z_m}{l} = f_3\left(\frac{V^2}{lg}, \frac{h_{tw}}{l}, \frac{B}{l}, \frac{H}{l}, F'_d, \frac{\Delta y}{l}\right)$$

Case-4 $$\frac{Z_m}{l} = f_3\left(\frac{V^2}{lg}, \frac{h_{tw}}{l}, \frac{b}{l}, \frac{H}{l}, F'_d, \frac{\Delta y}{l}\right)$$

Now using these variables subset regression is done for each case and subsequently formulas are derived for each of the cases

Table 8.2. Subset Regression for case-2

Variables	R-Sq	R-Sq (adj)	PRESS	R-Sq (pred)	Mallows C_p	*S*	AICc	BIC	Cond No	V^2/lg	h_{tw}/l	b/l	H/l	$\Delta y/l$	F_d
1	45.7	45.1	0.3	43.0	44.6	0.059	-244	-237	1.00	×	×	✓	×	×	×
1	29.3	28.4	0.4	24.8	83.6	0.067	-221	-218	1.00	×	×	×	✓	×	×
2	55.9	54.8	0.3	51.8	22.5	0.053	-260	-251	2.10	×	×	✓	✓	×	×
2	54.4	53.3	0.3	50.9	26.0	0.054	-257	-248	1.70	×	×	✓	×	✓	×
3	63.1	61.8	0.2	58.9	7.40	0.049	-278	-262	4.70	×	✓	✓	×	✓	×
3	60.2	58.8	0.2	56.8	14.3	0.051	-267	-255	1.90	✓	×	✓	×	✓	×
4	**65.6**	**64.0**	**0.2**	**60.2**	**3.40**	**0.048**	**-278**	**-264**	**5.40**	×	×	✓	✓	✓	✓
4	64.7	63.0	0.2	60.3	5.60	0.048	-275	-261	6.60	✓	✓	✓	×	✓	×
5	65.7	63.6	0.2	59.3	5.20	0.048	-275	-259	23.9	×	✓	✓	✓	✓	✓
5	65.7	63.6	0.2	59.5	5.30	0.048	-275	-259	12.7	✓	×	✓	✓	✓	✓
6	65.8	63.3	0.2	58.7	007	0.048	-273	-255	47.9	✓	✓	✓	✓	✓	✓

*Note-From subset regression the lowest Mallows C_p value is 3.40 and its corresponding R-Sq(adj) is 64. Now using the variables of this case the final formula will be

$$\frac{Z_m}{l} = 2.1\left(\frac{b}{l}\right)^{0.8}\left(\frac{H}{l}\right)^{0.46}\left(\frac{\Delta y}{l}\right)^{0.33}\left(F_d\right)^{0.33} \tag{8.1}$$

Table 8.3. Model summary for case-2

R	R^2	SSE	MSE	RMSE	% In(±10%)	% In (±20%)	% In(±30%)
0.860	0.740	0.143	0.0016	0.040	32.95	59.09	81.81

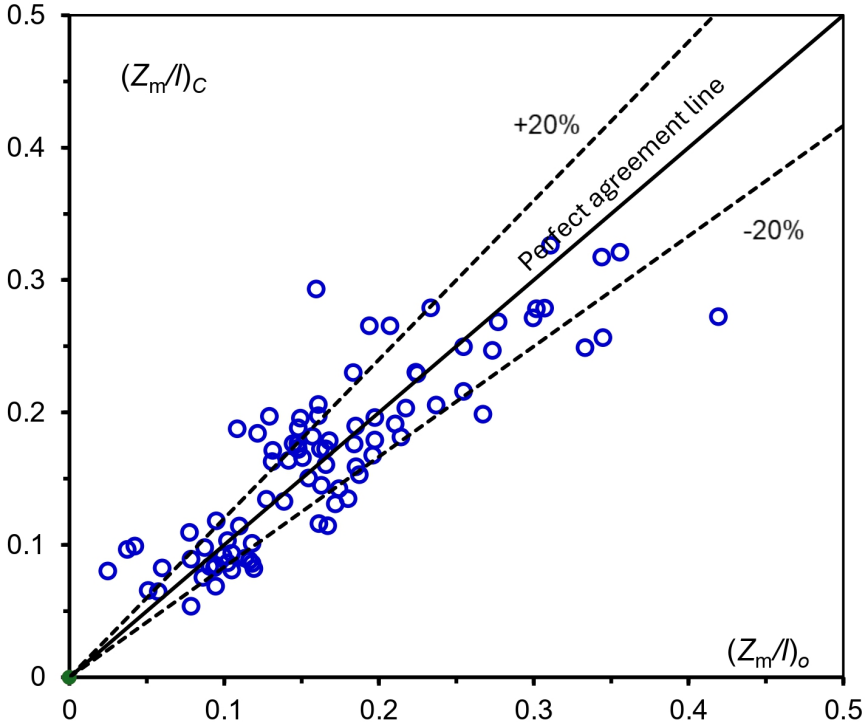


Fig. 8.30. Comparison between observed and predicted values of equilibrium scour depth.

Table 8.4. Subset Regression for case-1

Variables	R-Sq	R-Sq (adj)	PRESS	R-Sq (pred)	Mallows Cp	*S*	AICc	BIC	Cond No	V^2/lg	h_{tw}/l	B/l	H/l	$\Delta y/l$	F_d
1	35.0	34.3	0.4	32.0	42.9	0.064	-228	-221	01.00	×	×	✓	×	×	×
1	29.3	28.4	0.4	24.8	54.2	0.067	-221	-218	01.00	×	×	×	✓	×	×
2	53.5	52.4	0.3	49.4	8.90	0.054	-255	-246	02.22	×	✓	×	×	✓	×
2	44.3	43.0	0.3	39.4	26.8	0.060	-240	-230	02.67	×	×	✓	✓	×	×
3	56.6	55.0	0.3	51.9	4.90	0.053	-259	-248	05.15	×	✓	✓	×	✓	×
3	54.0	52.4	0.3	47.7	9.80	0.054	-254	-243	05.47	×	✓	×	✓	✓	×
4	**58.1**	**56.1**	**0.3**	**51.7**	**3.80**	**0.052**	**-260**	**-246**	**05.33**	×	×	✓	✓	✓	✓
4	57.4	55.4	0.3	52.5	5.20	0.053	-259	-245	07.47	✓	✓	✓	×	✓	×
5	58.5	56.0	0.3	50.9	5.00	0.052	-259	-243	27.69	×	✓	✓	✓	✓	✓
5	58.3	55.7	0.3	51.3	5.50	0.052	-258	-242	12.59	✓	×	✓	✓	✓	✓
6	58.5	55.5	0.3	50.0	07.0	0.053	-256	-238	51.91	✓	✓	✓	✓	✓	✓

*Note-From subset regression the lowest Mallows C_p value is 3.80 and its corresponding R-Sq(adj) is 56.1. Now using the variables of this case the final formula will be

$$\frac{Z_m}{l} = 1.14\left(\frac{B}{l}\right)^{0.63}\left(\frac{H}{l}\right)^{0.42}\left(\frac{\Delta y}{l}\right)^{0.38}\left(F_d\right)^{0.40} \tag{8.2}$$

Table 8.5. Model summary for case-1

R	R^2	SSE	MSE	RMSE	% In(±10%)	% In (±20%)	% In(±30%)
0.821	0.674	0.179	0.0020	0.045	30.68	59.09	82.95

*Note-(±10%), (±20%) and (±30%) indicate deviation from PAL by ±10%, ±20% and ±30% respectively.
**Note-% In indicates how much percentage of data is within the deviated line.

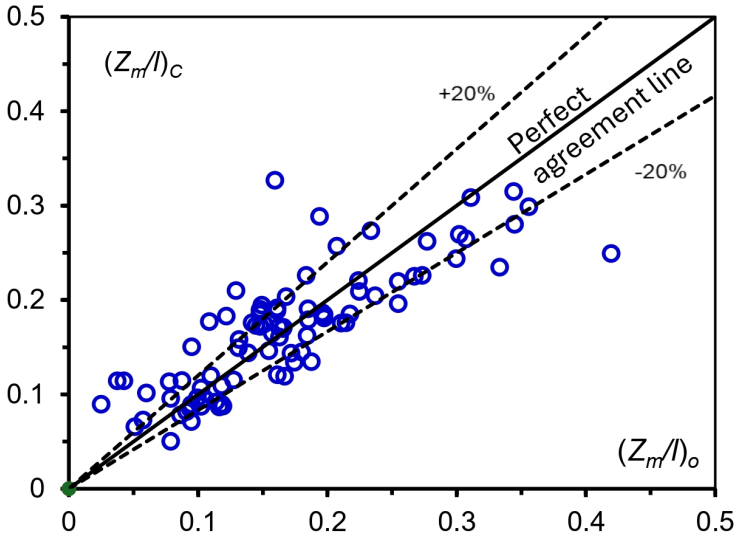


Fig. 8.31. Comparison between observed and predicted values of equilibrium scour depth.

Table 8.6. Subset Regression for case-4

Variables	**R-Sq**	**R-Sq (adj)**	**PRESS**	**R-Sq (pred)**	**Mallows Cp**	***S***	**AICc**	**BIC**	**Cond No**	***V²/lg***	***h_{tw}/l***	***b/l***	***H/l***	***Δy/l***	**F'_d**
1	45.7	45.1	0.3	43.0	43.2	0.058	-244	-237	1.00	×	×	✓	×	×	×
1	29.3	28.4	0.4	24.8	81.6	0.067	-221	-218	1.00	×	×	×	✓	×	×
2	55.9	54.8	0.3	51.8	21.3	0.053	-260	-251	2.12	×	×	✓	✓	×	×
2	54.4	53.3	0.3	50.9	24.8	0.054	-257	-248	1.73	×	×	✓	×	✓	×
3	63.1	61.8	0.2	58.9	6.40	0.049	-278	-262	4.73	×	✓	✓	×	✓	×
3	60.2	58.8	0.2	56.8	13.2	0.051	-267	-255	1.93	✓	×	✓	×	✓	×
4	**64.8**	**63.1**	**0.2**	**59.1**	**4.40**	**0.048**	**-275**	**-262**	**5.54**	×	×	✓	✓	✓	✓

4	64.7	63.0	0.2	60.3	4.60	0.048	-275	-261	6.55	✓	✓	✓	×	✓	×
5	65.4	63.3	0.2	59.1	5.00	0.048	-275	-259	9.90	✓	✓	✓	✓	✓	×
5	65.1	63.0	0.2	59.1	5.70	0.048	-274	-258	13.29	✓	✓	✓	×	✓	✓
6	65.4	62.8	0.2	58.0	7.00	0.048	-272	-254	61.26	✓	✓	✓	✓	✓	✓

*Note-From subset regression the lowest Mallows C_p value is 4.40 and its corresponding R-Sq(adj) is 63.1. Now using the variables of this case the final formula will be

$$\frac{Z_m}{l} = 1.31\left(\frac{b}{l}\right)^{0.83}\left(\frac{H}{l}\right)^{0.41}\left(\frac{\Delta y}{l}\right)^{0.32}\left(F'_d\right)^{0.31} \tag{8.3}$$

Table 8.7. Model summary for case-4

R	R^2	SSE	MSE	RMSE	% In(±10%)	% In (±20%)	% In(±30%)
0.846	0.717	0.156	0.0017	0.042	27.27	60.23	80.68

*Note-(±10%), (±20%) and (±30%) indicate deviation from PAL by ±10%, ±20% and ±30% respectively.
**Note-% In indicates how much percentage of data is within the deviated line.

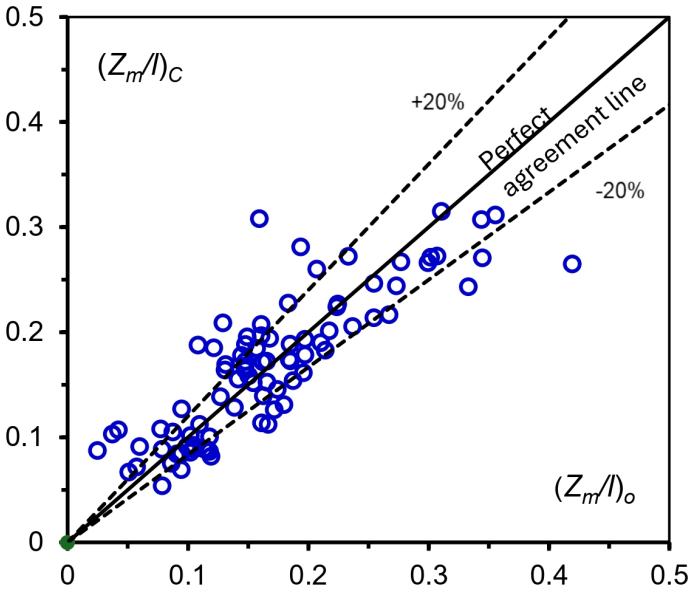


Fig. 8.32. Comparison between observed and predicted values of equilibrium scour depth.

Table 8.8. Subset Regression for case-3

Variable	R-Sq	R-Sq (adj)	PRESS	R-Sq (pred)	Mallows Cp	*S*	AICc	BIC	Cond No	V^2/lg	h_{tw}/l	*B/l*	*H/l*	Δ*y/l*	F'd
1	35.0	34.3	0.4	32.0	40.4	0.064	-228	-221	1.00	×	×	✓	×	×	×
1	29.3	28.4	0.4	24.8	51.5	0.067	-221	-218	1.00	×	×	×	✓	×	×
2	53.5	52.4	0.3	49.4	7.10	0.054	-255	-246	2.22	×	✓	×	×	✓	×
2	44.3	43.0	0.3	39.4	24.6	0.060	-240	-230	2.67	×	×	✓	✓	×	×
3	56.6	55.0	0.3	51.9	3.20	0.053	-259	-248	5.15	×	✓	✓	×	✓	×
3	54.0	52.4	0.3	47.7	8.00	0.054	-254	-243	5.47	×	✓	×	✓	✓	×
4	**57.4**	**55.4**	**0.3**	**52.5**	**3.50**	**0.053**	**-259**	**-245**	**7.47**	✓	✓	✓	×	✓	×
4	57.0	54.9	0.3	50.2	4.40	0.053	-258	-244	9.26	×	✓	✓	✓	✓	×
5	57.7	55.1	0.3	50.5	5.00	0.053	-257	-241	10.13	✓	✓	✓	✓	✓	×
5	57.6	55.0	0.3	50.8	5.20	0.053	-257	-241	14.91	✓	✓	✓	×	✓	✓
6	57.7	54.6	0.3	48.9	7.00	0.053	-254	-236	62.09	✓	✓	✓	✓	✓	✓

*Note- From subset regression the lowest Mallows C_p value is 3.50 and its corresponding R-Sq(adj) is 55.4. Now using the variables of this case the final formula will be

**Note-In this case can not find any equation because Minitab software can not get any correlation for iteration.

Formula derivation by using Spearman's rank coefficient and subset regression method.

Table 8.9. Correlation for Spearman's rank coefficient

Variables	Z_m/l	V^2/lg	h_{tw}/l	*B/l*	*b/l*	*H/l*	Δ*y/l*	F_d	F'd
Z_m/l	1.000								
V^2/lg	0.421	1.000							
h_{tw}/l	0.349	0.560	1.000						
B/l	0.563	0.230	0.378	1.000					
b/l	0.691	0.303	0.370	0.878	1.000				
H/l	0.504	0.354	0.313	0.358	0.264	1.000			
Δ*y/l*	0.407	-0.233	-0.483	0.191	0.196	0.314	1.000		
F_d	0.044	0.542	0.727	-0.121	-0.004	-0.200	-0.694	1.000	
F'd	0.024	0.560	0.760	-0.086	-0.020	-0.170	-0.701	0.990	1.000

Note: *. Correlation is significant at the 0.05 level (2-tailed); **. Correlation is significant at the 0.01 level (2-tailed). The correlation values between *B/l* and *b/l*, F_d, and F'd are 0.878, and 0.99 respectively, indicating strong correlations. Therefore, in both cases significance number <0.001 with **. Consequently, we may neglect one of the terms from *B/l* or *b/l* and F_d or F'd.

However, to create more options for analysis, we will consider one term from each group. **Hence, the non-dimensional group was reduced to the following form-**

Case-1 $$\frac{Z_m}{l} = f_3\left(\frac{V^2}{l\,\mathrm{g}}, \frac{h_{tw}}{l}, \frac{B}{l}, \frac{H}{l}, F_d, \frac{\Delta y}{l}\right)$$

Case-2 $$\frac{Z_m}{l} = f_3\left(\frac{V^2}{l\,\mathrm{g}}, \frac{h_{tw}}{l}, \frac{b}{l}, \frac{H}{l}, F_d, \frac{\Delta y}{l}\right)$$

Case-3 $$\frac{Z_m}{l} = f_3\left(\frac{V^2}{l\,\mathrm{g}}, \frac{h_{tw}}{l}, \frac{B}{l}, \frac{H}{l}, F'_d, \frac{\Delta y}{l}\right)$$

Case-4 $$\frac{Z_m}{l} = f_3\left(\frac{V^2}{l\,\mathrm{g}}, \frac{h_{tw}}{l}, \frac{b}{l}, \frac{H}{l}, F'_d, \frac{\Delta y}{l}\right)$$

*Note- In this case, if we perform subset regression and find the best combination of variables, it will yield the same output (Eq. 8.1, Eq. 8.2, Eq. 8.3) as the Pearson correlation with the subset regression method. Consequently, the formula will be the same, along with identical error metrics (**Table** 8.3, **Table**. 8.5, **Table**. 8.7)

Formula derivation by using Kendull's Tau-b correlation and subset regression method.

Table 8.10. Correlation for Kendull's Tau-b coefficient

Variables	Z_m/l	V^2/lg	h_{tw}/l	B/l	b/l	H/l	$\Delta y/l$	F_d	F'_d
Z_m/l	1.000								
V^2/lg	0.255	1.000							
h_{tw}/l	0.244	0.414	1.000						
B/l	0.382	0.256	0.279	1.000					
b/l	0.562	0.244	0.296	0.772	1.000				
H/l	0.354	0.249	0.227	0.284	0.216	1.000			
$\Delta y/l$	0.287	-0.147	-0.320	0.138	0.150	0.229	1.000		
F_d	0.041	0.380	0.554	-0.092	-0.006	-0.136	-0.484	1.000	
F'_d	0.028	0.399	0.584	-0.062	-0.018	-0.116	-0.497	0.948	1.000

Note: * Correlation is significant at the 0.05 level (2-tailed); **Correlation is significant at the 0.01 level (2-tailed). The correlation values between F_d and F'_d are 0.948, indicating strong correlations. Therefore, in this case, the significance number <0.001 with **. Consequently, we may neglect one of the terms from F_d or F'_d. However, to create more options for analysis, we will consider one term from each group. **Hence, the non-dimensional group was reduced to the following form-**

Case-1 $$\frac{Z_m}{l} = f_3\left(\frac{V^2}{l\,\mathrm{g}}, \frac{h_{tw}}{l}, \frac{b}{l}\frac{B}{l}, \frac{H}{l}, F_d, \frac{\Delta y}{l}\right)$$

Case-2 $$\frac{Z_m}{l} = f_3\left(\frac{V^2}{l\mathrm{g}}, \frac{h_{tw}}{l}, \frac{b}{l}\frac{B}{l}, \frac{H}{l}, F'_d, \frac{\Delta y}{l}\right)$$

*Note- Using these variables, subset regression was performed for each case, and subsequently, formulas were derived for each case.

Table 8.11. Subset Regression for case-1

Variables	R-Sq	R-Sq (adj)	PRESS	R-Sq (pred)	Mallows C_p	*S*	AICc	BIC	Cond No	V^2/lg	h_{tw}/l	B/l	b/l	H/l	$\Delta y/l$	F_d
1	45.7	45.1	0.3	43.0	61.3	0.06	-245	-237	1.00	×	×	×	✓	×	×	×
1	35.0	34.3	0.4	32.0	89.8	0.06	-229	-222	1.00	×	×	✓	×	×	×	×
2	55.9	54.8	0.3	51.8	36.1	0.05	-261	-251	2.10	×	×	×	✓	✓	×	×
2	54.4	53.3	0.3	50.9	40.0	0.05	-258	-248	1.70	×	×	×	✓	×	✓	×
3	63.1	61.8	0.2	58.9	18.7	0.05	-274	-262	4.70	×	✓	×	✓	×	✓	×
3	60.4	59.0	0.2	54.7	26.0	0.05	-268	-256	32.3	×	×	✓	✓	✓	×	×
4	67.4	65.9	0.2	62.3	9.10	0.05	-283	-269	30.7	×	✓	✓	✓	×	✓	×
4	65.6	64.0	0.2	60.2	14.0	0.05	-278	-264	5.40	×	×	×	✓	✓	✓	✓
5	**69.6**	**67.8**	**0.2**	**62.9**	**5.30**	**0.05**	**-287**	**-271**	**38.0**	×	✓	✓	✓	✓	✓	×
5	68.8	66.9	0.2	61.9	7.60	0.05	-284	-268	39.7	×	×	✓	✓	✓	✓	✓
6	70.1	67.8	0.2	62.9	6.10	0.05	-285	-267	39.0	✓	✓	✓	✓	✓	✓	×
6	69.8	67.5	0.2	62.1	6.90	0.05	-284	-266	49.4	×	✓	✓	✓	✓	✓	✓
7	70.1	67.5	0.2	61.9	8.00	0.05	-283	-263	68.8	✓	✓	✓	✓	✓	✓	✓

*Note- From subset regression the lowest Mallows C_p value is 5.0 and its corresponding R-Sq(adj) is 67.8. Now using the variables of this case the final formula will be

$$\frac{Z_m}{l} = 6.57\left(\frac{B}{l}\right)^{-1.25}\left(\frac{b}{l}\right)^{1.85}\left(\frac{\Delta y}{l}\right)^{0.25}\left(\frac{h_{tw}}{l}\right)^{0.24}\left(\frac{H}{l}\right)^{0.34} \tag{8.4}$$

Table 8.12. Model summary for case-1

R	R^2	SSE	MSE	RMSE	% In (±10%)	% In (±20%)	% In (±30%)
0.859	0.739	0.143	0.0016	0.040	36.36	63.63	79.55

*Note-(±10%), (±20%) and (±30%) indicate deviation from PAL by ±10%, ±20% and ±30% respectively.

**Note-% In indicates how much percentage of data is within the deviated line.

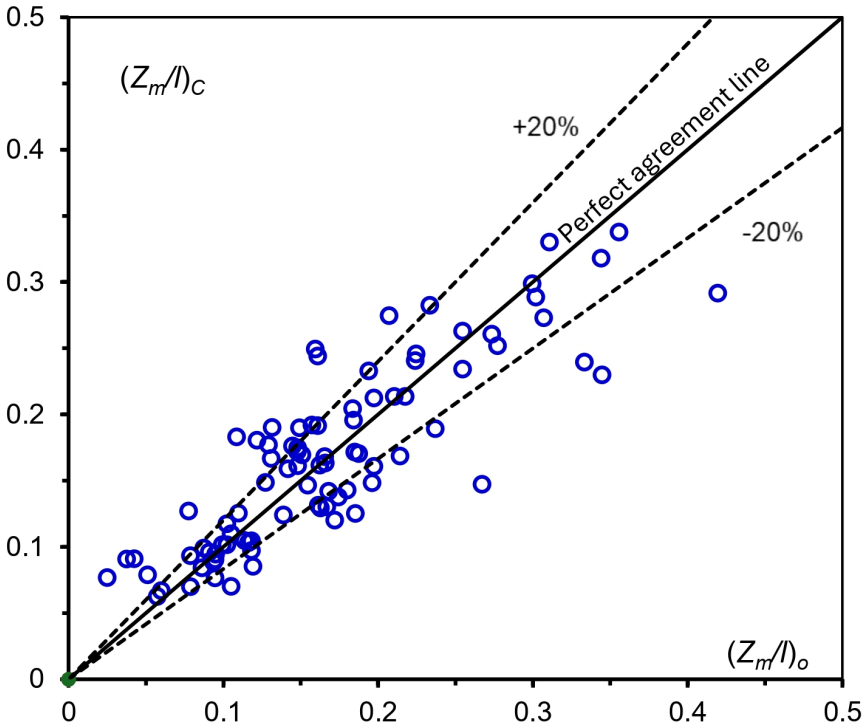


Fig. 8.33. Comparison between observed and predicted values of equilibrium scour depth.

Table 8.13. -Subset Regression for case-2

Variables	R-Sq	R-Sq (adj)	PRESS	R-Sq (pred)	Mallows C_p	S	AICc	BIC	Cond No	V^2/lg	h_{tw}/l	B/l	b/l	H/l	$\Delta y/l$	F'd
1	45.7	45.1	0.3	43.0	61.3	0.059	-244	-237	1.00	×	×	×	✓	×	×	×
1	35.0	34.3	0.4	32.0	89.8	0.064	-228	-222	1.00	×	×	✓	×	×	×	×
2	55.9	54.8	0.3	51.8	36.1	0.053	-260	-251	2.12	×	×	×	✓	✓	×	×
2	54.4	53.3	0.3	50.9	40.0	0.054	-257	-248	1.73	×	×	×	✓	×	✓	×
3	63.1	61.8	0.2	58.9	18.7	0.049	-278	-262	4.73	×	✓	×	✓	×	✓	×
3	60.4	59.0	0.2	54.7	25.9	0.051	-267	-256	32.2	×	×	✓	✓	✓	×	×
4	67.4	65.9	0.2	62.3	9.10	0.046	-282	-269	30.6	×	✓	✓	✓	×	✓	×
4	65.1	63.4	0.2	58.4	15.4	0.048	-276	-263	35.2	×	×	✓	✓	✓	✓	×
5	**69.6**	**67.8**	**0.2**	**62.9**	**5.20**	**0.045**	**-286**	**-271**	**37.9**	×	✓	✓	✓	✓	✓	×
5	68.9	67.1	0.2	62.1	7.10	0.046	-284	-269	37.4	×	×	✓	✓	✓	✓	✓
6	70.1	67.8	0.2	62.9	6.10	0.045	-285	-267	38.9	✓	✓	✓	✓	✓	✓	×
6	69.8	67.5	0.2	62.3	6.80	0.045	-284	-267	41.1	×	✓	✓	✓	✓	✓	✓
7	70.1	67.5	0.2	62.0	8.00	0.045	-283	-263	65.8	✓	✓	✓	✓	✓	✓	✓

*Note- From subset regression the lowest Mallows C_p value is 5.2 and its corresponding R-Sq(adj) is 67.8. Now using the variables of this case the final formula will be the same as that of Eq. 8.4.

$$\frac{Z_m}{l} = 6.57\left(\frac{B}{l}\right)^{-1.25}\left(\frac{b}{l}\right)^{1.85}\left(\frac{\Delta y}{l}\right)^{0.25}\left(\frac{h_{tw}}{l}\right)^{0.24}\left(\frac{H}{l}\right)^{0.34} \quad (8.4)$$

Formula derivation by using Stepwise regression and subset regression methods.

Table 8.14. Deduction of variables using Stepwise Regression

Model	Variables Entered	Method
1	*b/l*	Stepwise (Criteria: Probability-of-F-to-enter <= .050, Probability-of-F-to-remove >= .100).
2	*H/l*	Stepwise (Criteria: Probability-of-F-to-enter <= .050, Probability-of-F-to-remove >= .100).
3	*B/l*	Stepwise (Criteria: Probability-of-F-to-enter <= .050, Probability-of-F-to-remove >= .100).
4	$\Delta y/l$	Stepwise (Criteria: Probability-of-F-to-enter <= .050, Probability-of-F-to-remove >= .100).
5	h_{tw}/l	Stepwise (Criteria: Probability-of-F-to-enter <= .050, Probability-of-F-to-remove >= .100).

Table 8.15.:-Subset Regression from variables deducted by stepwise regression

Variables	R-Sq	R-Sq (adj)	PRESS	R-Sq (pred)	Mallows C_p	*S*	AICc	BIC	Cond No	*B/l*	*b/l*	*H/l*	$\Delta y/l$	h_{tw}/l
1	45.7	45.1	0.3	43.0	62.7	0.06	-245	-237	1.0	×	✓	×	×	×
1	35.0	34.3	0.4	32.0	91.4	0.06	-229	-222	1.0	✓	×	×	×	×
2	55.9	54.8	0.3	51.8	37.2	0.05	-261	-251	2.0	×	✓	✓	×	×
2	54.4	53.3	0.3	50.9	41.1	0.05	-258	-248	2.0	×	✓	×	✓	×
3	63.1	61.8	0.2	58.9	19.6	0.05	-274	-262	5.0	×	✓	×	✓	✓
3	60.4	59.0	0.2	54.7	26.9	0.05	-268	-256	32	✓	✓	✓	×	×
4	**67.4**	**65.9**	**0.2**	**62.3**	**9.90**	**0.05**	**-283**	**-269**	**31**	**✓**	**✓**	**×**	**✓**	**✓**
4	65.1	63.4	0.2	58.4	16.2	0.05	-277	-263	35	✓	✓	✓	✓	×
5	69.6	67.8	0.2	62.9	6.00	0.05	-287	-271	38	✓	✓	✓	✓	✓

*Note- From subset regression, the Mallows C_p value is taken as 9.9 and its corresponding R-Sq(adj) is 67.4. Now using the variables of this case the final formula will be

$$\frac{Z_m}{l} = 4.45\left(\frac{B}{l}\right)^{-0.92}\left(\frac{b}{l}\right)^{1.54}\left(\frac{\Delta y}{l}\right)^{0.34}\left(\frac{h_{tw}}{l}\right)^{0.34} \quad (8.5)$$

Table 8.16. Model summary for stepwise regression

R	R^2	SSE	MSE	RMSE	% In (±10%)	% In (±20%)	% In (±30%)
0.836	0.699	0.165	0.0019	0.043	31.82	57.95	77.27

*Note-(±10%), (±20%) and (±30%) indicate deviation from PAL by ±10%, ±20% and ±30% respectively.
**Note-% In indicates how much percentage of data is within the deviated line.

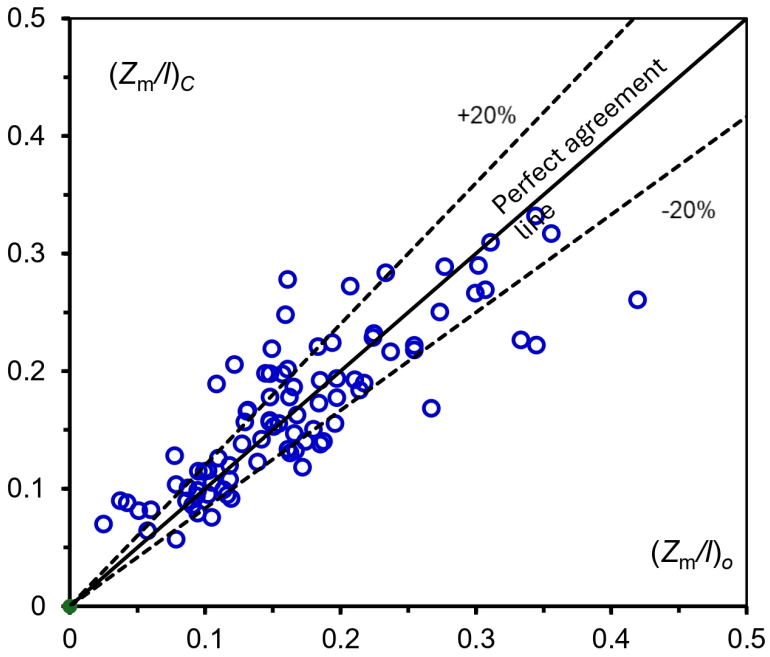


Fig. 8.34. Comparison between observed and predicted values of equilibrium scour depth.

Formula derivation by using backward regression and subset regression methods.

Table. 8.17. Deduction of variables using Back-word Regression

Variables Entered/Removed			
Model	**Variables Entered**	**Variables Removed**	**Method**
1			Enter
2		F'_d	Backward (criterion: Probability of F-to-remove >= .100).
3	All Variables	F_d	Backward (criterion: Probability of F-to-remove >= .100).
4		V^2/lg	Backward (criterion: Probability of F-to-remove >= .100).
Dependent Variable: Z_m/l			

Table. 8.18. Subset Regression from variables deducted by backward regression

Variables	R-Sq	R-Sq (adj)	PRESS	R-Sq (pred)	Mallows C_p	S	AICc	BIC	Cond No	h_{tw}/l	B/l	b/l	H/l	$\Delta y/l$
1	45.7	45.1	0.3	43	62.7	0.06	-245	-237	1	×	×	✓	×	×
1	35	34.3	0.4	32	91.4	0.06	-229	-222	1	×	✓	×	×	×
2	55.9	54.8	0.3	51.8	37.2	0.05	-261	-251	2	×	×	✓	✓	×
2	54.4	53.3	0.3	50.9	41.1	0.05	-258	-248	2	×	×	✓	×	✓
3	63.1	61.8	0.2	58.9	19.6	0.05	-274	-262	5	✓	×	✓	×	✓
3	60.4	59	0.2	54.7	26.9	0.05	-268	-256	32	×	✓	✓	✓	×
4	67.4	65.9	0.2	62.3	9.9	0.05	-283	-269	31	✓	✓	✓	×	✓
4	65.1	63.4	0.2	58.4	16.2	0.05	-277	-263	35	×	✓	✓	✓	✓
5	**69.6**	**67.8**	**0.2**	**62.9**	**6**	**0.05**	**-287**	**-271**	**38**	✓	✓	✓	✓	✓

*Note- From subset regression the lowest Mallows C_p value is 6.0 and its corresponding R-Sq(adj) is 67.8. Now using the variables of this case the final formula will be the same as that of Eq. 8.4

$$\frac{Z_m}{l} = 6.57\left(\frac{B}{l}\right)^{-1.25}\left(\frac{b}{l}\right)^{1.85}\left(\frac{\Delta y}{l}\right)^{0.25}\left(\frac{h_{tw}}{l}\right)^{0.24}\left(\frac{H}{l}\right)^{0.34} \tag{8.4}$$

Formula derivation by using Forward regression and subset regression methods.

In this method, after the forward regression total number of variables will remain the same in the process of the Stepwise or backward method. Therefore, the final formula will be the same likes Forward and Backward regression analysis like Eq. 8.4 or Eq. 8.5.

8.2(b). Formula derivation by using different statistical techniques.

This method first developed the equations by taking the non-dimensional parameter for the height of log vane(*H)*, i.e. the parameter obtained from dimensionless analysis (Eq. 6.6)

Formula derivation by using Pearson correlation and subset regression methods.

Table 8.19. Correlation for Pearson correlation coefficient

Variables	Z_m/H	V^2/Hg	h_{tw}/H	B/H	b/H	b/l	l/H	$\Delta y/H$	Fd	F'd
Z_m/H	1.000									
V^2/Hg	0.185	1.000								
h_{tw}/H	0.297	0.406	1.000							

B/H	0.539	0.053	0.418	1.000						
b/H	0.615	0.084	0.456	0.96	1.000					
b/l	0.499	-0.203	0.199	0.445	0.477	1.000				
l/H	0.218	0.179	0.27	0.593	0.605	-0.372	1.000			
Δy/H	0.382	-0.213	-0.527	0.244	0.215	0.078	0.166	1.000		
Fd	0.264	0.728	**0.886**	0.196	0.272	0.005	0.225	-0.528	1.000	
F'd	0.237	0.724	0.900	0.207	0.256	0.000	0.211	-0.543	**0.994**	1.000

Note: * Correlation is significant at the 0.05 level (2-tailed); **. Correlation is significant at the 0.01 level (2-tailed). The correlation values between h_{tw}/H and F_d, F_d and F'_d are 0.886, and 0.994 respectively, indicating strong correlations. Therefore, in both cases significance number<0.001 with **. Consequently, we may neglect one of the terms from h_{tw}/H or F_d and F_d or F'_d. However, to create more options for analysis, we will consider one term from each group. **Hence, the non-dimensional group was reduced to the following form-**

Case-1 $$\frac{Z_m}{H} = f_4\left(\frac{V^2}{H\,\mathrm{g}}, \frac{h_{tw}}{H}, \frac{B}{H}, \frac{b}{H}, \frac{b}{l}, \frac{l}{H}, F'_d, \frac{\Delta y}{H}\right)$$

Case-2 $$\frac{Z_m}{H} = f_4\left(\frac{V^2}{H\,\mathrm{g}}, \frac{B}{H}, \frac{b}{H}, \frac{b}{l}, \frac{l}{H}, F_d, \frac{\Delta y}{H}\right)$$

*Note- Using these variables, subset regression was performed for each case, and subsequently, formulas were derived for each case.

Table. 8.20. Subset regression for case-1

Variables	R-Sq	R-Sq (adj)	PRESS	R-Sq (pred)	Mallows C_p	*S*	AICc	BIC	Cond No	V^2/Hg	h_{tw}/H	B/H	b/H	b/l	l/H	Δy/H	F'd
1	37.8	37.1	6.8	34.8	77.5	0.275	27	34	1	×	×	×	✓	×	×	×	×
1	29.0	28.2	7.7	25.8	100	0.293	38	45	1	×	×	✓	×	×	×	×	×
2	49.0	47.8	5.7	45.3	50.3	0.250	11	21	3	×	✓	×	×	×	×	✓	×
2	44.3	43.0	6.3	39.9	62.5	0.261	19	28	2	×	×	×	✓	×	×	✓	×
3	62.5	61.1	4.3	58.8	17.5	0.216	-13	-2.	3	×	×	×	×	✓	×	✓	✓
3	59.2	57.7	4.7	55.0	26.0	0.225	-6.0	6	4	×	✓	×	×	✓	×	✓	×
4	65.5	63.8	4.0	61.2	11.6	0.208	-18	-5	5	×	×	×	×	✓	✓	✓	✓
4	64.3	62.6	4.2	59.8	14.7	0.212	-15	-2	6	×	×	×	✓	✓	×	✓	✓
5	**69.3**	**67.4**	**3.7**	**64.2**	**3.80**	**0.198**	**-26**	**-10**	**32**	×	×	✓	×	✓	✓	✓	✓
5	67.4	65.4	4.0	61.6	8.70	0.204	-21	-5	64	×	×	✓	✓	✓	×	✓	✓
6	69.4	67.2	3.9	62.5	5.40	0.198	-24	-6	141	×	×	✓	✓	✓	✓	✓	✓
6	69.4	67.1	3.8	63.6	5.40	0.199	-24	-6	41	✓	×	✓	×	✓	✓	✓	✓
7	69.5	66.8	4.0	61.9	7.10	0.199	-22	-2	150	✓	×	✓	✓	✓	✓	✓	✓
7	69.5	66.8	3.9	63.0	7.30	0.200	-22	-2	299	✓	✓	✓	×	✓	✓	✓	✓
8	69.6	66.5	8.1	61.2	9.00	0.201	-20	2	339	✓	✓	✓	✓	✓	✓	✓	✓

*Note- From subset regression the lowest Mallows C_p value is 3.8 and its corresponding R-Sq(adj) is 67.4. Now using the variables of this case the final formula will be

$$\frac{Z_m}{H} = 3.93\left(\frac{B}{H}\right)^{-0.80}\left(\frac{b}{l}\right)^{1.39}\left(\frac{l}{H}\right)^{0.96}\left(\frac{\Delta y}{H}\right)^{0.33}\left(F'_d\right)^{0.29} \tag{8.6}$$

Table 8.21. Model summary for case-1

R	R^2	SSE	MSE	RMSE	% In(±10%)	% In (±20%)	% In(±30%)
0.826	0.683	3.31	0.0376	0.194	37.50	64.77	80.68

*Note-(±10%), (±20%) and (±30%) indicate deviation from PAL by ±10%, ±20% and ±30% respectively.

**Note-% In indicates how much percentage of data within the deviated line.

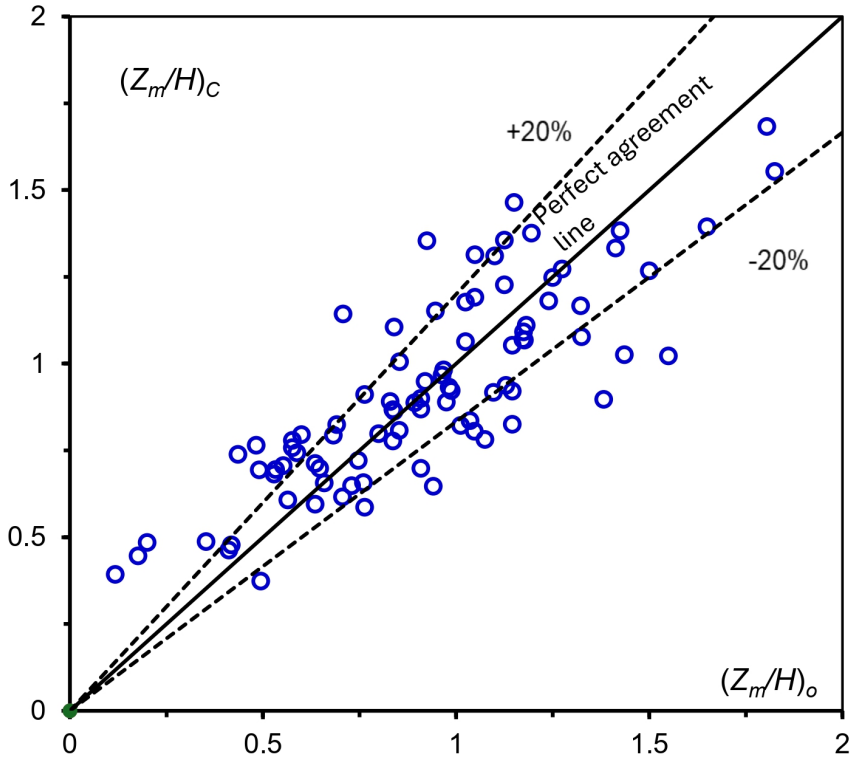


Fig. 8.35. Comparison between observed and predicted values of equilibrium scour depth

Table 8.22. Subset Regression for case-2

Variables	R-Sq	R-Sq (adj)	PRESS	R-Sq (pred)	Mallows Cp	*S*	AICc	BIC	Cond No	V^2/Hg	*B/H*	*b/H*	*b/l*	*l/H*	$\Delta y/H$	F_d
1	37.8	37.1	6.8	34.8	78.4	0.27	26.6	33.8	1.00	×	×	✓	×	×	×	×
1	29.0	28.2	7.7	25.8	101	0.29	38.2	45.4	1.00	×	✓	×	×	×	×	×
2	44.7	43.4	6.2	40.4	62.3	0.26	18.5	27.9	3.24	×	×	×	×	×	✓	✓
2	44.3	43.0	6.3	39.9	63.3	0.26	19.0	28.5	1.55	×	×	✓	×	×	✓	×
3	64.3	63.0	8.1	60.7	13.3	0.21	-18.0	-6.10	3.29	×	×	×	✓	×	✓	✓
3	55.5	53.9	5.1	51.5	36.3	0.24	1.68	13.3	5.07	×	×	✓	×	×	✓	✓
4	66.8	65.2	3.9	62.7	8.50	0.20	-22.0	-8.20	5.43	×	×	×	✓	✓	✓	✓
4	65.7	68.1	4.0	61.4	11.5	0.21	-19.0	-5.20	6.16	×	×	✓	✓	×	✓	✓
5	**69.3**	**67.4**	**3.7**	**68.1**	**4.20**	**0.20**	**-26.0**	**-10.0**	**32.3**	×	✓	×	✓	✓	✓	✓
5	67.8	65.9	3.9	62.6	8.00	0.20	-22.0	-6.40	77.6	×	×	✓	✓	✓	✓	✓
6	69.3	67.1	3.8	63.5	6.00	0.20	-24.0	-6.10	45.1	✓	✓	×	✓	✓	✓	✓
6	69.3	67.0	3.9	62.2	6.20	0.20	-24.0	-5.90	148	×	✓	✓	✓	✓	✓	✓
7	69.3	66.7	4.0	61.5	8.00	0.20	-22.0	-1.70	153	✓	✓	✓	✓	✓	✓	✓

*Note- From subset regression the lowest Mallows C_p value is 4.2 and its corresponding R-Sq(adj) is 67.4. Now using the variables of this case the final formula will be

$$\frac{Z_m}{H} = 3.93\left(\frac{B}{H}\right)^{-0.51}\left(\frac{b}{l}\right)^{1.1}\left(\frac{l}{H}\right)^{0.67}\left(\frac{\Delta y}{H}\right)^{0.33}\left(F_d\right)^{0.29} \tag{8.7}$$

Table 8.23. Model summary for case-2

R	R^2	SSE	MSE	RMSE	% In (±10%)	% In (±20%)	% In (±30%)
0.826	0.683	3.31	0.0376	0.194	37.50	64.77	80.68

*Note-(±10%), (±20%) and (±30%) indicate deviation from PAL by ±10%, ±20% and ±30% respectively.

**Note-% In indicates how much percentage of data is within the deviated line.

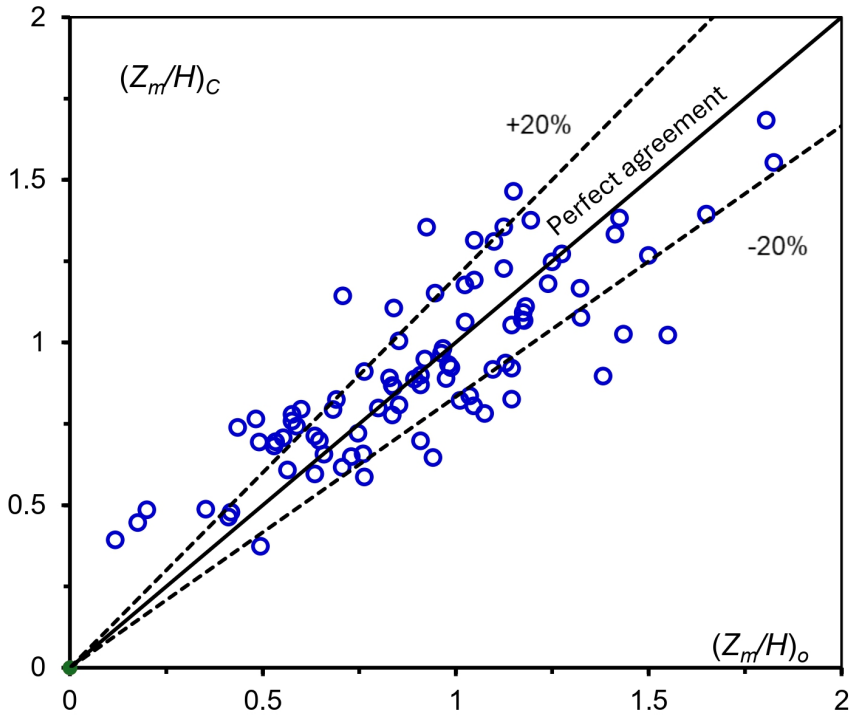


Fig. 8.36. Comparison between observed and predicted values of equilibrium scour depth

Formula derivation using Spearman's rank coefficient and subset regression methods.

Table 8.24. Correlation for Spearman's rank coefficient

Variables	Z_m/H	V^2/Hg	h_{tw}/H	B/H	b/H	b/l	l/H	$\Delta y/H$	F_d	F'_d
Z_m/H	1.000									
V^2/Hg	0.245	1.000								
h_{tw}/H	0.293	0.489	1.000							
B/H	0.552	0.266	0.313	1.000						
b/H	0.639	0.308	0.349	0.973	1.000					
b/l	0.494	-0.145	0.153	0.441	0.457	1.000				
l/H	0.272	0.393	0.249	0.643	0.686	-0.267	1.000			
$\Delta y/H$	0.268	-0.284	-0.617	0.209	0.212	0.033	0.181	1.000		
F_d	0.287	0.696	0.905	0.115	0.193	-0.004	0.197	-0.61	1.000	
F'_d	0.244	0.687	0.918	0.106	0.161	-0.020	0.165	-0.632	0.99	1.000

Note: * Correlation is significant at the 0.05 level (2-tailed); **. Correlation is significant at the 0.01 level (2-tailed). The correlation values between h_{tw}/H and F_d, F_d and F'_d are 0.905, and 0.99 respectively, indicating strong correlations. Therefore, in both cases significance number <0.001 with **. Consequently, we may neglect one of the terms from h_{tw}/H or F_d and F_d or F'_d. However, to create more options for analysis, we will consider one term from each group.

Hence, the non-dimensional group was reduced to the following form-

Case-1 $$\frac{Z_m}{H} = f_4\left(\frac{V^2}{H\,\mathrm{g}}, \frac{h_{tw}}{H}, \frac{B}{H}, \frac{b}{H}, \frac{b}{l}, \frac{l}{H}, F'_d, \frac{\Delta y}{H}\right)$$

Case-2 $$\frac{Z_m}{H} = f_4\left(\frac{V^2}{H\,\mathrm{g}}, \frac{B}{H}, \frac{b}{H}, \frac{b}{l}, \frac{l}{H}, F_d, \frac{\Delta y}{H}\right)$$

*Note-In this case if we do subset regression and find the best combination of variables, it also gives the same output as the Pearson correlation with the subset regression method. So, the formula will be the same along with the same error matrices. Therefore, the final formula will be

$$\frac{Z_m}{H} = 3.93\left(\frac{B}{H}\right)^{-0.80}\left(\frac{b}{l}\right)^{1.39}\left(\frac{l}{H}\right)^{0.96}\left(\frac{\Delta y}{H}\right)^{0.33}\left(F'_d\right)^{0.29} \tag{8.6}$$

$$\frac{Z_m}{H} = 3.93\left(\frac{B}{H}\right)^{-0.51}\left(\frac{b}{l}\right)^{1.1}\left(\frac{l}{H}\right)^{0.67}\left(\frac{\Delta y}{H}\right)^{0.33}\left(F_d\right)^{0.29} \tag{8.7}$$

Formula derivation by using Kendull's Tau-b correlation and subset regression methods.

Table 8.25.- Correlation for Kendull's Tau-b coefficient

Variables	Z_m/H	V^2/Hg	h_{tw}/H	B/H	b/H	b/l	l/H	$\Delta y/H$	Fd	F'd
Z_m/H	1.000									
V^2/Hg	0.161	1.000								
h_{tw}/H	0.202	0.354	1.000							
B/H	0.409	0.256	0.232	1.000						
b/H	0.473	0.272	0.244	0.908	1.000					
b/l	0.377	-0.112	0.116	0.346	0.345	1.000				
l/H	0.201	0.279	0.171	0.468	0.537	-0.217	1.000			
$\Delta y/H$	0.186	-0.176	-0.416	0.157	0.155	0.026	0.119	1.000		
Fd	0.201	0.522	0.766	0.089	0.144	-0.006	0.134	-0.392	1.000	
F'd	0.173	0.511	0.803	0.081	0.115	-0.018	0.110	-0.418	0.948	1.000

Note: *. Correlation is significant at the 0.05 level (2-tailed); **. Correlation is significant at the 0.01 level (2-tailed). The correlation values between F_d and F'_d are 0.948, indicating strong correlations. Therefore, in this case, the significance number <0.01 with **. Consequently, we may neglect one of the terms from F_d and F'_d. However, to create more options for analysis, we will consider one term from each group. **Hence, the non-dimensional group was reduced to the following form-**

Case-1 $$\frac{Z_m}{H} = f_4\left(\frac{V^2}{H\,\mathrm{g}}, \frac{h_{tw}}{H}, \frac{B}{H}, \frac{b}{l}, \frac{l}{H}, F'_d, \frac{\Delta y}{H}\right)$$

Case-2 $$\frac{Z_m}{H} = f_4\left(\frac{V^2}{H\,\mathrm{g}}, \frac{h_{tw}}{H}, \frac{b}{H}, \frac{b}{l}, \frac{l}{H}, F'_d, \frac{\Delta y}{H}\right)$$

Case-3 $$\frac{Z_m}{H} = f_4\left(\frac{V^2}{Hg}, \frac{B}{H}, \frac{b}{l}, \frac{l}{H}, F_d, \frac{\Delta y}{H}\right)$$

Case-4 $$\frac{Z_m}{H} = f_4\left(\frac{V^2}{Hg}, \frac{b}{H}, \frac{b}{l}, \frac{l}{H}, F_d, \frac{\Delta y}{H}\right)$$

*Note- Using these variables, subset regression is performed for each case, and subsequently, formulas are derived for each case.

Table 8.26. Subset Regression for case-1

Variables	R-Sq	R-Sq (adj)	PRESS	R-Sq (pred)	Mallows C_p	*S*	AICc	BIC	Cond No	V^2/Hg	*b/l*	*l/H*	*Δy/H*	h_{tw}/H	F_d'	B/H
1	29.0	28.2	7.7	25.8	102	0.3	38.2	45.4	1.0	×	×	×	×	×	×	✓
1	24.9	24.0	8.2	21.6	113	0.3	43.2	50.4	1.0	×	✓	×	×	×	×	×
2	49.0	47.8	5.7	45.3	52	0.3	11.3	20.7	3.2	×	×	×	✓	✓	×	×
2	43.8	42.5	6.3	39.8	65	0.3	19.9	29.3	2.2	×	✓	✓	×	×	×	×
3	62.5	61.1	4.3	58.8	18	0.2	-13.4	-1.7	3.4	×	✓	×	✓	×	✓	×
3	59.2	57.7	4.7	55.0	27	0.2	-6.0	5.6	3.8	×	✓	×	✓	✓	×	×
4	65.5	63.8	4.0	61.2	12	0.2	-18.5	-4.7	5.5	×	✓	✓	✓	×	✓	×
4	62.9	61.1	4.4	58.3	19	0.2	-12.1	1.8	5.8	×	✓	×	✓	×	✓	✓
5	**69.3**	**67.4**	**3.7**	**64.2**	**4.5**	**0.2**	**-26.3**	**-10.4**	**32.3**	×	✓	✓	✓	×	✓	✓
5	65.8	63.7	8.1	60.6	14	0.2	-16.8	-0.8	42.3	×	✓	✓	✓	✓	✓	×
6	69.4	67.1	3.8	63.6	6	0.2	-24.3	-6.3	41.1	✓	✓	✓	✓	×	✓	✓
6	69.3	67.0	3.8	63.4	6	0.2	-24.0	-6.0	48.5	×	✓	✓	✓	✓	✓	✓
7	69.5	66.8	3.9	63.0	8	0.2	-22.0	-2.0	298.5	✓	✓	✓	✓	✓	✓	✓

*Note- From subset regression the lowest Mallows C_p value is 4.50 and its corresponding R-Sq(adj) is 67.4. Now using the variables of this case the final formula will be the same as that of case 1 of Pearson Correlation or Spearsman rank cofficient (Eq. 8.6) method.

$$\frac{Z_m}{H} = 3.93\left(\frac{B}{H}\right)^{-0.80}\left(\frac{b}{l}\right)^{1.39}\left(\frac{l}{H}\right)^{0.96}\left(\frac{\Delta y}{H}\right)^{0.33}\left(F'_d\right)^{0.29} \tag{8.6}$$

Table 8.27. Subset Regression for case-1

Variables	R-Sq	R-Sq (adj)	PRESS	R-S(pre	Mallows C_p	*S*	AICc	BIC	Cond No	V^2/Hg	*b/l*	*l/H*	*Δy/H*	h_{tw}/H	F_d'	b/H	
1	38	37.1	7	35	65	0.27	27	34	1	×	×	×	×	×	×	×	✓
1	25	24.0	8	22	96	0.30	43	50	1	×	✓	×	×	×	×	×	×
2	49	47.8	6	45	40	0.25	11	21	3	×	×	×	✓	✓	×	×	×
2	44	43.0	6	40	52	0.26	19	28	2	×	×	×	✓	×	×	✓	
3	63	61.1	4	59	10	0.22	-13	-2	3	×	✓	×	✓	×	✓	×	
3	59	57.7	5	55	18	0.23	-6	6	4	×	✓	×	✓	✓	×	×	
4	**66**	**63.8**	**4**	**61**	**4.8**	**0.21**	**-18**	**-5**	**5**	×	✓	✓	✓	×	✓	×	
4	64	62.6	4	60	7.7	0.21	-15	-2	6	×	✓	×	✓	×	✓	✓	
5	66	64.3	4	61	4.6	0.21	-18	-3	77	×	✓	✓	✓	×	✓	✓	
5	66	63.7	4	61	6.1	0.21	-17	-1	42	×	✓	✓	✓	✓	✓	×	
6	67	64.2	4	60	6.0	0.21	-17	1	115	×	✓	✓	✓	✓	✓	✓	
6	67	68.1	4	60	6.3	0.21	-16	2	99	✓	✓	✓	✓	×	✓	✓	
7	67	63.7	4	60	8.0	0.21	-14	6	277	✓	✓	✓	✓	✓	✓	✓	

*Note-From subset regression the lowest Mallows Cp value is 4.8 and its corresponding R-Sq(adj) is 63.8. Now using the variables of this case the final formula will be

$$\frac{Z_m}{H} = 1.51\left(\frac{b}{l}\right)^{0.64}\left(\frac{l}{H}\right)^{0.19}\left(\frac{\Delta y}{H}\right)^{0.34}\left(\mathrm{F'_d}\right)^{0.31} \tag{8.8}$$

Table 8.28. Model summary for case-2

R	R^2	SSE	MSE	RMSE	% In (±10%)	% In (±20%)	% In (±30%)
0.806	0.651	7.533	0.0856	0.292	30.68	63.63	82.95

*Note-(±10%), (±20%) and (±30%) indicate deviation from PAL by ±10%, ±20% and ±30% respectively.

**Note-% In indicates how much percentage of data is within the deviated line.

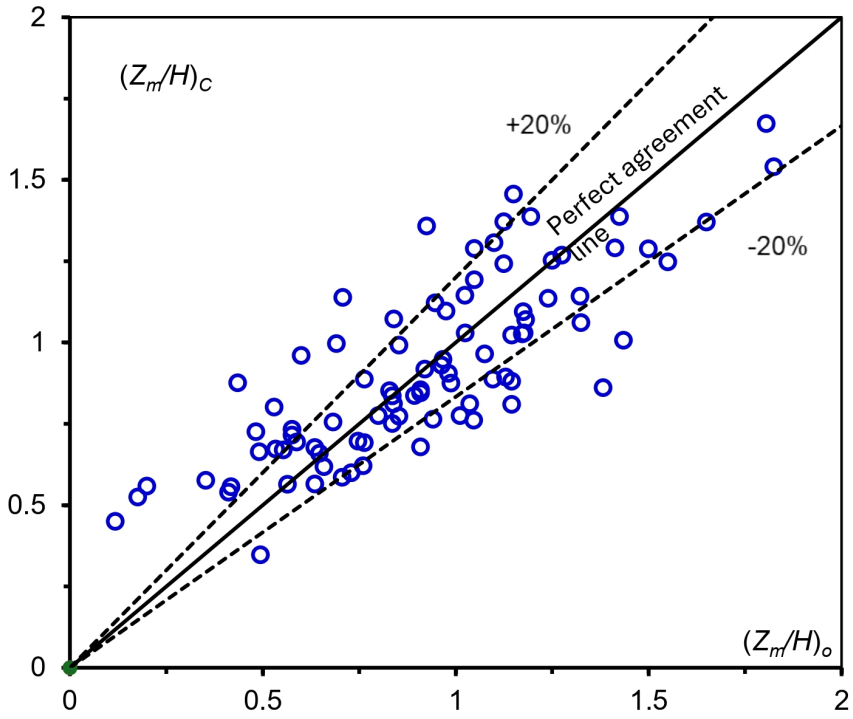


Fig. 8.37. Comparison between observed and predicted values of equilibrium scour depth

Table 8.29. Subset regression for case-3

Variables	R-Sq	R-Sq (adj)	PRESS	R-Sq (pred)	Mallows C_p	S	AICc	BIC	CondNo	V^2/Hg	b/l	l/H	$\Delta y/H$	B/H	F_d
1	29	28.2	8	25.8	104	0.29	38	45	1	×	×	×	×	✓	×
1	25	24.0	8	21.6	115	0.30	43	50	1	×	✓	×	×	×	×
2	45	43.4	6	40.4	68.1	0.26	18	28	3	×	×	×	✓	×	✓
2	44	42.5	6	39.8	66.6	0.26	20	29	2	×	✓	✓	×	×	×
3	64	63.0	4	60.7	14.4	0.21	-18	-6	3	×	✓	×	✓	×	✓
3	52	50.0	6	47.3	47.6	0.24	9.0	20	5	×	×	×	✓	✓	✓
4	67	65.2	4	62.7	9.60	0.20	-22	-8	5	×	✓	✓	✓	×	✓
4	65	63.1	4	60.3	15.1	0.21	-17	-3	5	×	✓	×	✓	✓	✓
5	**69**	**67.4**	**4**	**68.1**	**5.20**	**0.20**	**-26**	**-10**	**32**	×	✓	✓	✓	✓	✓
5	67	64.8	4	62.0	11.6	0.21	-20	-4	17	✓	✓	✓	✓	×	✓
6	69	67.1	4	63.5	7.00	0.20	-24	-6	45	✓	✓	✓	✓	✓	✓

*Note- From subset regression the lowest Mallows C_p value is 5.2 and its corresponding R-Sq(adj) is 67.4. Now using the variables of this case the final formula will be the same as that of Eq. 8.7.

$$\frac{Z_m}{H} = 3.93\left(\frac{B}{H}\right)^{-0.51}\left(\frac{b}{l}\right)^{1.1}\left(\frac{l}{H}\right)^{0.67}\left(\frac{\Delta y}{H}\right)^{0.33}\left(F_d\right)^{0.29} \tag{8.7}$$

Table 8.30. Subset Regression for case-4

Variables	R-Sq	R-Sq (adj)	PRESS	R-Sq (pred)	Mallows C_p	S	AICc	BIC	Cond No	V^2/Hg	b/l	l/H	Δy/H	b/H	F_d
1	38	37.1	7	35	73	0.3	27	34	1	×	×	×	×	✓	×
1	25	24.0	8	22	105	0.3	43	50	1	×	✓	×	×	×	×
2	45	43.4	6	40	57	0.3	18	28	3	×	×	×	✓	×	✓
2	44	43.0	6	40	58	0.3	19	28	2	×	×	×	✓	✓	×
3	64	63.0	4	61	10	0.2	-18	-6	3	×	✓	×	✓	×	✓
3	56	53.9	5	52	32	0.2	2	13	5	×	×	×	✓	✓	✓
4	**67**	**65.2**	**4**	**63**	**5.6**	**0.2**	**-22**	**-8**	**5**	×	✓	✓	✓	×	✓
4	66	68.1	4	61	8.4	0.2	-19	-5	6	×	✓	×	✓	✓	✓
5	68	65.9	4	63	5.1	0.2	-22	-6	78	×	✓	✓	✓	✓	✓
5	67	64.8	4	62	7.6	0.2	-20	-4	17	✓	✓	✓	✓	×	✓
6	68	65.5	4	62	7.0	0.2	-20	-2	100	✓	✓	✓	✓	✓	✓

*Note- From subset regression the lowest Mallows C_p value is 5.6 and its corresponding R-Sq(adj) is 65.2. Now using the variables of this case the final formula will be

$$\frac{Z_m}{H} = 2.28\left(\frac{b}{l}\right)^{0.61}\left(\frac{l}{H}\right)^{0.16}\left(\frac{\Delta y}{H}\right)^{0.34}\left(F_d\right)^{0.32} \tag{8.9}$$

Table 8.31. Model summary for case-4

R	R^2	SSE	MSE	RMSE	% In (±10%)	% In (±20%)	% In (±30%)
0.820	0.672	3.428	0.039	0.197	35.22	60.27	84.09

*Note-(±10%), (±20%) and (±30%) indicate deviation from PAL by ±10%, ±20% and ±30% respectively.

**Note-% In indicates how much percentage of data is within the deviated line.

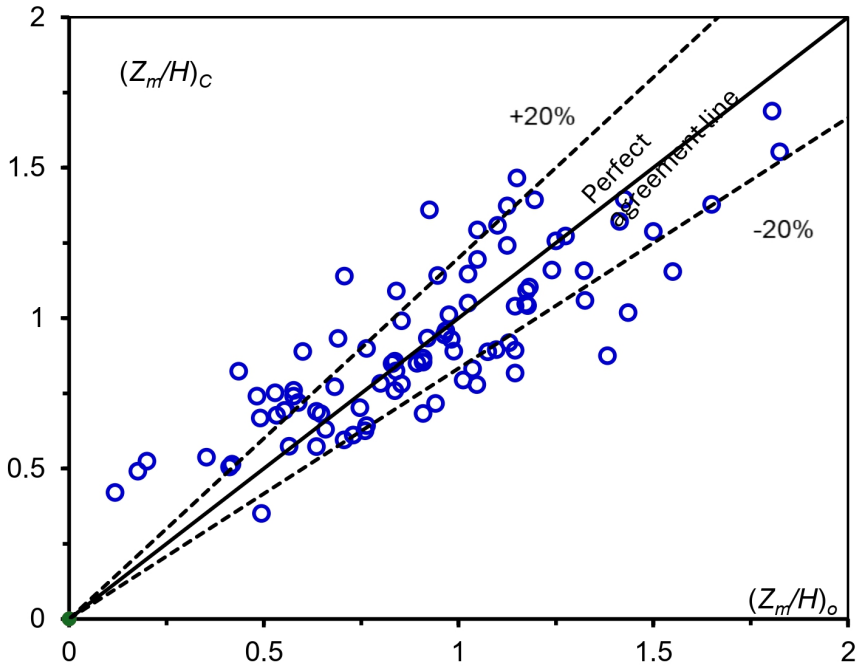


Fig. 8.38. Comparison between observed and predicted values of equilibrium scour depth

Formula derivation by using forward regression and subset regression methods.

Table 8.32. Forward regression analysis.

Model	Variables Entered	Method
1	***b/H***	Forward (Criterion: Probability-of-F-to-enter <= .050)
2	**Δ*y/H***	Forward (Criterion: Probability-of-F-to-enter <= .050)
3	**F_d**	Forward (Criterion: Probability-of-F-to-enter <= .050)
4	***b/l***	Forward (Criterion: Probability-of-F-to-enter <= .050)
5	***l/H***	Forward (Criterion: Probability-of-F-to-enter <= .050)
6	***B/H***	Forward (Criterion: Probability-of-F-to-enter <= .050)

Table 8.33. Subset regression analysis.

Variables	R-Sq	R-Sq (adj)	PRESS	R-Sq (pred)	Mallows Cp	*S*	AICc	BIC	Cond No	*b/l*	*l/H*	Δ*y/H*	F_d	*B/H*	*b/H*
1	37.8	37.1	7	35	80	0.27	27	34	1	×	×	×	×	×	✓
1	29.0	28.2	8	26	103	0.29	38	45	1	×	×	×	×	✓	×
2	44.7	43.4	6	40	64	0.26	18	28	3	×	×	✓	✓	×	×
2	44.3	43	6	40	65	0.26	19	28	2	×	×	✓	×	×	✓
3	64.3	63	4	61	14	0.21	-18	-6	3	✓	×	✓	✓	×	×
3	55.5	53.9	5	52	37	0.24	2.0	13	5	×	×	✓	✓	×	✓
4	66.8	65.2	4	63	9	0.20	-22	-8	5	✓	✓	✓	✓	×	×
4	65.7	68.1	4	61	12	0.21	-19	-5	6	✓	×	✓	✓	×	✓
5	**69.3**	**67.4**	**4**	**64**	**5**	**0.20**	**-26**	**-10**	**32**	✓	✓	✓	✓	✓	×
5	67.8	65.9	4	63	9	0.20	-22	-6	78	✓	✓	✓	✓	×	✓
6	69.3	67	3.9	62	7	0.20	-24	-6	148	✓	✓	✓	✓	✓	✓

*Note- From subset regression the lowest Mallows C_p value is 5.0 and its corresponding R-Sq(adj) is 67.4. Now using the variables of this case the final formula will be like Eq. 8.7.

$$\frac{Z_m}{H} = 3.93\left(\frac{B}{H}\right)^{-0.51}\left(\frac{b}{l}\right)^{1.1}\left(\frac{l}{H}\right)^{0.67}\left(\frac{\Delta y}{H}\right)^{0.33}\left(F_d\right)^{0.29} \tag{8.7}$$

Formula derivation by using Stepwise regression/Backward and subset regression methods.

*Note- In this case if we do subset regression and find the best combination of variables it also gives the same output as Pearson correlation with the subset regression method. So, the formula will be the same along with the same error matrices. Therefore, the final formula will be

$$\frac{Z_m}{H} = 3.93\left(\frac{B}{H}\right)^{-0.80}\left(\frac{b}{l}\right)^{1.39}\left(\frac{l}{H}\right)^{0.96}\left(\frac{\Delta y}{H}\right)^{0.33}\left(F'_d\right)^{0.29} \tag{8.6}$$

$$\frac{Z_m}{H} = 3.93\left(\frac{B}{H}\right)^{-0.51}\left(\frac{b}{l}\right)^{1.1}\left(\frac{l}{H}\right)^{0.67}\left(\frac{\Delta y}{H}\right)^{0.33}\left(F_d\right)^{0.29} \tag{8.7}$$

Table 8.34. List of formulas along with error matrices for different deviation conditions.

Serial Number	Formula	R^2	RMSE	%In (±10%)	% In (±20%)	% In (±30%)
1	$\frac{Z_m}{l}=2.1\left(\frac{b}{l}\right)^{0.8}\left(\frac{H}{l}\right)^{0.46}\left(\frac{\Delta y}{l}\right)^{0.33}\left(F_d\right)^{0.33}$	0.740	0.040	32.95	59.09	81.81
2	$\frac{Z_m}{l}=1.14\left(\frac{B}{l}\right)^{0.63}\left(\frac{H}{l}\right)^{0.42}\left(\frac{\Delta y}{l}\right)^{0.38}\left(F_d\right)^{0.40}$	0.674	0.045	30.68	59.09	82.95
3	$\frac{Z_m}{l}=1.31\left(\frac{b}{l}\right)^{0.83}\left(\frac{H}{l}\right)^{0.41}\left(\frac{\Delta y}{l}\right)^{0.32}\left(F'_d\right)^{0.31}$	0.717	0.042	27.27	60.23	80.68
4	$\frac{Z_m}{l}=6.57\left(\frac{B}{l}\right)^{-1.25}\left(\frac{b}{l}\right)^{1.85}\left(\frac{\Delta y}{l}\right)^{0.25}\left(\frac{h_{tw}}{l}\right)^{0.24}\left(\frac{H}{l}\right)^{0.34}$	0.739	0.040	36.36	63.63	79.55
5	$\frac{Z_m}{l}=4.45\left(\frac{B}{l}\right)^{-0.92}\left(\frac{b}{l}\right)^{1.54}\left(\frac{\Delta y}{l}\right)^{0.34}\left(\frac{h_{tw}}{l}\right)^{0.34}$	0.699	0.043	31.82	57.95	77.27
6	$\frac{Z_m}{H}=3.93\left(\frac{B}{H}\right)^{-0.80}\left(\frac{b}{l}\right)^{1.39}\left(\frac{l}{H}\right)^{0.96}\left(\frac{\Delta y}{H}\right)^{0.33}\left(F'_d\right)^{0.29}$	0.683	0.194	37.50	64.77	80.68
7	$\frac{Z_m}{H}=3.93\left(\frac{B}{H}\right)^{-0.51}\left(\frac{b}{l}\right)^{1.1}\left(\frac{l}{H}\right)^{0.67}\left(\frac{\Delta y}{H}\right)^{0.33}\left(F_d\right)^{0.29}$	0.683	0.194	37.50	64.77	80.68
8	$\frac{Z_m}{H}=1.51\left(\frac{b}{l}\right)^{0.64}\left(\frac{l}{H}\right)^{0.19}\left(\frac{\Delta y}{H}\right)^{0.34}\left(F'_d\right)^{0.31}$	0.651	0.292	30.68	63.63	82.95
9	$\frac{Z_m}{H}=2.28\left(\frac{b}{l}\right)^{0.61}\left(\frac{l}{H}\right)^{0.16}\left(\frac{\Delta y}{H}\right)^{0.34}\left(F_d\right)^{0.32}$	0.672	0.197	35.22	60.27	84.09

8.3. General discussion on newly developed formulas

If the derived formula adheres to dimensional consistency, conservation laws, boundary conditions, and empirical validation, and accurately represents nonlinearities and scaling behaviors, it follows the physical significance of flow physics and can be used for future analysis; otherwise, it may produce results but will not accurately describe the behavior of the parameters. In the present study, a total of nine number formulas were developed. Now we discuss all the developed formulas one by one by focusing on serial numbers.

- In Eq. 8.1 the non-dimensional scour is the function of orientation angle (i.e. $\frac{b}{l} = \sin\theta$) and F_d. We know that non-dimensional scour increases with the value b/l ratio and F_d. Here also it justifies this phenomenon.

  Scour due to the H/l ratio is a complex phenomenon. If H increases keeping l constant, then scour will be increased and vice versa. Conversely, if l is increased while keeping H constant then scour will be also increased or vice versa. When the values of H and l are changed simultaneously, the scour pattern can not be predicted. It may be an upward or downward trend. However, at present, a clear upward trend is shown in **Fig. 8.39**, which satisfies Eq. 8.1. Therefore, this ratio may be used in the equation.

  Scour due to the $\Delta y/l$ ratio is a complex phenomenon. If Δy is increased keeping l constant, then scour will be increased and vice versa. Conversely, keeping Δy constant, if l is increased then scour will be also increased or vice versa. When the values of H and l are changed simultaneously, the scour pattern can not be predicted; it may be a trend upward or downward. However, at present, a clear upward trend is shown in **Fig. 8.40,** which satisfies Eq. 8.1. Therefore, this ratio may be used in the equation.

  Here, it is seen that all the parameters used in this equation justify the normal flow physics of the fluid, so Eq. 8.1 may be used for future analysis. For the same reason Eq. 8.3 may be used for scour analysis.

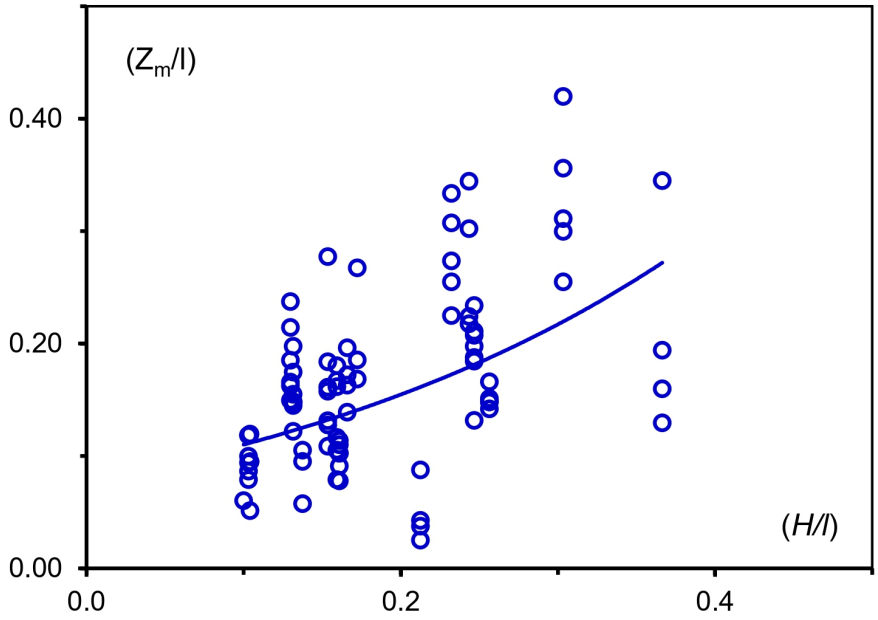


Fig. 8.39. The effect of aspect ratio (H/l) on non-dimensional scour depth (Z_m/l).

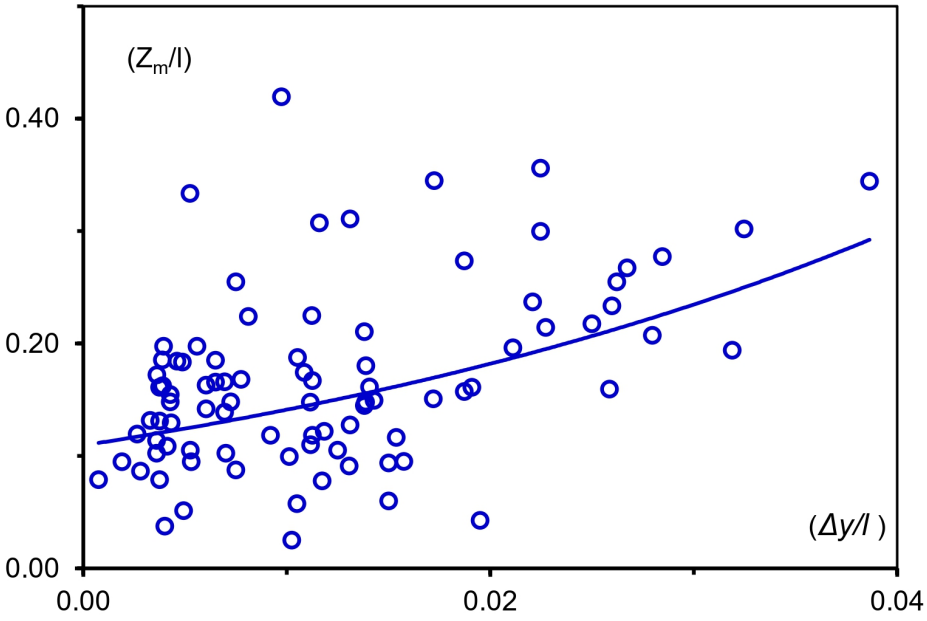


Fig. 8.40. The effect of aspect ratio ($\Delta y /l$) on non-dimensional scour depth (Z_m/l).

- If we compare Eq. 8.1 and Eq. 8.2 then we can see the B/l ratio is added in replace of the b/l ratio. We know that if the B/l ratio is increased then scour will be reduced but here gives the opposite result. So this equation simply does not obey the flow physis of fluid. Therefore, it may not be used for future scour depth prediction which will give a result that will not follow the physical significance of the flow parameters.

  In Eq. 8.4 a new non-dimensional parameter is used i.e. h_{tw}/l. Scour due to the h_{tw}/l ratio is a complex phenomenon. If h_{tw} is increased keeping l constant, then scour will be decreased and vice versa. Conversely, keeping *the* h_{tw} constant, if l is increased then scour

will be also increased or vice versa, in either of the cases this result is contradictory to the present formula. However, in the present study the pattern (see **Fig. 8.20**, **Fig. 8.21**, **Fig. 8.22**) will not follow the behavior of the fluid. Therefore, this ratio with positive power may not used in the equation. Similarly for the same reason Eq. 8.5 is also not used for future analysis.

- In Eq. 8.6 and Eq. 8.7, *H/B* does not follow the natural behavior of the fluid so this equation may not be used for future modeling of structures that increase the risk of failure.
- In Eq. 8.8 and Eq.8.9, all the independent non-dimensional parameters follow the general theory of fluid mechanics. Thus, why these two equations may be used for the prediction of non-dimensional scour depth.

Now the Present list of formulas that may be used for scour depth prediction is given below.

Table 8.35. List of formulas along with error matrices and percentages for different deviation conditions.

Eq. Number	Formula	R^2	RMSE	%In (±10%)	% In (±20%)	% In (±30%)
8.1	$\frac{Z_m}{l}=2.1\left(\frac{b}{l}\right)^{0.8}\left(\frac{H}{l}\right)^{0.46}\left(\frac{\Delta y}{l}\right)^{0.33}\left(F_d\right)^{0.33}$	0.740	0.040	32.95	59.09	81.81
8.3	$\frac{Z_m}{l}=1.31\left(\frac{b}{l}\right)^{0.83}\left(\frac{H}{l}\right)^{0.41}\left(\frac{\Delta y}{l}\right)^{0.32}\left(F'_d\right)^{0.31}$	0.717	0.042	27.27	60.23	80.68
8.8	$\frac{Z_m}{H}=1.51\left(\frac{b}{l}\right)^{0.64}\left(\frac{l}{H}\right)^{0.19}\left(\frac{\Delta y}{H}\right)^{0.34}\left(F'_d\right)^{0.31}$	0.651	0.292	30.68	63.63	82.95
8.9	$\frac{Z_m}{H}=2.28\left(\frac{b}{l}\right)^{0.61}\left(\frac{l}{H}\right)^{0.16}\left(\frac{\Delta y}{H}\right)^{0.34}\left(F_d\right)^{0.32}$	0.672	0.197	35.22	60.27	84.09

8.4. Comparison between shortlisted formulas

Based on **Table 8.35**, Eq. 8.1 has a higher R^2 value and a lower RMSE value compared to the other equations, indicating it has the least error involved. Additionally, **Fig. 8.40** shows that the percentage of data for each formula gives similar results, with narrow margins. Therefore, considering both **Table 8.35** and **Fig. 8.40**, my recommended formula is Eq. 8.1 and Eq. 8.9.

$$\frac{Z_m}{l}=2.1\left(\frac{b}{l}\right)^{0.8}\left(\frac{H}{l}\right)^{0.46}\left(\frac{\Delta y}{l}\right)^{0.33}\left(F_d\right)^{0.33} \tag{8.1}$$

Now considered $\psi=\left(\frac{\Delta y}{l}F_d\right)$, which is the non-dimensional parameter. Now, Eq. 8.1 may be written as

$$\frac{Z_m}{l} = 2.1\left(\frac{b}{l}\right)^{0.8}\left(\frac{H}{l}\right)^{0.46}(\psi)^{0.33} \tag{8.10}$$

Equation 8.10 is similar to the model proposed by Pagliara and Kurdistani (2016) and Pagliara (2015), where three functional groups were considered: l/B, h_{tw}/H and η.

Another formula that may suggested concerning H is Eq. 8.9.

$$\frac{Z_m}{H} = 2.28\left(\frac{b}{l}\right)^{0.61}\left(\frac{l}{H}\right)^{0.16}\left(\frac{\Delta y}{H}\right)^{0.34}(F_d)^{0.32} \tag{8.9}$$

These two formulae may be used for calculations of scour.

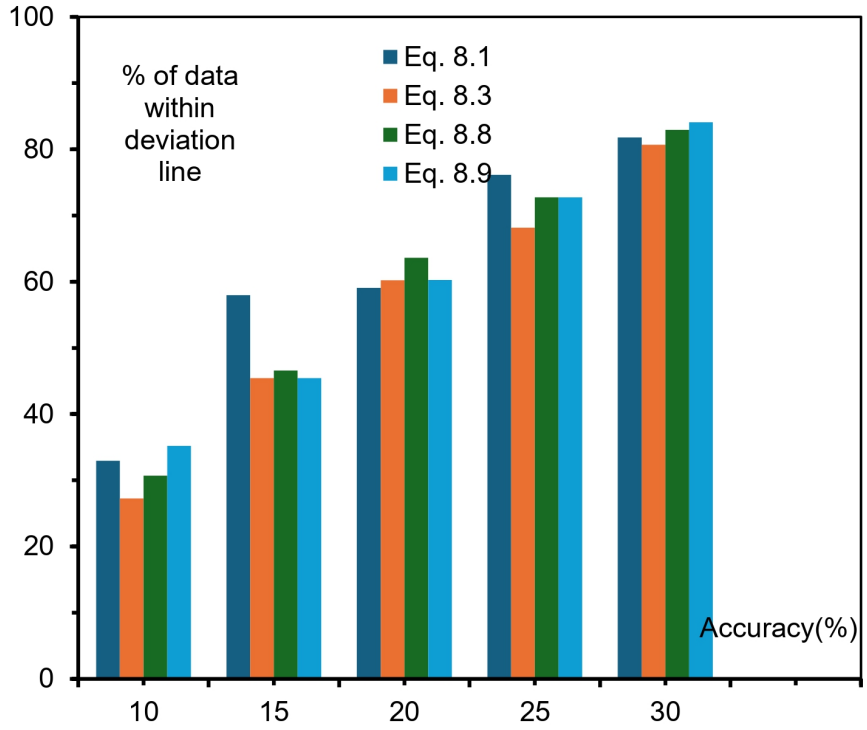


Fig. 8.40. The effect of accuracy (%) versus percentage of data within the deviation line in the numbers of equations (represented as bar diagram).

8.6. Validation of formula

Based on **Fig. 8.41**, **Fig. 8.42**, and **Table 8.36,** it is observed that when plots are created using the formulas of other researchers, very few data points remain within the deviation line. However, when the data from other researchers is plotted using Eq. 8.1, better results are obtained, as shown in **Fig. 8.43**. Therefore, it is clear from **Fig. 8.43.** that Eq. 8.1 is more accurate than the formulas of the other researchers. Hence, this formula can be used for the calculation of non-dimensional scour depth. In the present study considered±30% deviation line then there were no points below the -30% line which indicates the accuracy of the formula

in terms of overestimating the scour depth. So this formula may not be given under estimated scour value.

Table 8.36. List of formulas along with error matrices and percentage-in values for different deviation conditions.

Data collected from	Statistical influence parameter	The formula used for evaluation		
		Pagliara and Kurdistani (2016)	**Pagliara et al. (2014)**	**Pagliara et al. (2015)**
Pagliara and Kurdistani (2016)	R	0.75	0.64	0.75
	R^2	0.56	0.41	0.56
	SSE	0.41	0.28	7.7
	MSE	0.05	0.03	0.86
	RMSE	0.21	0.18	0.92
	% In	44.44	44.44	44.44
Pagliara et al. (2014)	R	0.25	0.59	0.25
	R^2	0.06	0.35	0.06
	SSE	27.23	12.37	27.23
	MSE	0.68	0.31	0.62
	RMSE	0.83	0.56	0.79
	% In	0	5	0
Pagliara et al. (2015)	R	0.27	0.49	0.27
	R^2	0.07	0.24	0.07
	SSE	15.11	6.07	15.11
	MSE	0.39	0.16	0.39
	RMSE	0.62	0.39	0.62
	% In	7.69	30.77	7.69

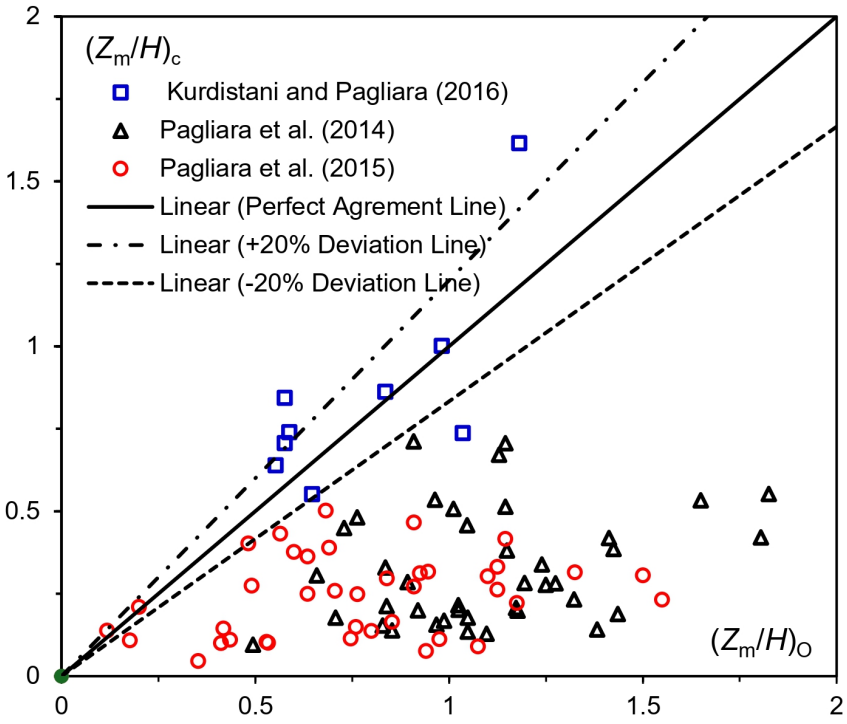


Fig. 8.41. Comparison between observed and predicted values of equilibrium scour depth using Pagliara and Kurdistani (2016) and Pagliara (2015) formula.

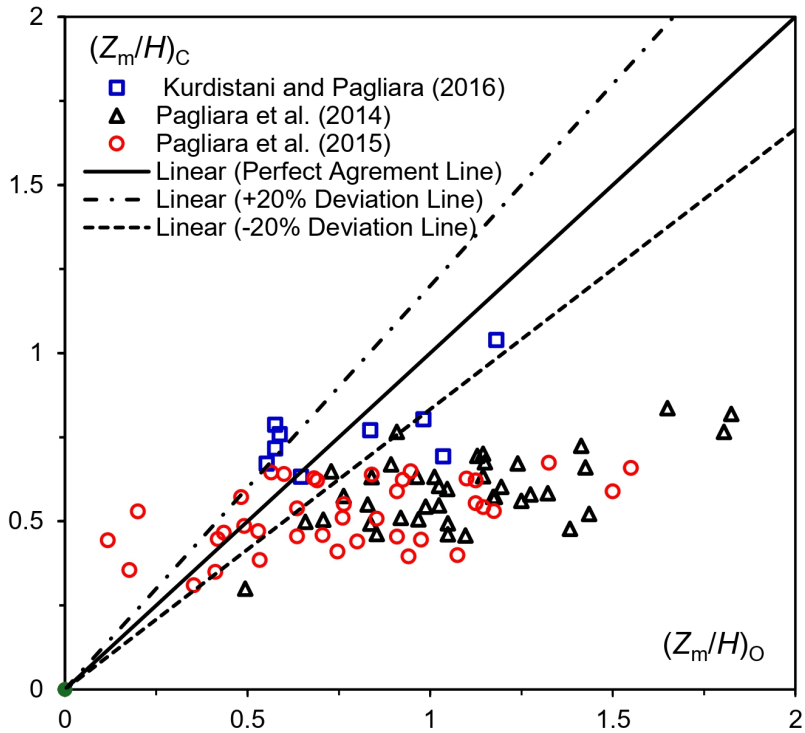


Fig. 8.42. Comparison between observed and predicted values of equilibrium scour depth using the Pagliara (2014) formula.

Table 8.39. List of formulas along with error matrices and percentage-in formulas for different deviation conditions.

Data collected from	Statistical influence parameter	The formula used for evaluation			
		Pagliara and Kurdistani (2016)	**Pagliara et al. (2014)**	**Pagliara et al. (2015)**	**Present Study**
Present Study	R	0.15	0.45	0.15	0.861
	R^2	0.02	0.2	0.02	0.74
	SSE	42.75	18.72	42.75	0.143
	MSE	0.49	0.21	0.49	0.0016
	RMSE	0.70	0.46	0.70	0.04
± 20% deviation	%In	7.95	20.45	7.95	59.09
± 30% deviation	%In	14.77	34.09	14.77	81.8
± 40% deviation	%In	21.59	48.86	21.59	90.91
± 50% deviation	%In	30.68	72.73	30.68	92.05

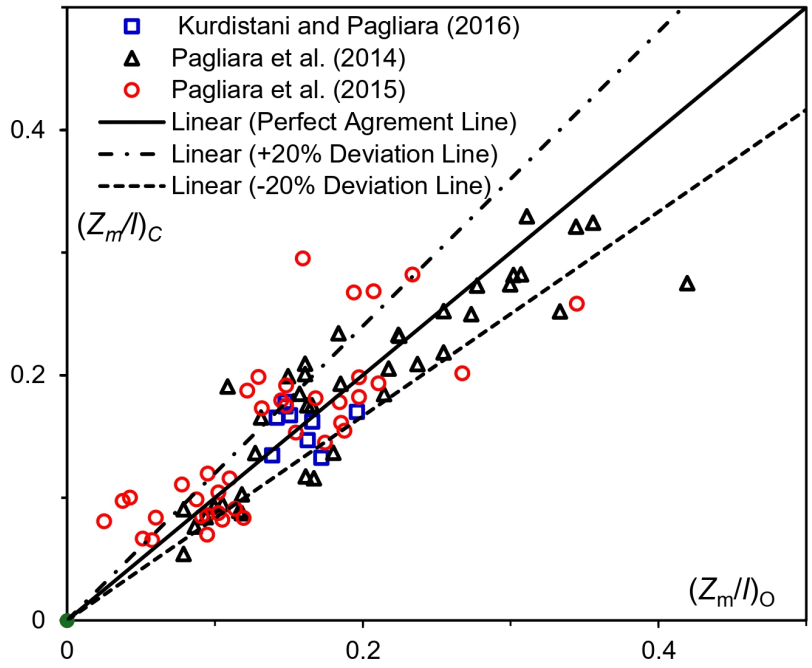


Fig. 8.43. Comparison between observed and predicted values of equilibrium scour depth using the newly developed equation.

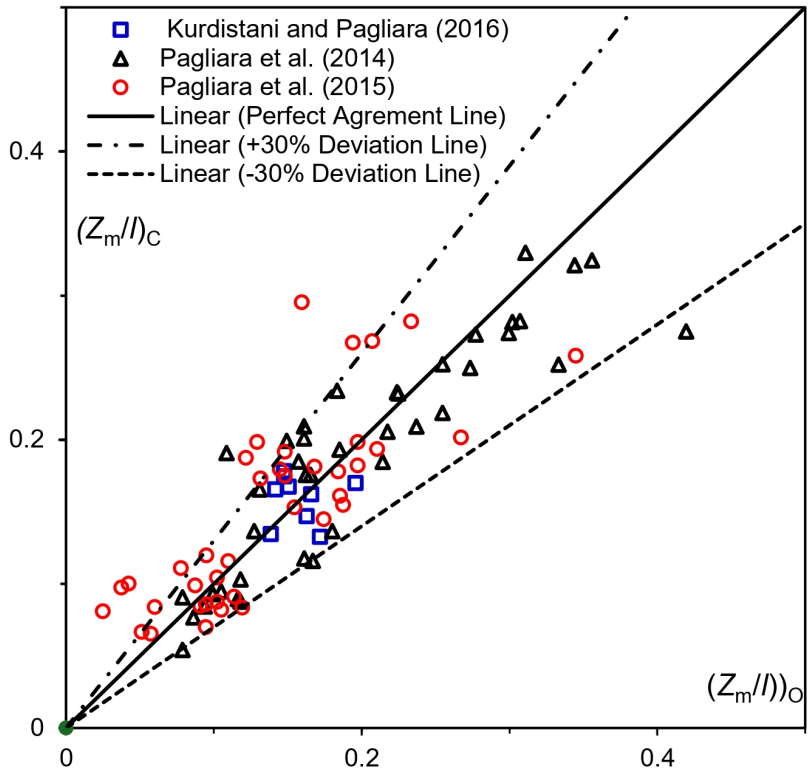


Fig. 8.43. Comparison between observed and predicted values of equilibrium scour depth using the newly developed equation.

CHAPTER -09

Conclusive remarks

9.1. Conclusions

In conclusion, this thesis presents a comprehensive study aimed at deriving a new equilibrium scour depth equation specifically for log vanes. Through a systematic and rigorous approach, we have developed an empirical model that better predicts scour depth in the vicinity of log vanes under varying hydraulic conditions.

Our research began with an extensive review of existing literature on scour phenomena around various hydraulic structures, highlighting the unique characteristics and challenges posed by log vanes. We identified the limitations of current scour depth prediction models, particularly their lack of specific log vane structures.

Using the experimental data, we applied multiple regression analysis and dimensional analysis techniques to derive a new equilibrium scour depth equation. The proposed equation incorporates dimensionless parameters that effectively account for the influence of flow intensity, sediment characteristics, and geometric properties of the log vane. This novel equation was validated against both our experimental data and a set of field observations, demonstrating improved accuracy and reliability over existing models.

Based on the present study there are several conclusions are there in which are described below

- When all the data is plotted in a newly developed equation using ±30% deviation from the perfect agreement line, no data falls below the -30% line. This indicates that all the non-dimensional scour depths are overestimated. Therefore, there is a lower chance of any structure's failure due to scouring.
- In this process, it is observed that the value of R^2 (0.02) is much lower when all the data is plotted using the Pagliara and Kurdistani (2016) formula, and it does not match the R^2 (0.91) mentioned in their paper.
- Based on all the experimental data used in this analysis, a clear pattern was not always observed, therefore formula derivation by non-linear regression gives few scrap formulas which do not satisfy the normal behavior of the fluid.
- Since no data on woody structures are available in the literature, the closest structural geometry belongs to spur dikes. Therefore, the observed data from Kuhnle et al. (1999, 2002) on a 90° spur dike and angled spur dike, respectively, have been used for comparison with the derived equation of Pagliara and Kurdistani (2016). Thus, there are more chances of involving error in the calculation of scour.
- Pagliara et al. (2014) compared the derived formula with the J hook data of Pagliara et al. (2013), while Pagliara et al. (2015) compared it with the cross-vane data of Pagliara and Kurdistani (2013) and the W-weir data of Pagliara (2014b). Additionally, Pagliara and Kurdistani (2016) compared the derived formula with the data from Kuhne et al. (1999,

2002). Therefore, the previous formula was always compatible with the less scour depth. Consequently, when comparisons of the present study are made with those of Pagliara et al. (2014), Pagliara et al. (2015), or Pagliara and Kurdistani (2016), all the data shows a downward movement from the -20% deviation line. This satisfies the comments of Pagliara et al. (2015) that a log vane with the same hydraulic conditions results in less scours compared to the cross vane.

9.2. Limitations of the study

The comprehensive approach to analyzing and developing a new formula based on the literature to estimate clearwater equilibrium scour depth downstream of a log vane study, there is involves a few limitations which are described below-

- The accuracy and reliability of the results heavily rely on the quality and availability of the data collected from various graphs and literature sources. If the data is sparse, outdated, or inconsistent, it could introduce biases or errors in the analysis.
- One of the primary limitations of this study is the potential presence of errors in the data obtained from various literature sources.
- The formula derivation is done using a nonlinear regression method, which provides the best possible fit curve; however, it may or may not fulfill the physical significance of flow.
- Dimensional analysis, subset regression, and other dimensionality reduction techniques often rely on simplifying assumptions. These assumptions may not always hold in real-world scenarios, leading to potential inaccuracies in the results.
- The findings of the study may be specific to the conditions, parameters, and datasets used in the analysis. Extrapolating these findings to different geographical locations, hydraulic conditions, or types of vane dikes may not be appropriate without further validation.
- It is crucial to validate the selected formula against independent datasets or field measurements to assess its predictive accuracy and reliability. Failure to validate the chosen formula could lead to misleading conclusions. In the present study, the formula suggested by different researcher validate their formula by using J-hook data and cross-vane data which may give inaccurate results.
- The study's reliance on existing literature may introduce publication bias, where only studies with positive or significant results are published, leading to an overestimation of the effectiveness of certain formulas.
- Since the study focuses on equilibrium scour depth formulas, it is essential to consider the equilibrium variability of hydraulic conditions and scour processes. Failure to account for equilibrium dynamics could limit the applicability of the selected formula over different time scales.

9.3. Future scopes of the work

- In this field, very few studies have been conducted, providing ample opportunity for further exploration of scour and its morphology. Based on the present study, the equation can be validated with additional experimental data and potentially applied in practical structures for scour calculations, with efforts made to minimize the error in predicting scour in practical applications.
- Previously Pagliara et al (2014) and Pagliara et al. (2015) compared the derived formula with the data of J-hook and cross vane respectively. Therefore, there is scope for further research to compare the other river restoration structures with this formula (Eq. 8.1) and to determine the most effective techniques for river restoration work.

9.4 Notations

Notation used in this study-

b	=	Vertical projection vane from river bank (m)
B	=	Width of the channel (m)
D	=	Effective width of vane (m)
d_{50}	=	Median grain size (m)
Fr	=	Froude number of flow
F_d	=	Densimetric Particle Froude number (dimensionless)
F'_d	=	Densimetric Particle Froude number (dimensionless)
g	=	Acceleration due to gravity (m/sec^2)
G_s	=	Specific gravity of sediment particle(dimensionless)
H	=	Log vane height (m)
h_{tw}	=	Tail water depth (m)
L	=	Length of abutment (m)
l	=	Log vane length (m)
Q	=	Discharge of flow (m^3/sec)
Re	=	Reynolds number (dimensionless)
S_o	=	Bed Slope (°)
u_*	=	Shear velocity in (m/sec)
u_{*c}	=	Critical shear velocity (m/sec)
V	=	Depth-averaged flow velocity (m/sec)
V_c	=	Critical flow velocity (m/sec)
y	=	Depth of flow in u/s (m)
Δy	=	Difference in water level in between u/s and d/s
ρ	=	Density of water (kg/m^3)
ρ_s	=	Sediment density (kg/m^3)
Δ	=	Relative density (dimensionless)
σ	=	Geometric standard deviation (dimensionless)
θ	=	Orientation angle of log vane (degree)
μ	=	Dynamic viscosity (kg/m-.sec)
υ	=	Kinematic viscosity (m^2/sec)
τ	=	Shear stress (N/m^2)
τ_c	=	Critical shear stress (N/m^2)
Z_m	=	Equilibrium scour depth (m)

References

Ahmed, F., and Rajaratnam, N. (1998). Flow around bridge piers. *Journal of Hydraulic Engineering*, Vol. 124, Issue 3, pp. 288-300 .https://doi.org/10.1061/(ASCE)0733-9429(1998)124:3(288).

Ahmed, F., and Rajaratnam, N. (2000). Observations on flow around bridge abutment. *Journal of Engineering Mechanics*, Vol. 126, Issue 1, pp. 51-59. https://doi.org/10.1061/(ASCE)0733-9399(2000)126:1(51).

Al-Shukur, A. H. K., and Obeid, Z. H. (2016). Experimental study of bridge pier shape to minimize local scour. *International Journal of Civil Engineering and Technology*, Vol. 7, Issue 1, pp. 162-171.

Azamathulla, H. M. A. H. M., Ab Ghani, A., Zakaria, N. A. (2010). Prediction of scour around hydraulic structure using soft computing techniques. *Malaysian Journal of Civil Engineering*, Vol. 22, Issue 1, pp. 53-65, https://doi.org/10.11113/mjce.v22.15799.

Behbahan, T.S. (2011). Laboratory Investigation of Submerged Vane Shapes Effect on River Banks Protection. *Australian Journal of Basic and Applied Sciences*, Vol. 5, Issue 12, pp. 1402- 1407. http://www.insipub.com/ajbas/2011/December-2011/1402-1407.pdf.

Bejestan, M.S. and Azizi, R. (2012). Experimental Investigation of Scour Depth at the Edge of Different Submerged Vanes Shapes. *World Environmental and Water Resources Congress* 2012, pp. 1376-1385. https://doi.org/10.1061/9780784412312.138.

Bejestan, M.S., Khademi, K. and Kozeymehnezhad, H. (2015). Submerged vane-attached to the abutment as scour Countermeasure. *Ain Shams Engineering Journal*, Vol. 6, Issue 3, pp. 775-783. https://doi.org/10.1016/j.asej.2015.02.006.

Bhuiyan, F., Hey, R. D., and Wormleaton, P. R. (2007). "Hydraulic evaluation of W-weir for river restoration." *Journal of Hydraulic Engineering*, Vol. 133, Issue 6, pp. 596-609. https://doi.org/10.1061/(ASCE)0733-9429(2007)133:6(596).

Breusers, H. N. C., Nicollet, G., and Shen, H. W. (1977). Local scour around cylindrical piers. *Journal of Hydraulic Research*, Vol. 15, Issue 3, pp. 211-252. https://doi.org/10.1080/00221687709499645.

Dargahi, B. (1990). Controlling mechanism of local scouring. *Journal of Hydraulic Engineering*, Vol. 116, Issue 10, pp. 1197-1214. https://doi.org/10.1061/(ASCE)0733-9429(1990)116:10(1197).

Das, R., Das, S., Jaman, H., and Mazumdar, A. (2019). Impact of upstream bridge pier on the scouring around adjacent downstream bridge pier. *Arabian Journal for Science and Engineering*, Vol. 44, pp. 4359-4372. https://doi.org/10.1007/s13369-018-3418-5.

Das, R., Khwairakpam, P., Das, S., Mazumdar A. (2014) Clear-water local scour around eccentric multiple piers to shift the line of sediment deposition. *Asian Journal of Water Environment and Pollution,* Vol. 11, Issue 3, pp. 47–54.

Das, S., and Mazumdar, A. (2018). Evaluation of hydrodynamic consequences for horseshoe vortex system developing around two eccentrically arranged identical piers of diverse

shapes. *KSCE Journal of Civil Engineering*, Vol. 22, pp. 2300-2314. https://doi.org/10.1007/s12205-017-1842-9.

Das, S., Das, R., and Mazumdar, A. (2013). Circulation characteristics of horseshoe vortex in scour region around circular piers. *Water Science and Engineering*, Vol. 6, Issue 1, pp. 59-77. https://doi.org/10.3882/j.issn.1674-2370.2013.01.005.

Das, S., Das, R., Kuila, A., and Mazumdar, A. (2014). Analysis of clear-water equilibrium scour around two eccentric circular piers to increase self-dredging. In *Seminar on Dredging: Equipment and Applications, (EADA), Kolkata, India*.

Das, S., Das, R., Mazumdar, A. (2016). Comparison of local scour characteristics around two eccentric piers of different shapes. *Arabian Journal of Science and Engineering,* Vol. 41, Issue 4, pp. 1199-1213. https://doi.org/10.1007/s13369-015-1817-4.

Das, S., Ghosh, R., Das, R., and Mazumdar, A. (2014). Clear water scour geometry around circular piers. *Ecology Environment and Conservation*, Vol. 20, Issue 2, pp. 479-492.

Das, S., Ghosh, S., and Mazumdar, A. (2014). Kinematics of Horseshoe Vortex in a Scour Hole around Two Eccentric Triangular Piers. *International Journal of Fluid Mechanics Research*, Vol. 41, Issue 4, pp. 296-317. https://doi.org/10.1615/InterJFluidMechRes.v41.i4.20.

Das, S., Jaman, H., Chatterjee, A., Das, R., and Mazumdar, A. (2017). Hydrodynamic behaviour of Flow past three typically arranged circular piers on different horizontal planes. *International Journal of Fluid Mechanics Research*, Vol. 44, Issue 5, pp. 457-468. https://doi.org/10.1615/InterJFluidMechRes.2017019421.

Das, S., Midya, R., Das, R., and Mazumdar, A. (2013). A study of wake vortex in the scour region around a circular pier. *International Journal of Fluid Mechanics Research*, Vol. 40, Issue 1, pp. 42-59. https://doi.org/10.1615/InterJFluidMechRes.v40.i1.40.

Dey, S., and Barbhuiya, A. K. (2004). Clear-water scour at abutments in thinly armored beds. *Journal of Hydraulic Engineering*, Vol. 130, issue 7, pp. 622-634. https://doi.org/10.1061/(ASCE)0733-9429(2004)130:7(622).

Dey, S., and Raikar, R. V. (2007). Characteristics of horseshoe vortex in developing scour holesat piers. *Journal of Hydraulic Engineering*, Vol. 133, Issue 4, pp. 399-413. https://doi.org/10.1061/(ASCE)0733-9429(2007)133:4(399).

Dey, S., Bose, S. K., & Sastry, G. L. (1995). Clear water scour at circular piers: a model. *Journal of Hydraulic Engineering*, Vol. 121, Issue 12, pp. 869-876. https://doi.org/10.1061/(ASCE)0733-9429(1995)121:12(869).

Doe, J., and Smith, J. (2020). Subset Regression in Machine Learning: A Comprehensive Review. Journal of Machine Learning Research, Vol.21, Issue 3, pp. 112-135. https://doi.org/10.5555/123456789012.

Efroymson, M. A. (1960). Multiple Regression Analysis.Technometrics, Vol.2, pp.269-290, https://doi.org/10.1080/00401706.1960.10489866.

Flokstra, C. (2006). Modelling of submerged vanes. *Journal of Hydraulic Research*, Vol. 44, Issue 5, pp. 591-602. https://doi.org/10.1080/00221686.2006.9521709.

Ghorbani, B. and Kells, J.A. (2008). Effect of submerged vanes on the scour occurring at a cylindrical pier. *Journal of Hydraulic Research*, Vol. 46, Issue 5, pp. 610-619. https://doi.org/10.3826/jhr.2008.3003.

Gupta, U.P; Sharma, N; Ojha C.S.P (2007). Performance evaluation of tapered vane, *Journal of Hydraulic Research,* Vol. 45, Issue 4, pp. 472-477. https://doi.org/10.1080/00221686.2007.9521781.

Johnson, P. A., Hey, R. D., Tessier, M., and Rosgen, D. L. (2001). Use of vanes for control of scour at vertical wall abutments. *Journal of Hydraulic Engineering*, Vol. 127, Issue 9, pp. 772-778.https://doi.org/10.1061/(ASCE)0733-9429(2001)127:9(772).

Jueyi, S. U. I., Afzalimehr, H., Samani, A. K., and Maherani, M. (2010). Clear-water scour around semi-elliptical abutments with armored beds. *International Journal of Sediment Research*, Vol. 125, Issue 3, pp. 233-245. https://doi.org/10.1016/S1001-6279(10)60041-8

Khwairakpam, P., Ray, S. S., Das, S., Das, R., & Mazumdar, A. (2012). Scour hole characteristics around a vertical pier under clear water scour conditions. *ARPN Journal of Engineering and Applied Sciences*, Vol. 7, Issue 6, pp. 649-654.

Legates, D. R., and McCabe Jr, G. J. (1999). Evaluating the use of "goodness-of-fit" measures in hydrologic and hydroclimatic model validation. Water Resources Research, Vol.35, Issue.1, pp. 233-241.

Marelius, F., Sinha, S.K. (1998). Experimental Investigation of Flow past Submerged Vanes, *Journal of Hydraulic Engineering*, 124(5), pp. 542-545. https://doi.org/10.1061/(ASCE)0733-9429(1998)124:5(542).

Melville, B. W. (1992). Local scour at bridge abutments. *Journal of Hydraulic Engineering,* Vol. 118, Issue 4, pp. 615-631. https://doi.org/10.1061/(ASCE)0733-9429(1992)118:4(615).

Melville, B. W., & Raudkivi, A. J. (1977). Flow characteristics in local scour at bridge piers. *Journal of Hydraulic Research*, Vol. 15, issue 4, pp. 373-380. https://doi.org/10.1061/(ASCE)0733-9429(2004)130:7(622).

Melville, B. W., and Chiew, Y. M. (1999). Time scale for local scour at bridge piers. *Journal of Hydraulic Engineering*, Vol. 125, Issue 1, pp. 59-65. https://doi.org/10.1061/(ASCE)0733-9429(1999)125:1(59).

Melville, B.W. (1975). Local scour at bridge sites. Report no. 117, School of Engineering, University of Auckland. Auckland, New Zealand.

Michael, S.A., Mohamed, G.M., Mohamed, S.B.A.M. (1991). Wake vortex scour at bridge piers. *Journal of Hydraulic Engineering*, Vol. 117, Issue 7, pp. 891-904. https://doi.org/10.1061/(ASCE)0733-9429(1991)117:7(891)

Muzzammil, M., and Gangadhariah, T. (2003). The mean characteristics of horseshoe vortex at a cylindrical pier. *Journal of Hydraulic Research*, Vol. 41, Issue 3, pp. 285-39*741*. https://doi.org/10.1080/00221680309499973.

Nandi, B. (2019): Analysis of Time Variation of Scour around Three Cylindrical Tandem Piers. M.E. Thesis, School of Water Resources Engineering, Jadavpur University, Kolkata, India.

Nandi, B., and Das, S. (2023*a*). Equation for time-dependent local scour at pier-like structures with eccentric in-line arrangements. In *Proceedings of the Institution of Civil Engineers-Water Management*, pp. 1-14. https://doi.org/10.1680/jwama.23.00006.

Nandi, B., Das, S., (2023*b*). Identify most promising temporal scour depth formula for circular piers proposed over last six decades. *Ocean Engineering.* Vol. 286, Art. No. 115639. https://doi.org/10.1016/j.oceaneng.2023.115639.

Nandi, B., Patel, G., Das, S. (2024b). Prediction of maximum scour depth at clear water conditions: Multivariate and robust comparative analysis between empirical equations and machine learning approaches using extensive reference metadata. *Journal of Environmental Management*, Vol. 354, Art. No. 120349. https://doi.org/10.1016/j.jenvman.2024.120349.

Nandi, B., Sasmal, K., and Das, S. (2024*a*). Evolution of Four Formulae Derived Over Five Decades to Predict Temporal Scour at Circular Pier. In International Conference on Science, Technology and Engineering, pp. 131-139. Singapore: Springer Nature Singapore. https://doi.org/10.1007/978-981-99-4665-5_14.

Nash, J. E., and Sutcliffe, J. V. (1970). River flow forecasting through conceptual models' part I—A discussion of principles. The North-Holland Publishing Co, Amsterdam, Journal of Hydrology, Vol. 10, Issue 3, pp.282-290.

Odgaard, A. J., & Kennedy, J. F. (1983). River-bend bank protection by submerged vanes. *Journal of Hydraulic Engineering*, Vol. 109, Issue *8*, pp. 1161-1173. https://doi.org/10.1061/(ASCE)0733-9429(1983)109:8(1161).

Odgaard, A. J., and Kennedy, J. F. (1983). River-bend bank protection by submerged vanes. *Journal of Hydraulic Engineering*, Vol. 109, Issue 8, pp. 1161-1173. https://doi.org/10.1061/(ASCE)0733-9429(1983)109:8(1161).

Odgaard, A. J., and Spoljaric, A. (1986). Sediment control by submerged vanes. Journal of Hydraulic Engineering, Vol. 112, Issue 12, pp. 1164-1180. https://doi.org/10.1061/(ASCE)0733-9429(1986)112:12(1164).

Odgaard, A.J. and Spoljaric, A. (1986). Sediment Control by Submerged Vanes. *Journal of Hydraulic Engineering*, Vol. 112, Issue 12, pp. 1164-1180. https://doi.org/10.1061/(ASCE)0733-9429(1986)112:12(1164).

Odgaard, A.J. and Spoljaric, A. (1986). Sediment Control by Submerged Vanes. Journal of Hydraulic Engineering, 112(12), pp. 1164-1180.

Odgaard, A.J. and Wang, Y. (1991). Sediment Management with Submerged Vanes. I: Theory. *Journal of Hydraulic Engineering*, Vol. 117, Issue 3 pp. 267-283. https://doi.org/10.1061/(ASCE)0733-9429(1991)117:3(267).

Odgaard, A.J. and Wang, Y. (1991). Sediment Management with Submerged Vanes. I: Applications. *Journal of Hydraulic Engineering*, Vol. 117, Issue 3, pp. 284-302. https://doi.org/10.1061/(ASCE)0733-9429(1991)117:3(267).

Oliveto, G., and Hager, W. H. (2002). Temporal evolution of clear-water pier and abutment scour. *Journal of Hydraulic Engineering*, Vol. 128, Issue 9, pp. 811-820. https://doi.org/10.1061/(ASCE)0733-9429(2002)128:9(811).

Pagliara, S. (2007). Influence of sediment gradation on scour downstream of block ramps. *Journal of Hydraulic Engineering*, Vol. 133, Issue 11, pp. 1241-1248. https://doi.org/10.1061/(ASCE)0733-9429(2007)133:11(1241).

Pagliara, S., and Kurdistani, S. M. (2013). Scour downstream of cross-vane structures. *Journal of Hydro-environment Research*, Vol. 7, Issue 4, pp. 236-242. https://doi.org/10.1016/j.jher.2013.02.002.

Pagliara, S., and Kurdistani, S. M. (2014). “Scour characteristics downstream of grade-control structures.” River flow 2014, A. J. Schleiss, et al., eds., Taylor & Francis, London.

Pagliara, S., and Kurdistani, S. M. (2014). Scour characteristics downstream of grade-control structures. *River flow 2014*, pp. 2093-2098.

Pagliara, S., and Kurdistani, S. M. (2016). Flume experiments on scour downstream of wood stream Restoration structures. *Geomorphology*, Vol. *279*, pp. 141-149. https://doi.org/10.1016/j.geomorph.2016.10.013.

Pagliara, S., and Palermo, M. (2008). Scour control and surface sediment distribution downstream of block ramps. *Journal of Hydraulic Research*, Vol. 46, Issue 3, pp. 334-343. https://doi.org/10.3826/jhr.2008.3208.

Pagliara, S., Hassanabadi, L., and Kurdistani, S. M. (2015). Clear water scour downstream of log deflectors in horizontal channels. *Journal of Irrigation and Drainage Engineering*, Vol. 141, Issue 9, Art. No. 04015007. https://doi.org/10.1061/(ASCE)IR.1943-4774.0000869.

Pagliara, S., Kurdistani, S. M., and Cammarata, L. (2014b). “Scour of clear water rock W-weirs in straight rivers.” *Journal of Hydraulic Engineering*, Vol. 140, Issue 4, Art. No. 06014002. https://doi.org/10.1061/(ASCE)HY.1943-7900.0000842.

Pagliara, S., Lotti, I., and Palermo, M. (2008). Hydraulic jump on rough bed of stream rehabilitation structures. *Journal of Hydro-environment research*, Vol. 2, Issue 1, pp. 29-38. https://doi.org/10.1016/j.jher.2008.06.001.

Pagliara, S., Sagvand Hassanabadi, L., and Mahmoudi Kurdistani, S. (2015). Log-vane scour in clear water condition. *River Research and Applications*, Vol. 31, Issue 9, pp. 1176-1182. https://doi.org/10.1002/rra.2799.

Raudkivi, A. J., and Ettema, R. (1983). Clear water scour at cylindrical piers. *Journal of Hydraulic Engineering*, Vol. 109, Issue 3, pp. 338-350. https://doi.org/10.1061/(ASCE)0733-9429(1983)109:3(338).

Raudkivi, A. J., and Ettema, R. (1985). Scour at cylindrical bridge piers in armored beds. *Journal of Hydraulic Engineering*, Vol. 111, Issue 4, pp. 713-731. https://doi.org/10.1061/(ASCE)0733-9429(1985)111:4(713).

Scurlock, S. M., Cox, A. L., Thornton, C. I., & Baird, D. C. (2012). Maximum velocity effects from vane-dike installations in channel bends. In *World Environmental and Water Resources Congress 2012,* pp.2614-2626. https://doi.org/10.1061/9780784412312.261.

Scurlock, S. M., Thornton, C. I., and Abt, S. R. (2012*a*, b). “Equilibrium scour downstream of three-dimensional grade-control structures. *Journal of Hydraulic Engineering*, Vol. 138, issue 2, pp. 167-176. https://doi.org/10.1061/(ASCE)HY.1943-7900.0000493.

weirs in straight rivers.” *Journal of Hydraulic Engineering*, Vol. 140, Issue 4. https://doi.org/10.1061/(ASCE)HY.1943-7900.0000842.

Willmott, C.J. (1981). On the validation of models. Physical Geography, Vol. 2, Issue 2, pp. 184–194.